ISSN : 0973-0613

JOURNAL OF Wind and Engineering

Vol. 5 No. 2 July 2008

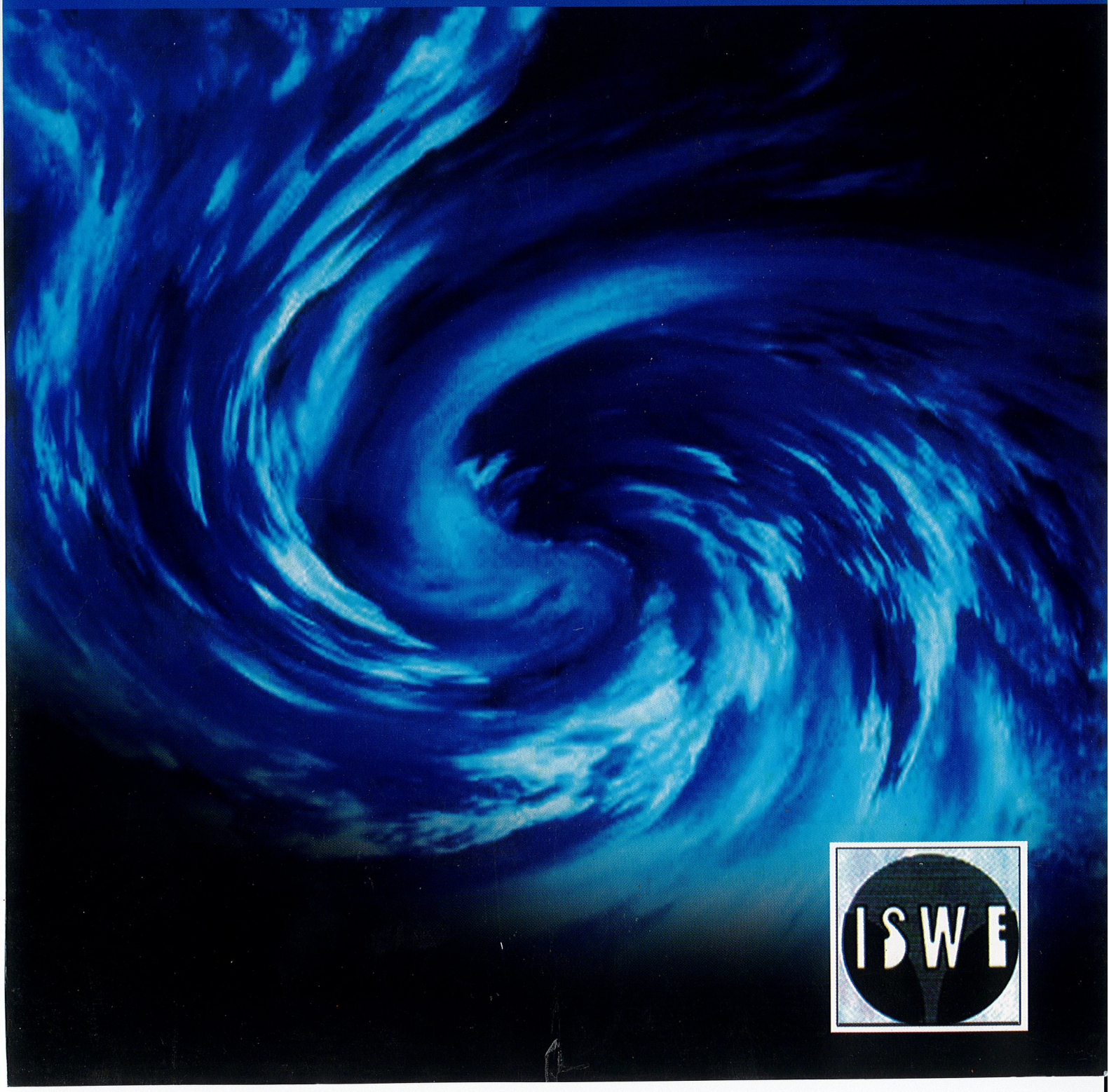

Journal of Wind and Engineering

JOURNAL OF WIND & ENGINEERING

Vol. 5 No. 2 July 2008

CONTENTS

Journal of Wind & Engineering, Vol. 5, No. 2, July 2008, pp. 1-16

A TIME DOMAIN ANALYSIS TECHNIQUE FOR AERODYNAMIC WIND TUNNEL MODEL STUDIES

K.T. Tse[1], P.A. Hitchcock[2], and K.C.S. Kwok[2,3]

[1]Department of Building and Construction, City University of Hong Kong
[2]CLP Power Wind/Wave Tunnel Facility, HKUST, Hong Kong
[3]Department of Civil Engineering, HKUST, Hong Kong

ABSTRACT

Owing to the limited storage capacity and computational power of computers in the 1980s, analyses for aerodynamic model studies, such as high-frequency base balance (HFBB) or synchronous multi-pressure sensing system (SMPSS), have been traditionally conducted in the frequency domain. As computer technology has improved and the necessity to conduct the vibration control analysis in the time domain grows, this paper investigates the feasibility of implementing analyses for aerodynamic model studies in the time domain. A series of wind tunnel tests was conducted at the CLP Power Wind/Wave Tunnel Facility, The Hong Kong University of Science and Technology to determine the wind forces exerted on a benchmarking building using the simultaneous pressure measurement technique. The base overturning moments and torque were subsequently synthesised using the measured pressure data and analysed in both time domain and frequency domain from which the base overturning moment responses and the building tip acceleration responses from both analyses were compared. In addition, a parametric study on the frequency ratio between the first and the second modes of the example building was carried out to examine its effects on the resultant responses. The base overturning moment response design envelopes obtained from both analysis approaches were also evaluated. The detailed analysis procedures of both domains and their resulting comparisons are presented in this paper.

INTRODUCTION

The high-frequency base balance (HFBB) testing technique was developed in the early 1980s (Davenport and Tschanz, 1981). It is an efficient and effective alternative approach to aeroelastic testing for the prediction of wind-induced forces and moments for tall building design and it has become one of the most common wind tunnel testing techniques for tall buildings. The fundamental premise of the HFBB technique is that the modal forces exerted on a building by the wind can be estimated by measuring the overturning and torsional moments experienced by a lightweight and stiff model in which only a building's external geometry is modelled. Predictions of mean and dynamic loads and responses are determined analytically from the estimated modal forces. In contrast, building mass, stiffness and damping are all physically modelled in the aeroelastic technique, thereby allowing time varying forces, moments, displacements and/or accelerations to be measured directly. However, the time and cost involved in aeroelastic modelling techniques, particularly for complicated multi-degree of freedom models, has mainly limited the use of this technique to special structures.

Building responses can be obtained by analysing HFBB data in the time domain or frequency domain using random vibration theory or spectral analysis for stationary random loads. Probably owing to the limited storage capacity and computational power of computers in the 1980s, it has been common practice

in wind engineering to conduct the analysis in the frequency domain. There are a number of issues associated with the HFBB test and analysis technique, as discussed by Boggs and Peterka (1989) and Yip and Flay (1995), that need to be considered in its application to real tall buildings. These include: (a) the likely significance of aeroelastic effects, as they cannot be measured in a HFBB test; (b) the significance and effects of non-ideal and/or three-dimensional (3D) mode shapes; and (c) the selection of an appropriate method of estimating the effects of cross-correlation between the modal responses of a tested building.

For analyses conducted in the frequency domain, it is necessary to use an appropriate technique to combine the statistical values, such as standard deviation, of the responses of different modes to determine the total loads and responses affecting the building. For structures with well-separated natural frequencies and coincident centres of mass and stiffness, it is convenient to combine components using the square-root-of-sum-of-squares (SRSS) rule, developed by Rosenblueth (1951), in which it is assumed that the cross-correlation terms are negligible. .For structures with eccentricities between the centre of mass and centre of stiffness at each floor, 3D mode shapes are likely for at least the first few modes of vibration, meaning that intermodal coupling may be significant (Chen and Kareem, 2005a). This can be complicated further through the effect of building shape on the cross-correlation of wind loads and if the building has closely-spaced natural frequencies. In the latter case, more sophisticated frequency domain analyses may be required (Der Kiureghian, 1980; Yip and Flay, 1995; Chen and Kareem, 2005b; Huang et al., 2007).

Recent advancements in computer technology have allowed the more computationally demanding time domain analysis techniques to become a practical option, whereby the modal responses can be directly superimposed rather than neglecting or estimating cross-correlation terms, and hence more accurate results can be obtained (Flay and Li, 2007). In addition, Flay and Li (2007) illustrated the suitability of utilising time domain analysis for the assessment of accelerations for a building with 3D mode shapes and highlighted the potential for its use in assisting in damper design to ameliorate the magnitude of predicted accelerations. It is possible to investigate further the feasibility of various mitigation solutions, such as strengthening/ resizing the structural members and incorporating extra damping via vibration control devices, within a limited timeframe.

For vibration control analyses in the frequency domain, the effects of a control device would be routinely approximated by the modal damping values and subsequently incorporated into the HFBB analysis. On one hand, the approximation of modal damping values in a frequency domain analysis does not precisely reveal the performance of the control device and it is generally applicable only to passive-type dampers. On the other hand, it is difficult to characterise the effects of some damping devices through only a modal damping ratio because their damping forces may be coupled with the inter-storey displacement and velocity where they are installed. Therefore, it is highly desirable for vibration control analyses to be performed in the time domain using the wind force information obtained from an aerodynamic model test, such as HFBB or SMPSS.

The primary objective of this study is to investigate the feasibility of time domain analysis for aerodynamic model studies and to examine its potential advantages. The time domain and frequency domain dynamic analysis procedures considered in this study are outlined in the following sections. An example building was wind tunnel tested and employed to demonstrate the differences between the analysis methods in the two domains.

FORMULATION OF ANALYSIS TECHNIQUES

Equations of motion

Rigid floor diaphragms are commonly adopted in the finite element modelling of the majority of building structures, except those with significant openings on the floor system and braced frame structures. The concept of rigid floor diaphragms was introduced nearly 40 years ago as a means of increasing the efficacy in the solution process associated with the structural dynamics (Clough, 1963). The motions of each floor plate are confined to two translations in plan and one rotation about a vertical axis as a rigid body, under the assumption that no in-plane deformations occur in the floor plate. A general matrix formulation of the

equation of motion for such a tall structure with rigid floor systems subject to random wind loads can be expressed as:

$$\mathbf{M}\ddot{\mathbf{x}} + \mathbf{C}\dot{\mathbf{x}} + \mathbf{K}\mathbf{x} = \mathbf{W} \tag{1}$$

where **M**, **C**, and **K** are the structural mass matrix in kg or kg·m^2, proportional damping matrix in N·s/m or N·s·m/rad, and stiffness matrix in N/m or N·m/rad respectively; $\mathbf{x} = [x_1, x_2,\ldots, x_{n-1}, x_n, y_1, y_2,\ldots, y_{n-1}, y_n, \theta_1,\theta_2,\ldots, \theta_{n-1}, \theta_n]'$ is the displacement vector in metres or radians, where x_i, and y_i, are the ith storey translational displacements along the x-, and y-axes, respectively, θ_i are the rotations about the vertical axis at the ith storey mass centre; and **W** is the wind excitation time history vector in N or N·m.

Method of classical modal analysis

In general, the simultaneous solution of the coupled equations of motion is not practical for systems with many degrees of freedom, for example typical building structures, that are subjected to random wind loads. It is advantageous to transform these equations to modal coordinates by way of classical modal analysis, leading to a set of uncoupled modal equations. Each modal equation is independently solved to determine the modal contributions to the physical response, and these modal responses are combined with the mode shapes to obtain the total response.

In accordance with classical modal analysis, the dynamic displacement response, $\mathbf{x}(t)$, can be expanded in terms of modal contributions as follows:

$$\mathbf{x}(t) = \sum_j \phi_j(z_i)\xi_j(t) \tag{2}$$

in which $\phi_j(z_i) = [\phi_{jx}(z_1), \phi_{jx}(z_2),\ldots, \phi_{jx}(z_n), \phi_{jy}(z_1), \phi_{yx}(z_2),\ldots, \phi_{jy}(z_n), \phi_{j\theta}(z_1), \phi_{j\theta}(z_2),\ldots, \phi_{j\theta}(z_n)]'$ is the jth mode shape vector in metres or radians, where $\phi_{jx}(z_i)$, $\phi_{jy}(z_i)$, $\phi_{j\theta}(z_i)$ are the mode shape values for the ith storey at a height of z_i, along the x- and y-axes and about the mass centre, respectively; $\xi_j(t)$ is the dimensionless generalised coordinate for the jth mode.

Substituting Eqn 2 in Eqn 1 and pre-multiplying each term in the ensuing equation by the transpose of the corresponding mode shape $\phi_j^T(z_i)$ gives:

$$m_j\ddot{\xi}_j(t) + c_j\dot{\xi}_j(t) + k_j\xi_j(t) = w_j(t) \tag{3}$$

where: generalised mass, $m_j = \sum_i \left[m(z_i)\phi_{jx}^2(z_i) + m(z_i)\phi_{jy}^2(z_i) + I(z_i)\phi_{j\theta}^2(z_i)\right]$;

generalised damping, $c_j = 2m_j\omega_j\zeta_j$;

generalised stiffness, $k_j = \omega_j^2 m_j$; and

generalised force, $w_j = \sum_i \left[w_x(z_i,t)\phi_{jx}(z_i) + w_y(z_i,t)\phi_{jy}(z_i) + w_\theta(z_i,t)\phi_{j\theta}(z_i)\right]$

and where $m(z_i)$, and $I(z_i)$ denote the mass and mass moment of inertia respectively for the ith storey at a height of z_i; ω_j, and ζ_j are the natural frequency and damping ratio respectively for the jth mode; $w_x(z_i,t)$, $w_y(z_i,t)$, and $w_\theta(z_i,t)$ are the wind force components impacting on the ith storey at a height of z_i along x-, y-axes and about the mass centre, respectively. The generalised mass and stiffness can be easily determined from the storey masses and mass moments of inertia, natural frequencies, and mode shapes output from FEM software, such as ETABS and SAP2000. The generalised damping is computed in conjunction with the estimated modal damping ratio.

Time domain dynamic analysis

For the current study, the time domain dynamic analysis procedures use a state-space technique in which the modal system is first of all solved to determine the generalised coordinate time histories (i.e. $\xi_j(t), \dot{\xi}_j(t)$,

and $\xi_j(t)$). The physical responses (i.e. $\ddot{\mathbf{x}}(t)$, $\dot{\mathbf{x}}(t)$, and $\mathbf{x}(t)$) can be computed subsequently in a mode-by-mode manner by multiplying the generalised coordinates with the corresponding mode shape, as denoted in Eqn 2. The state-space form of Eqn 3 is:

$$\dot{\mathbf{Z}} = \mathbf{A}\mathbf{Z} + \mathbf{B}w_j(t) \tag{4}$$

where: state vector, $\mathbf{Z} = \begin{Bmatrix} \xi_j(t) \\ \dot{\xi}_j(t) \end{Bmatrix}$;

system matrix, $\mathbf{A} = \begin{bmatrix} 0 & 1 \\ -k_j/m_j & -c_j/m_j \end{bmatrix}$; and

location vector, $\mathbf{B} = \begin{Bmatrix} 0 \\ 1/m_j \end{Bmatrix}$

The output modal response is governed by a so-called *observer*, **Y**, defined in Eqn 5, by regulating the output matrix, **E**, and feedforward matrix, **D**, as summarised in Table 1.

$$\mathbf{Y} = \mathbf{E}\mathbf{Z} + \mathbf{D}w_j(t) \tag{5}$$

Table 1. Summary of output and feedforward matrices for *observer*

	Modal Response	**E**	**D**
i	$\xi_j(t)$	[1 0]	0
ii	$\dot{\xi}_j(t)$	[0 1]	0
iii	$\ddot{\xi}_j(t)$	$\begin{bmatrix} -k_j/m_j & -c_j/m_j \end{bmatrix}$	$1/m_j$

By adopting the equivalent static force concept of earthquake engineering (Chopra, 1995), the internal forces associated with the displacement along the x-axis for the jth mode, $x_j(t)$, are formulated in Eqn 6. These equivalent static forces $Fx_j(z_i,t)$, by definition, will cause displacements $x_j(t)$ when imposed externally. The associated base overturning moment responses, $Myy_j(t)$, about the y-axis are obtained by summing the moments induced by these force distributions along the building height. The base overturning moment responses about the x-axis, $Mxx_j(t)$, and the base torsional moment responses about a vertical axis, $Mzz_j(t)$, are determined in a similar manner, as expressed in Eqn 7.

$$Fx_j(z_i,t) = \omega_j^2 \xi_j(t) m(z_i) \phi_{jx}(z_i) \tag{6}$$

$$\begin{Bmatrix} Mxx_j(t) \\ Myy_j(t) \\ Mzz_j(t) \end{Bmatrix} = \omega_j^2 \xi_j(t) \begin{Bmatrix} \sum_i m(z_i)\phi_{jy}(z_i) \cdot z_i \\ \sum_i m(z_i)\phi_{jx}(z_i) \cdot z_i \\ \sum_i I(z_i)\phi_{j\theta}(z_i)/r(z_i) \end{Bmatrix} \tag{7}$$

The total base overturning moment response about the x-axis, namely the x-moment response $Mxx(t)$, is the direct superposition of the base overturning moment for each mode in the time domain and is defined in Eqn 8:

$$Mxx(t) = \sum_j Mxx_j(t) \tag{8}$$

It is convenient to decompose the total x-moment response into mean, background fluctuating, and resonant components. The background fluctuating component, $Mxx_{bg}(t)$, can be considered as the moment response due solely to the aerodynamic wind force that is independent of dynamic effects related to the building structure, and which may be computed from Eqn 9. The resonant component, $Mxx_{j,res}(t)$, attributable primarily to the dynamic characteristics of the building, may be determined by directly subtracting the background component from the total fluctuating moment response, given in Eqn 10.

$$Mxx_{j,bg}(t) = \frac{w_j(t)}{m_j}\sum_i m(z_i)\phi_{jy}(z_i)\cdot z_i \tag{9}$$

$$Mxx_{j,res}(t) = Mxx_j(t) - Mxx_{j,bg}(t) \tag{10}$$

The calculation procedures for the total, background fluctuating and resonant component of the y-moment and z-moment responses are similar to those described in Eqns 8 – 10, although the background fluctuating component of the z-moment is of a slightly different format to Eqn 9.

The standard deviations of the three components of moment response are computed statistically, as given in Eqn 11, where the superscript *t* denotes time domain calculations.

$$\sigma_M^t = \sqrt{\lim_{T\to\infty}\frac{1}{T}\int_0^T [M(t)-\overline{M}]^2\,dt} \tag{11}$$

where mean moment, $\overline{M} = \lim_{T\to\infty}\frac{1}{T}\int_0^T M(t)dt$

In modern, slender tall buildings serviceability limit state design to control accelerations at the highest habitable floor is often the governing factor for their design. The second derivative of the generalised coordinates can be obtained by solving the generalised equation of motion in state-space form, Eqns 4 – 5, by using the appropriate output matrix, **E**, and feedforward matrix, **D,** as listed in the last row of Table 1. The building tip dynamic acceleration responses of jth mode are computed from:

$$\begin{Bmatrix}\ddot{x}_j(t)\\ \ddot{y}_j(t)\\ \ddot{\theta}_j(t)\end{Bmatrix} = \ddot{\xi}_j(t)\begin{Bmatrix}\phi_{jx}(h)\\ \phi_{jy}(h)\\ \phi_{j\theta}(h)\end{Bmatrix} \tag{12}$$

where h is the height of the highest habitable floor. The maximum building tip resultant acceleration response of the jth mode at a distance of *r* from the mass centre is given by Eqn 13 and is schematically illustrated in Figure 1.

$$a_j(t) = \sqrt{\ddot{x}_j^2 + \ddot{y}_j^2} + r(h)\ddot{\theta}_j \tag{13}$$

The resultant acceleration response is the combined effect of the translational accelerations (i.e. $\ddot{x}$ and $\ddot{y}$) and the angular acceleration (i.e. $\ddot{\theta}$). The first term on the right hand side of Eqn 13, which is the resultant of the two translational accelerations (i.e. $\sqrt{\ddot{x}_j^2 + \ddot{y}_j^2}$), is a constant throughout the whole plane. The second term, which is the equivalent translational acceleration induced by the angular acceleration, varies for different locations, depending on the distance from the mass centre. At a distance of *r* from the mass centre, indicated by the dashed circle in Figure 1, the angular acceleration induces a translational/tangential acceleration with a magnitude equal to $r\ddot{\theta}$ and for which the direction depends on the selected location on the circle. The maximum resultant acceleration response will occur when the vector sum of and is at its maximum value, and hence it will occur when the tangential acceleration is parallel to $\sqrt{\ddot{x}_j^2 + \ddot{y}_j^2}$.

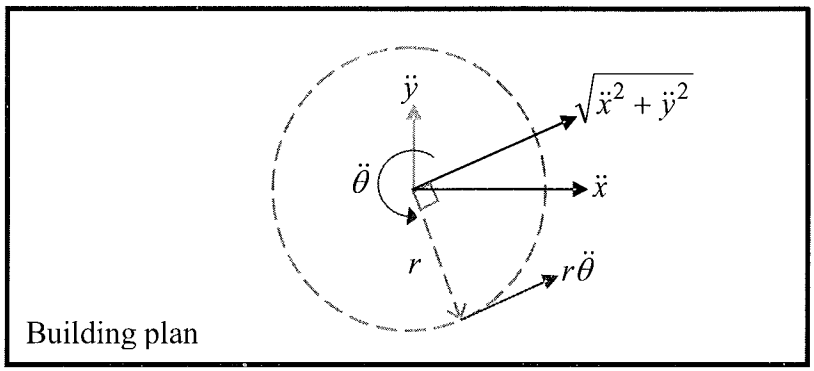

Figure 1. Schematics of acceleration components at the building top

Frequency domain dynamic analysis

For wind engineering, it has been found convenient to express and analyse the effects of wind on a given tall building in the frequency domain, assuming that the wind loads are stationary and normally distributed. The power spectral density (PSD) of the generalised coordinate for the jth mode is determined according to Eqn 14.

$$S_{\xi_j}(\omega) = \frac{1}{k_j^2}\left|H_j(\omega)\right|^2 S_{w_j}(\omega) \tag{14}$$

where: mechanical admittance function, $\left|H_j(\omega)\right|^2 = \dfrac{1}{\left[1-\left(\dfrac{\omega}{\omega_j}\right)^2\right]^2 + \left(\dfrac{2\omega\zeta_j}{\omega_j}\right)^2}$

PSD of generalised wind load, $S_{w_j}(\omega) = \dfrac{1}{2\pi}\int_{-\infty}^{\infty} R_{w_j}(\tau)e^{-i\omega\tau}d\tau$

autocorrelation of generalised wind forces, $R_{w_j}(\tau) = \lim_{T\to\infty}\dfrac{1}{T}\int_0^T w_j(t)w_j(t+\tau)dt$

Unlike the time domain calculations, where the standard deviation is computed statistically from the time history data, the standard deviation of the modal response for the jth mode is determined by integrating its PSD as follows:

$$\sigma_{\xi_j} = \left[\int_0^{\infty} S_{\xi_j}(\omega)d\omega\right]^{1/2} \tag{15}$$

The resonant component of the modal response may then be estimated by subtracting the background fluctuating component from the total dynamic modal response:

$$\sigma_{\xi_j,res} = \sqrt{\sigma_{\xi_j}{}^2 - \sigma_{\xi_j,bg}{}^2} \tag{16}$$

where: standard deviation of background component, $\sigma_{\xi_j,bg} = \dfrac{1}{k_j}\left[\int_0^{\infty} S_{w_j}(\omega)d\omega\right]^{1/2}$.

The mean and background fluctuating components of the moment responses are determined statistically from the mean and standard deviation of the moments measured directly by the base balance and subsequently

adjusted to prototype scale. The resonant components of the jth mode are related to the building storey mass and mode shape of the corresponding mode, expressed as Eqn 17, and may be combined with the background component using the square-root-of-sum-of-squares (SRSS) modal combination method, as demonstrated in Eqn 18, to determine the standard deviations of the total moment responses.

$$\begin{Bmatrix} \sigma^f_{Mxx_j,res} \\ \sigma^f_{Myy_j,res} \\ \sigma^f_{Mzz_j,res} \end{Bmatrix} = \omega_j^2 \sigma_{\xi_j,res} \begin{Bmatrix} \sum_i m(z_i)\phi_{jy}(z_i)\cdot z_i \\ \sum_i m(z_i)\phi_{jx}(z_i)\cdot z_i \\ \sum_i I(z_i)\phi_{j\theta}(z_i)/r(z_i) \end{Bmatrix} \tag{17}$$

$$\sigma^f_M = \sqrt{{\sigma^f_{M_{bg}}}^2 + \sum_j {\sigma^f_{M_{j,res}}}^2} \tag{18}$$

where the superscript *f* denotes the calculation in the frequency domain.

The SRSS modal combination method, in which the cross-correlation terms are neglected, provides satisfactory response estimates only for structures with well-separated natural frequencies, for example $1/1.2 \le \omega_i/\omega_{i+1} \le 1.2$ (Chopra, 1995). For structures with closely-spaced natural frequencies, the SRSS method may overestimate or underestimate the resultant responses as the cross-correlation terms may be positive or negative and should not be ignored. To overcome the limitations of the SRSS method, Der Kiureghian (1980) developed the complete quadratic combination (CQC) method for the modal combination, in which the cross-correlation terms are weighted by a pre-defined correlation coefficient under the assumption of white noise excitation. According to the CQC formulation, the total moment responses can be determined as follows:

$$\sigma^f_M = \sqrt{{\sigma^f_{M_{bg}}}^2 + \sum_j {\sigma^f_{M_{j,res}}}^2 + \sum_{j\neq k}\sum_k \rho_{jk}\sigma^f_{M_{jk,res}}\sigma^f_{M_{kj,res}}} \tag{19}$$

where $$\rho_{jk} = \frac{8\sqrt{\zeta_j\zeta_k\omega_j\omega_k}(\zeta_j\omega_j + \zeta_k\omega_k)\omega_j\omega_k}{(\omega_j^2-\omega_k^2)^2 + 4\zeta_j\zeta_k\omega_j\omega_k(\omega_j^2+\omega_k^2) + 4\omega_j^2\omega_k^2(\zeta_j^2+\zeta_k^2)}$$

Chen and Kareem (2005b) have further improved the CQC method for application to wind engineering by taking into account the correlations of the associated generalised forces, instead of assuming white noise excitation. Huang et al. (2007) have also derived a more precise formula in terms of spectral moments to evaluate the intermodal correlation coefficient. Analysis results using these formulations for the modal combination in the frequency domain were compared with those determined from the direct superposition in the time domain and are presented in the next section.

The standard deviation of the building tip resultant acceleration of the jth mode can be computed using Eqn 20.

$$\sigma^f_{a_j} = \sqrt{{\sigma^f_{\ddot{x}_j}}^2 + {\sigma^f_{\ddot{y}_j}}^2} + r(z_i)\sigma^f_{\ddot{\theta}_j} \tag{20}$$

where $$\begin{Bmatrix} \sigma_{\ddot{x}_j} \\ \sigma_{\ddot{y}_j} \\ \sigma_{\ddot{\theta}_j} \end{Bmatrix} = \omega_j^2\sigma_{\xi_j}\begin{Bmatrix} \phi_{jx}(h) \\ \phi_{jy}(h) \\ \phi_{j\theta}(h) \end{Bmatrix} = \sigma_{\ddot{\xi}_j}\begin{Bmatrix} \phi_{jx}(h) \\ \phi_{jy}(h) \\ \phi_{j\theta}(h) \end{Bmatrix}$$

EXPERIMENTAL SETUP

Example Building

The building model considered in this study is a modification of the second generation wind-excited benchmark building (Tse *et al.*, 2007). The shape and dimensions of the building were retained in this study, whereas the natural frequencies of the first two modes were deliberately set to be closely-spaced (i.e. $\omega_2/\omega_1 \leq 1.2$) and the mode shapes of the first three modes of vibration were lateral-torsional coupled within each mode. The building is a 60-storey, 240 metre tall reinforced concrete structure with a uniform rectangular floor plan of 72 m by 24 m throughout its height, as shown in Figure 2. The reinforced concrete building comprises two reinforced concrete cores, reinforced concrete frames, and two steel out-rigger trusses. Core setbacks at the two refuge floors induce a significant shift of mass, resulting in eccentricities between the level-by-level shear centre and mass centre over the building height. The asymmetrical structural configuration and the associated eccentricities cause the building to experience 3D modes of vibration.

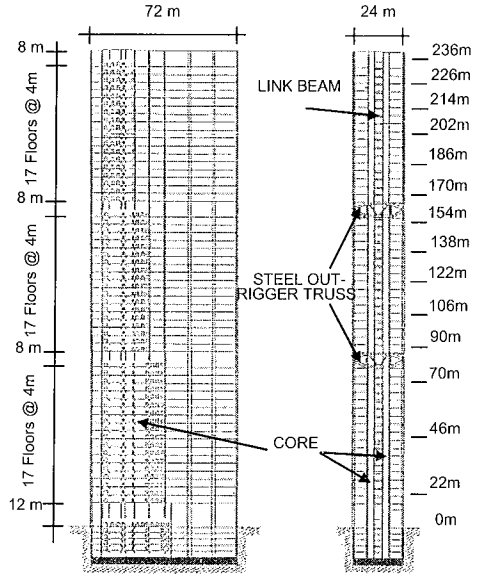

Figure 2. The shape and dimensions of the second generation wind-excited benchmark building.

The mode shapes corresponding to the first three modes of vibration, associated with the storey mass centres over the building height, are displayed in Figure 3. The first two modes have dominant sway components along the y- and x-axes, respectively. The third mode is a predominantly torsional mode of vibration with modest translational components. It should be noted that the torsional mode shapes (θ) were multiplied by the overall radius of gyration (i.e. ~20.4 m) of the building to maintain dimensional consistency among the three (x, y, z) components for the sake of presentation. To illustrate the accuracy of SRSS technique for the combination of modal responses, the corresponding natural frequencies were deliberately set at 0.230, 0.240 and 0.415 Hz, respectively.

Wind Force Measurements

A 1:400 scal\e rigid model of the benchmark building, as shown in Figure 4, was constructed from acrylic and tested at the CLP Power Wind/Wave Tunnel Facility (WWTF) at The Hong Kong University of Science and Technology (HKUST) to measure simultaneously the wind-induced pressures acting over the surfaces of the building model. The model was installed with 14 layers of pressure-taps over its height, with 32 pressure-taps in each layer. The elevations of the 14 layers are presented in Figure 2. The surface pressures measured from the test were converted into 14 layers of alongwind, crosswind, and torsional wind load

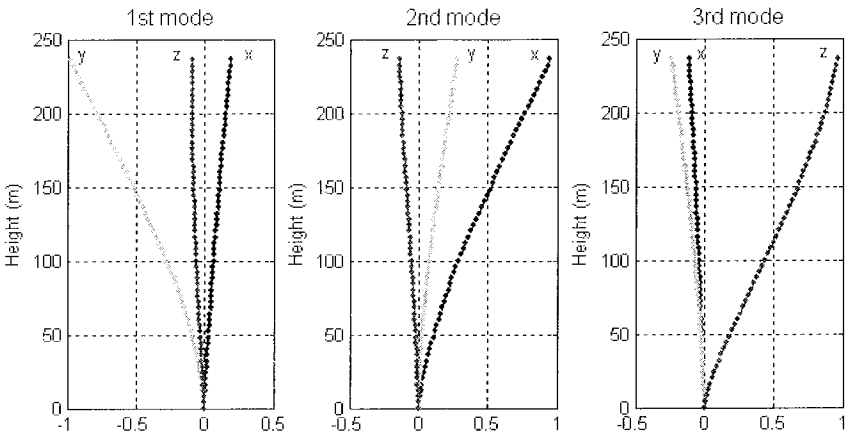

Figure 3. Mode shapes of the modified benchmark building.

distributions, from which the overall base overturning and torsional moments acting on the model were subsequently synthesised.

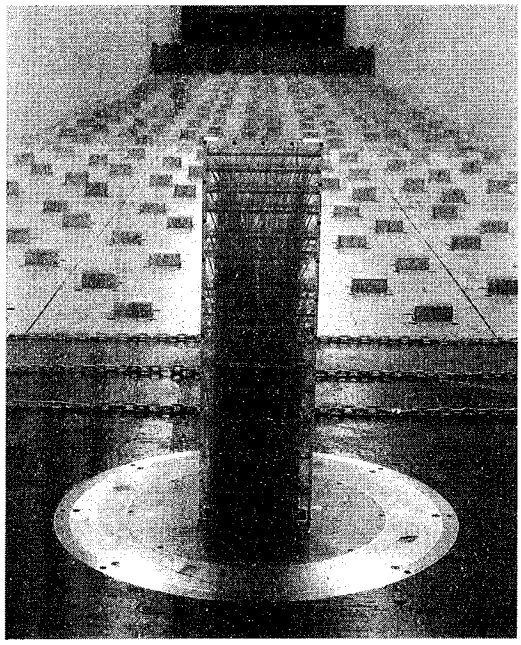

Figure 4. Pressure-tapped benchmark building model inside wind tunnel.

The pressure model was tested in a modelled boundary layer wind flow corresponding to open country terrain (i.e. Category 3 in Australian/New Zealand Standard 2002 AS/NZS 1170.2:2002). The test mean wind speed was approximately 13 m/s at the model height in order to satisfy the minimum Reynolds number requirement of 5×10^4 for a building model with sharp edges, as recommended by AWES-QAM-1-2001 (Australasian Wind Engineering Society 2001). Surface pressures were measured at a sampling frequency of 400 Hz, which was sufficient to measure pressure fluctuations with frequencies of up to around 2 Hz at prototype scale and which is four times higher than the natural frequencies of the first 3 modes of vibration. The pressure data were recorded for 36 seconds, which is equivalent to approximately 1 hour at prototype scale. Measurements were taken for five different incident wind angles at 22.5° increments from 0° to 90°, where 0° corresponds to wind normal to the wide face of the building.

Instantaneous pressure coefficients, normalised with respect to the mean wind speed at building height, were measured at each pressure-tap location and subsequently analysed to determine the 14 layers of prototype scale external wind force time histories:

$$W_q(t) = \frac{1}{2}\rho \overline{U}^2 \sum_s C_{pqs}(t)\Delta A_{qs} \tag{21}$$

where ρ is the density of air in kg/m^3; $\overline{U}$ is the prototype scale mean wind speed at building height in m/s; $C_{pqs}(t)$ is the pressure coefficient time history measured in the wind tunnel at pressure-tap s in layer q; and ΔA_{qs} is the corresponding tributary area in m^2. 5 year and 50 year return period mean wind speeds of 29.8 m/s and 51.1 m/s were used in the serviceability limit state design (i.e. acceleration) and ultimate limit state design (i.e. base overturning moment responses), respectively, for the building located in a coastal cyclone region, in accordance with AS/NZS 1170.2:2002.

Base overturning and torsional moments equivalent to the measurements of a HFBB test were numerically synthesised using the 14 layers of surface pressure time series. The base overturning moments, Mxx and Myy, were calculated by multiplying storey forces by the appropriate layer height while the base torsional moment, Mzz, was calculated by summing the storey torsional moment about the geometrical centre of the building. The normalised PSDs of the base overturning and torsional moments were used in the subsequent frequency domain analysis. The time series and the normalised PSDs are presented in Figures 5 and 6, respectively.

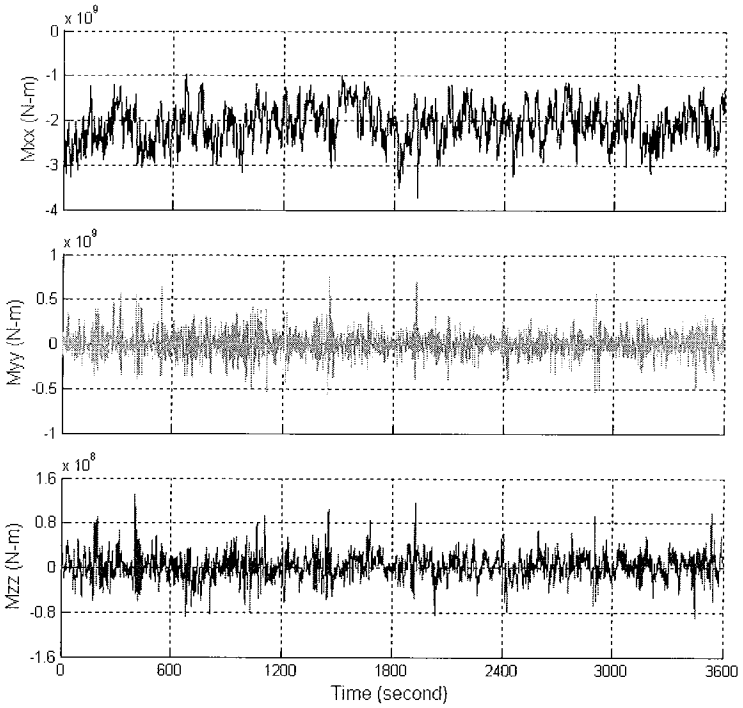

Figure 5. The synthesised base overturning and torsional moment time series.

A COMPARISON OF TIME DOMAIN AND FREQUENCY DOMAIN ANALYSES

Standard Deviations of resultant responses

The time series and normalised PSDs of the base overturning and torsional moments were used in the subsequent time domain and frequency domain dynamic analyses to determine the base overturning moment responses and the accelerations at the highest habitable floor. For both time and frequency domain analyses, the coupled equations of motion for the building model were at the outset transformed into a set of uncoupled

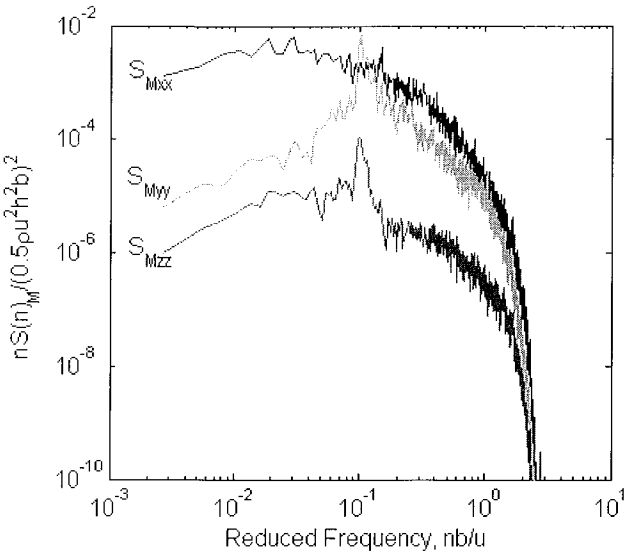

Figure 6. The normalised PSDs of the synthesised base overturning and torsional moments.

modal equations in terms of generalised coordinates by means of classical modal analysis. For the time domain analysis, the modal equations were sequentially solved using the state-space technique described previously, and the x-moment, y-moment, and z-moment responses for the jth mode were subsequently determined from the equivalent static forces associated with the displacements of the jth mode. The PSDs of the moment responses were then computed from the moment time histories by conducting a spectral analysis.

For the frequency domain analysis, the PSDs of the generalised wind loads were integrated with the mechanical admittance function to determine the PSDs of the generalised coordinates. The PSDs of the moment responses were computed by multiplying the PSDs of the generalised coordinates with the appropriate modal quantities. The PSDs of the moment responses determined from both analyses were compared, as shown in Figure 7. The results show a close agreement between both time and frequency domain techniques for the determination of the modal moment responses.

The resultant moment responses were computed by direct superposition of the modal moment responses in the time domain and the SRSS and CQC modal combination techniques in the frequency domain, respectively. In the time domain analysis, the standard deviations of the total, background fluctuating component and resonant component of the moment responses were computed statistically from the time series; whereas they were determined in the frequency domain by integrating the PSDs of the corresponding moment responses. The standard deviations of the resultant moment responses together with those of the background fluctuating components and resonant components of each mode are listed in Table 2. The differences between the standard deviations of the background fluctuating components are zero because they were computed statistically from the time series for both analysis techniques.

Table 2. Standard deviation and percentage difference of component moment responses

	Standard Deviation of Base Moment Responses [MNm]								
	Frequency Domain			Time Domain			Percentage difference [%]		
	M_{xx}	M_{yy}	M_{zz}	M_{xx}	M_{yy}	M_{zz}	M_{xx}	M_{yy}	M_{zz}
Background	416	133	22.6	416	133	22.6	0.00	0.00	0.00
Mode 1	796	159	14.2	792	158	14.2	0.48	0.49	0.48
Mode 2	119	415	8.17	118	412	8.10	0.81	0.81	0.81
Mode 3	49.1	24.5	31.3	48.8	24.4	31.1	0.55	0.55	0.55
Resultant	907	465	41.9	957	441	40.4	-5.51	5.00	3.70

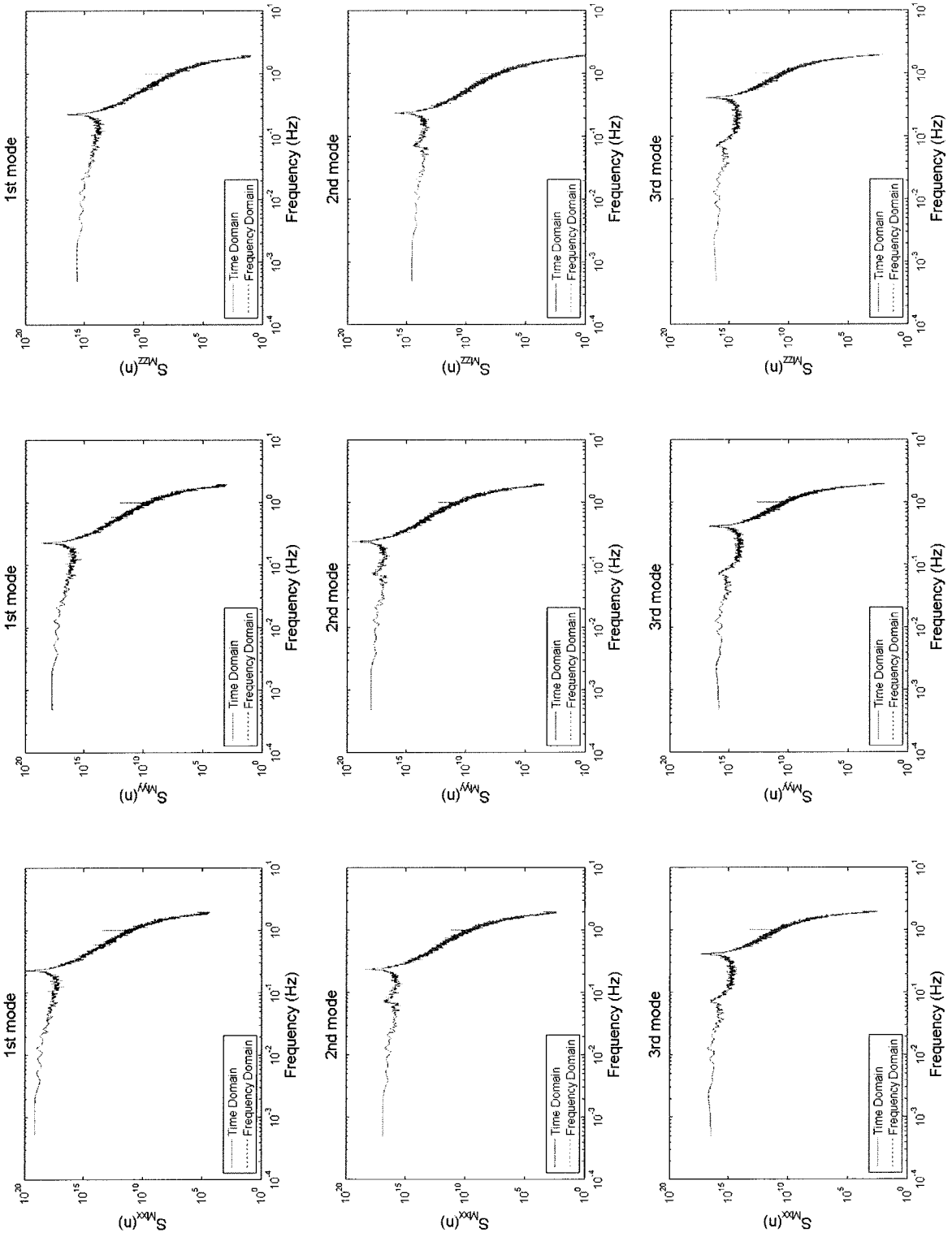

Figure 7. The power spectral densities of base overturning moment responses

The very low percentage differences between the resonant components, less than 1%, indicate that the frequency domain analysis technique is reasonably accurate for determining the responses of each mode for the modelled building considered in this study. However, more notable discrepancies were found between the two approaches for the standard deviations of the resultant moment responses, attributable to the various modal combination methods used (i.e. superposition for time domain and SRSS technique for frequency domain). It was found that the resultant responses from the frequency domain analysis were sometimes larger (i.e. for Myy and Mzz) and sometimes smaller (i.e. for Mxx) than those determined from time domain analyses, which is attributed to the cross-correlation terms, which can be positive or negative, being neglected when the SRSS technique is used. To investigate the significance of neglecting the cross-correlation terms, the resultant moment responses were also determined using various CQC modal combination techniques in which the cross-correlation terms were considered. The results together with the percentage difference with respect to the resultant moment responses obtained in the time domain are tabulated in Table 3.

Table 3. Standard deviation and percentage difference of resultant moment responses

	Standard deviation of Base Moment Resultant Responses					
	M_{xx} [MNm]	Difference [%]	M_{yy} [MNm]	Difference [%]	M_{zz} [MNm]	Difference [%]
Time Domain	957	-	441	-	40.4	-
SRSS	907	5.51	465	-5.00	41.9	-3.70
CQC (Der Kiureghian)	915	4.37	462	-4.58	41.7	-3.28
CQC (Chen and Kareem)	928	3.04	456	-3.29	41.2	-2.09
CQC (Huang et al.)	925	3.34	450	-2.02	41.2	-1.92

Among these methods, the resultant moment responses obtained from the SRSS rule deviate most from those obtained from the time domain analysis, attributable to the neglecting of cross-correlation terms. The CQC method developed by Der Kiureghian (1980) has improved the estimation of the resultant moment responses as the cross-correlation terms were considered in the calculations. The resultant moment responses were further improved by the CQC methods suggested by Chen and Kareem (2005b) and Huang et al. (2007) and evidently converge towards the value determined from the time domain analysis technique. Therefore, by nature, the time domain analysis gives a more accurate prediction of the resultant moments through the direct superposition of different modes, avoiding the need to assume or estimate their correlations.

The standard deviations and percentage differences of building tip resultant accelerations are shown in Table 4. For the time domain analysis, the building tip translational and torsional acceleration response time histories (i.e. $\ddot{x}_j$, $\ddot{y}_j$, and $\ddot{\theta}_j$) about the centre of mass were determined first. The resultant acceleration responses at a location corresponding to one radius of gyration from the centre of mass were then computed using Eqn 13, and the standard deviations were determined statistically and listed in Table 4. In contrast, for the frequency domain analysis, the standard deviations of building tip accelerations at the centre of mass were determined by integrating their PSDs, which were then combined according to Eqn 20 to compute the standard deviations of acceleration responses at a location corresponding to one radius of gyration from the mass centre. The positive percentage differences shown in Table 4 indicate that the results obtained from the frequency domain analysis are higher than those from the time domain analysis, again due to the differences in the modal combination techniques.

Effect of frequency ratio

As indicated in Tables 2 and 3, the percentage differences between the frequency and time domain analyses of the resultant moment responses were attributed to the different modal combination techniques. The accuracy of the SRSS modal combination method, used in the frequency domain analysis, depends on the frequency ratio (i.e. ω_2/ω_1) of two consecutive modes. It has been shown that the cross-correlation

Table 4. Standard deviation and percentage difference of building tip accelerations

	Standard Deviation of Building Tip Acceleration [milli-g]		
	Frequency Domain	Time Domain	Percentage difference [%]
Mode 1	17.45	16.86	3.39
Mode 2	9.49	9.11	3.95
Mode 3	5.09	4.78	6.11

coefficient among the modal responses diminishes rapidly as the separation between corresponding natural frequencies increases (Rosenblueth, 1951). For a system with a 2% damping ratio, the cross-correlation coefficient is significantly smaller when $\omega_2/\omega_1 \geq 1.2$.

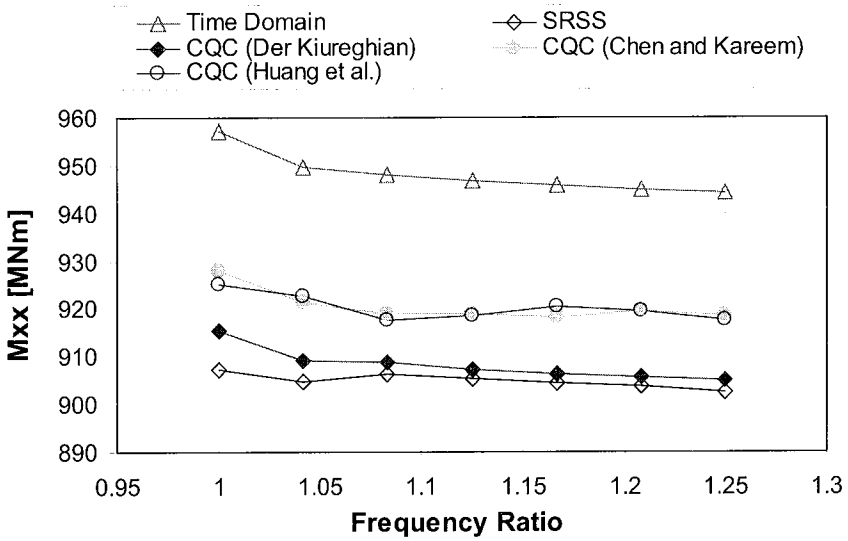

Figure 8. Percentage differences of base overturning moments for various frequency ratios

In this study, the natural frequency of the second mode of vibration was artificially and sequentially increased from 0.24 to 0.30 (i.e. up to a frequency ratio of 1.25) to investigate the influence of the frequency ratio ω_2/ω_1 on the accuracy of the combined building responses. The resultant moment responses obtained from direct superposition in the time domain, SRSS and CQC modal combination techniques in the frequency domain were plotted against the frequency ratio ranging from 1 to 1.25, as displayed in Figure 8. It is observed that the resultant moment responses gradually decrease as the frequency ratio increases regardless the modal combination methods used. And the percentage differences stabilise for all modal combination methods as the frequency ratio approaches 1.2 or higher. These results are consistent with the conclusions reached by Rosenblueth (1951).

Base Overturning Moment Design Envelope

For design purposes, the base overturning moment responses of a building structure obtained from an analysis of aerodynamic wind tunnel test results may be interpreted as a moment response design envelope as illustrated in Figure 9. In the frequency domain analysis, because of the absence of the cross-correlation information among moment responses *Mxx* and *Myy*, the moment design envelope is normally assumed to be an ellipse centred at $(\overline{Mxx}, \overline{Myy})$ with a major axis of magnitude $g_f \cdot \sigma^f_{Mxx}$ and a minor axis of magnitude $g_f \cdot \sigma^f_{Myy}$, where g_f is a peak factor defined in Eqn 22.

$$g_f = \sqrt{2\ln(3600 \times 2\pi\omega_j)} + \frac{0.57}{\sqrt{2\ln(3600 \times 2\pi\omega_j)}} \tag{22}$$

In the time domain analysis, the actual moment response design envelope can be directly constructed from the trace of $Mxx(t)$ and $Myy(t)$ moment response time histories, also displayed in Figure 9. The moment response design envelope obtained from the time domain analysis is concentric with that of the frequency domain analysis but it is skewed due to the cross-correlation. In addition, the magnitudes of the major and minor axes are noticeably smaller than those of frequency domain analysis, resulting in a smaller load envelope. Evidently, the moment response time history trace from the time domain analysis gives a more accurate representation of the moment response design envelope, which overcomes, in this instance, some conservatism in the estimated design loads which has potential implications for the design of structural members.

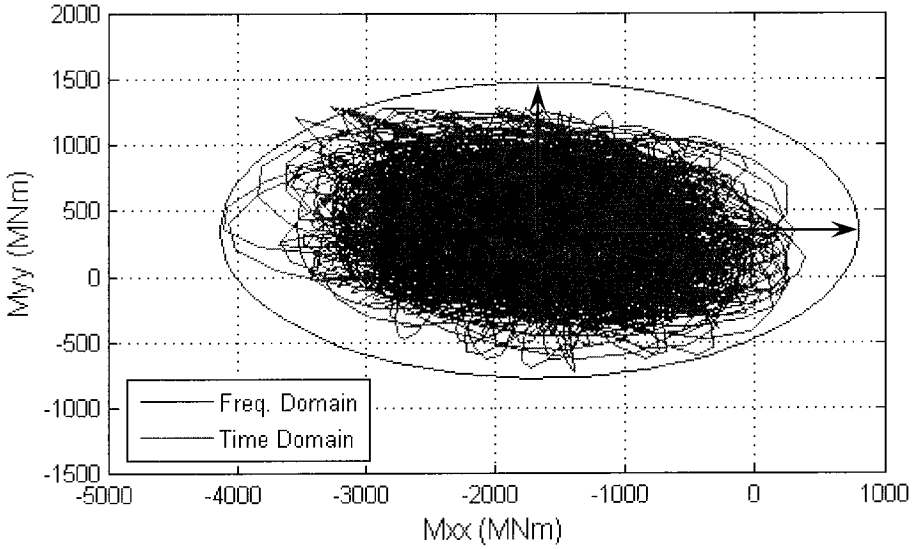

Figure 9. Base overturning moment design envelope

CONCLUSIONS

The high-frequency base balance time domain analysis was investigated in this paper. A series of wind tunnel tests were conducted to determine the wind loads experienced by the benchmark building, from which base overturning and torsional moments were synthesised. The base moment data were used in the subsequent time domain and frequency domain analyses to determine the base overturning and torsional moment responses and the building tip acceleration responses. Compared with the more accurate time domain analysis, which accounts for cross-correlation between the different modes, the frequency domain analysis technique was found to be accurate in determining the modal responses with percentage differences of less than 1%. However, the percentage differences for the resultant moment responses were noticeably higher, at around 5%, when the cross-correlation terms were ignored using the SRSS modal combination method. The percentage differences were further diminished by using various CQC modal combination methods, taking into account the cross-correlation terms.

The impact of the cross-correlation terms on the resultant moment responses was also analysed for frequency ratio between the first two translational modes ranging from 1 to 1.25 by artificially increasing the natural frequency of second mode. The percentage differences stabilised when the frequency ratio was greater than approximately 1.2. An evaluation of the base overturning moment response design envelopes demonstrated that the time domain analysis provides a more accurate moment response design envelope. The results of this study demonstrate that the high-frequency base balance time domain analysis is not only feasible, but its application for determining resultant responses is also advantageous.

ACKNOWLEDGEMENTS

This research project is funded by a Research Grants Council of Hong Kong Special Administrative Region, China (Project HKUST6301/04E). Thanks also go to the staff of the CLP Power Wind/Wave Tunnel Facility at HKUST for their assistance in this project.

REFERENCES

1. Australasian Wind Engineering Society, Wind Engineering Studies of Buildings, AWES–QAM–1–2001, 2001.
2. Boggs, D.W. and Peterka, J.A., Aerodynamic model tests of tall buildings, Journal of Engineering Mechanics, ASCE, 1989, Vol. 115, No. 3, pp 618-635.
3. Chen, X. and Kareem, A., Coupled dynamic analysis and equivalent static wind loads on buildings with three-dimensional modes, Journal of Structural Engineering, ASCE, 2005a, Vol. 131, No. 7, 1071-1082.
4. Chen, X. and Kareem, A., Dynamic wind effects on buildings with 3D coupled modes: application of high frequency force balance measurements, Journal of Structural Engineering, ASCE, 2005b, Vol. 131, No. 11, 1115-1125.
5. Chopra, A.K., Dynamics of structures – theory and applications to earthquake engineering, Prentice Hall International (UK) Limited, London, 1995, Chapter 6.
6. Clough, R. W., King, I. P. and Wilson, E. L., Structural Analysis of Multistory Buildings, Journal of the Structural Division, ASCE, 1963, Vol. 89, No. 8.
7. Davenport, A.G. and Tschanz, T., The response of tall buildings to wind, Proc. 4th U.S. Nat. Conf. of Wind Engineering, July 27-29, Seattle, Washington, U.S.A., 1981.
8. Der Kiureghian, A., Structural response to stationary excitation, Journal of Engineering Mechanics, ASCE, 1980, Vol. 106, No. 6, pp 1195-1213.
9. Flay, R.G.J. and Li, Y.F., On predicting accelerations in tall buildings from wind tunnel model tests using spectral and time history methods, Proc. 12th Int. Conf. on Wind Engineering, July 1-6, Cairns, Australia, Vol.1, pp 1215-1222.
10. Huang, M.F., Chan. C.M., Kwok., K.C.S. and Hitchcock, P.A., Dynamic analysis of wind-induced lateral-torsional response of tall buildings with coupled modes, Proc. 12th Int. Conf. on Wind Engineering, July 1-6, Cairns, Australia, Vol.1, pp 295-302.
11. Rosenblueth, E., A basis for aseismic design, PhD. Thesis, Uni. of Illinois, Urbana, I11., 1951.
12. Standards Australia, AS/NZS 1170.2:2002, Australian/New Zealand Standard, Structural design actions Part 2: Wind actions, 2002.
13. Tse, K.T., Kwok, K.C.S., Hitchcock, P.A., Samali, B. and Huang, M.F., Vibration control of a wind-excited benchmark tall building with complex lateral-torsional modes of vibration, Advances in Structural Engineering, 2007, Vol. 10, No. 3, pp 283-304.
14. Yip, D.Y.N. and Flay, R.G.J., A new force balance data analysis method for wind response predictions of tall buildings, Journal of Wind Engineering and Industrial Aerodynamics, 1995, 54/55, pp 457-471.

Journal of Wind & Engineering, Vol. 5, No. 2, July 2008, pp. 17-30

DESIGN WIND LOADS FOR ARCHED ROOFS

Michael Kasperski

Ruhr-University Bochum, Department of Civil Engineering, 44780 Bochum, Germany
michael.kasperski@rub.de

ABSTRACT

Arched roofs are used in modern architecture as an element of functional aesthetics to bridge large clear spans. In the design process, special care has to be taken since arched roof structures are sensitive to non-uniform load distributions as they may occur for wind loads. Most codes, however, present for arched roofs either mean pressure distributions or the envelope of local extreme pressures. To balance the shortcomings of this approach, some codes recommend neglecting all favourable load contributions. Based on wind tunnel experiments, the load model of the Eurocode, the new Australian/New Zealand Standard and the approach by Cook are discussed. The paper demonstrates that applying the specified pressure distribution considering the favourable load contributions may lead to considerable under-design. Following the very simple rule of neglecting all favourable loads will usually lead to a conservative but considerable uneconomic design. Examples for realistic load distributions are presented which have been identified applying the LRC-method.

INTRODUCTION

Arched roofs are used in modern architecture as an element of functional aesthetics to bridge large clear spans. They are typical of industrial buildings but are also associated with entertainment and exhibition halls. In the design process, special care has to be taken since arched roof structures are sensitive to non-uniform load distributions as they may occur for wind loads. Although the method of identifying the required effective wind load distributions has been developed almost 20 years ago, most wind load codes present for arched roofs either mean pressure distributions or the envelope of local extreme pressures. To balance the shortcomings of this approach, some codes recommend neglecting all favourable load contributions. Based on boundary layer wind tunnel experiments, the paper discusses on two example structures the different codal approaches. Especially, the paper deals with the recent version of the Eurocode, the new Australian/ New Zealand Standard and the approach by Cook. The comparison of the design values is presented and more realistic wind load distributions, which have been obtained with the LRC-method, are also discussed.

WIND TUNNEL EXPERIMENTS

Boundary layer flow

The wind tunnel experiments have been performed in a boundary layer flow corresponding to open country. The flow has a geometric scale λ_L of a 1:250 (λ - scale = ratio of wind tunnel parameter to full-scale parameter). In figure 1, the wind tunnel flow profiles of the normalized mean wind speed and the turbulence intensity are compared to the expected full-scale profiles. The latter values are based on ESDU [7] applying for the roughness length z_0 a range from 0.03 to 0.07 m. Altogether, the wind tunnel flow can be assumed to be a good representation of full-scale flow in open country.

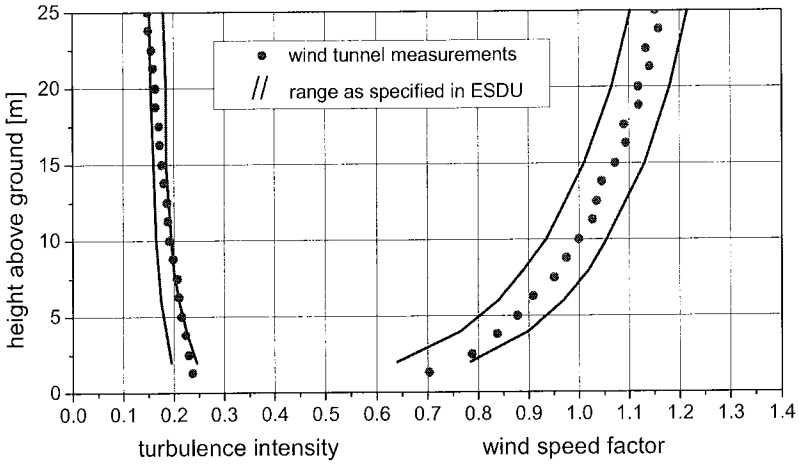

Figure 1: Wind tunnel profiles of the turbulence intensity and the wind speed factor for the mean wind speed compared to the target values for the full-scale flow

Model

Two building models have been tested in the wind tunnel. Both buildings have the length l = 37.5m, the span d = 25.0m and the same height of the eaves h = 5 m. The rise of the arch for the first building is f = 2.5 m, for the second building f = 5 m. The shape of the arched roof follows a parabola. Due to the low ratio of f/d, there is practically no difference to an equivalent segment of a circle. Along the centre bay, three pressure taps are provided on each wall and eleven pressure taps are positioned along the arch itself (Figure 2). The relative positions of the taps along the walls and the arch are summarized in Table 1.

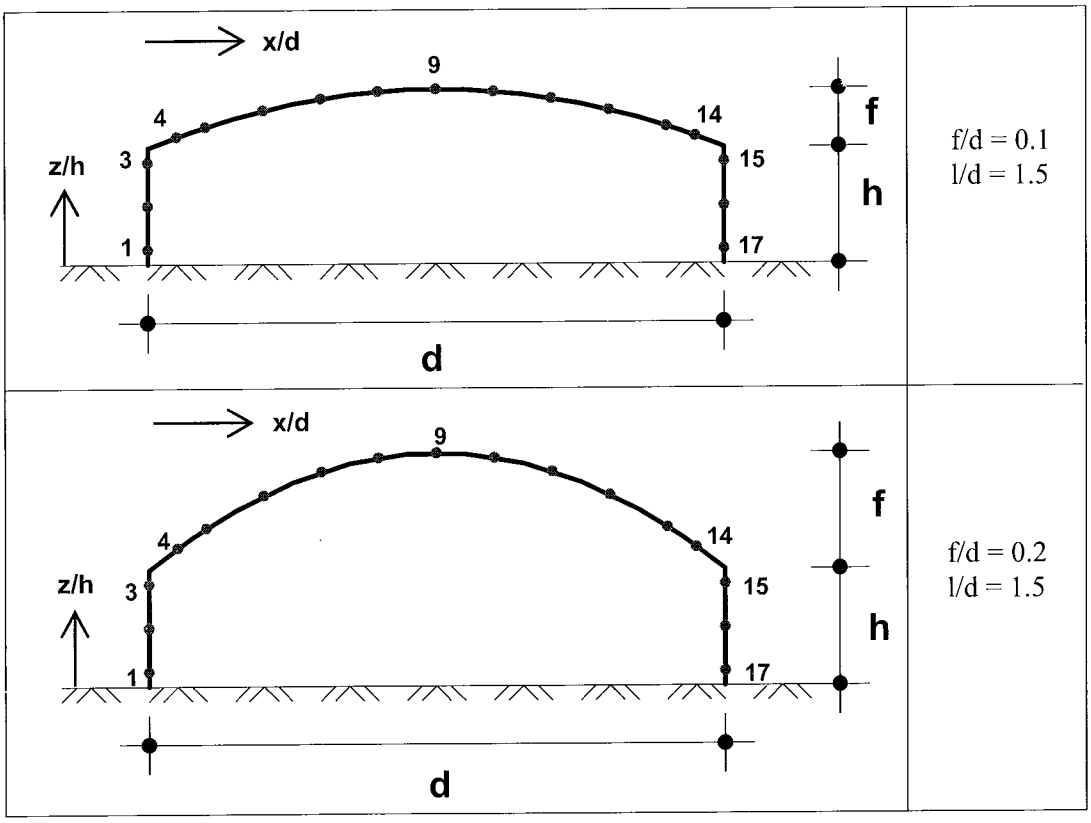

Figure 2: Basic geometry of the investigated arches and position of the taps

Table 1: Relative position of the taps along the walls and the arch

	walls										
no.	1		2		3		15		16		17
z/h	0.125		0.5		0.875		0.875		0.5		0.125
	arch										
no.	4	5	6	7	8	9	10	11	12	13	14
x/d	0.05	0.1	0.2	0.3	0.4	0.5	0.6	0.7	0.8	0.9	0.95

Data processing

The pressure signals are sampled with a frequency of 1024 Hz and are digitized by a 16 bit A/D converter leading to a resolution of $\Delta p = 0.03$ Pa. The wind tunnel in Bochum suffers from noticeable distortions induced by the noise of the motor and the noise of the fan. These acoustic distortions can be removed by two measures: the low-frequency part can be measured simultaneously using floor-mounted pressure taps at an appropriate along-wind position at the side of the model and then can be removed by simply subtracting the noise signal from the signals measured at the different taps along the building. The high-frequency fan noise forms a complex rotating multi-harmonic pattern and can be removed by digital filtering.

A single run is assumed in this study to correspond to 10 minutes in full-scale. To allow for a stable statistical analysis, 200 independent runs are performed. All pressures are normalized to the mean velocity pressure at eaves height. The simultaneous time series of the pressure coefficients are stored on hard disk.

From the simultaneously measured local pressures, in a second step, wind induced global actions - like drag and lift - and wind induced structural effects - like support reactions or bending moments - can be calculated. For both cases, the local pressures are combined in each time step with weighting factors. For the wind induced global actions drag and lift wind, the weighting factors are simply the relative contributing areas. For structural responses the weighting factors are obtained in terms of structural reactions due to unit loads in the different positions. These factors are also called influence coefficients. Figure 3 gives an example of influence coefficients for a vertical support reaction and a bending moment. In this example, the stiffness of the arch has been assumed to be constant along the axis; the roof system is supported by the walls which are idealized as rigid.

Extreme value analysis

From each independent run, one maximum and one minimum value are sampled. For the further simplified analysis, it is assumed that the extremes follow the extreme value distribution type I, which is given as follows:

$$F(x) = \exp\left[-\exp\left(-\left[\gamma + \frac{\pi}{\sqrt{6}}\,\frac{x - m}{\sigma}\right]\right)\right] \tag{1}$$

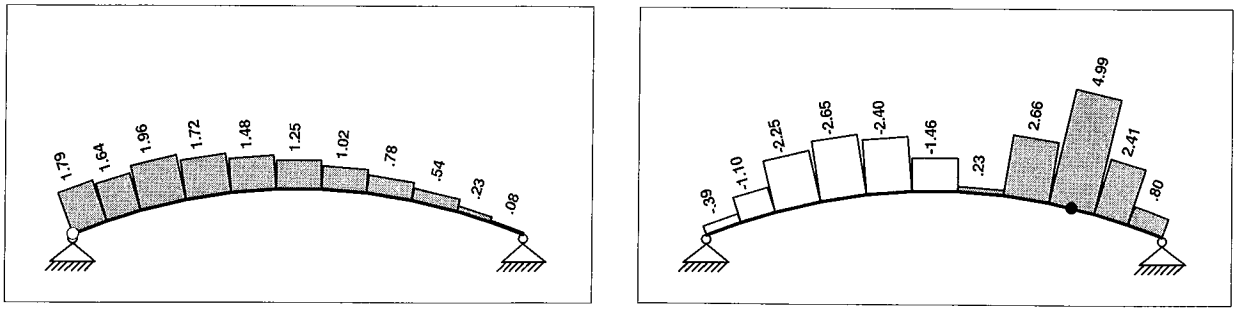

vertical support reaction of the arched roof **bending moment at pos. 17 for the arched roof**

Figure 3: Influence coefficients for a vertical support reaction and a bending moment

m - mean value of the extremes
σ - standard deviation of the extremes
γ - Euler constant = 0.5772

As recommended in the new ISO-code on wind loads [8], the design value of the aerodynamic coefficients is obtained as the 80%-fractile value of the extremes with reference to the storm duration of one hour. It can be estimated as follows:

$$\hat{c}_{80\%,1\,\text{hour}} = \hat{c}_{\text{mean},10\,\text{min}} \pm 2.1 \cdot \hat{c}_{\text{sdev},10\,\text{min}} \tag{2}$$

$\hat{c}_{\text{mean},10\,\text{min}}$ - mean value of the extremes obtained from 10 min samples
$\hat{c}_{\text{sdev},10\,\text{min}}$ - standard deviation of the extremes obtained from 10 min samples
$\hat{c}_{80\%,1\,\text{hour}}$ - 80%-fractile with reference to one hour

In the following, the design values of aerodynamic coefficients are calculated for local pressures along the arch, for global loads (drag and lift) and for structural load effects (support reactions, bending moments).

WIND INDUCED ACTIONS FROM CODES AND OTHER SOURCES

Eurocode

In the Eurocode [6], the wind induced actions in terms of pressure coefficients are always specified with two values, one value $c_{pe,1}$ applicable for areas smaller or equal 1 m², and a second value for areas larger or equal to 10 m². A lot of the information in the Eurocode is not presented as strict rules but in form of recommendations, i.e. the National Annexes may specify different approaches. This is also the case for the pressure coefficients for vaulted roofs. In the recommended approach, the roof is sub-divided into three parts: an upwind quarter, a centre half and a downwind quarter. Depending on the actual geometry, for the upwind quarter two pressure coefficients with different sign may have to be considered. For the two structures investigated in the actual study, the specified pressure coefficients are all negative. For counteracting pressures, the Eurocode demands to neglect the actions which will produce a beneficial effect. Then, two values for the wind induced actions have to be considered, namely the specified values and zero. This rule applies to all regions. The recommended pressure coefficients of the Eurocode are summarized in Table 2.

As reference pressure, the gust velocity pressure at the highest point of the roof is used. It is important to note that the Eurocode is again not strict in regard to the profile of the gust velocity pressure, i.e. each partner country may specify its own gust velocity pressure profile in the respective National Annex. The recommended gust velocity profile is given as:

$$q_p(z) = \left(1 + 7 \cdot I_v(z)\right) \cdot \frac{1}{2} \cdot \rho \cdot v_m^2(z) \tag{3}$$

$I_v(z)$ - profile of the turbulence intensity
ρ - air density
$v_m(z)$ - profile for the mean wind speed
z - height above ground

For flat, open country the Eurocode recommends the following profiles:

$$I_v(z) = \frac{1}{\ln(z/z_0)}, \quad v_m(z) = 0.19 \cdot \ln(z/z_0) \cdot v_{ref} \tag{4}$$

$z_0 = 0.05$ m
v_{ref} - reference wind speed depending on the geographic position

Table 2: Recommended pressure coefficients for the two arched roofs from EN 1991-1-4

	upwind quarter	centre half	downwind quarter
f/d = 0.1	-0.384	-0.8	-0.4
f/d = 0.2	-0.288	-0.9	-0.4

German DIN 1055

The new German DIN 1055 [5] has become effective by law with the beginning of 2007. It will be replaced in some years by the Eurocode and a German National Annex. The actual German DIN does not specify pressure coefficients for arched roofs. However, it is important to note that the general recommendation in regard to favourable load effects is even stricter than that in the Eurocode. The German DIN explains that there is no guarantee that the specified pressures will occur simultaneously along the structure. It therefore demands, that the effects of possible non-simultaneous actions have to be considered, stating that generally a conservative approach is obtained by neglecting the favourable loads, i.e. generally it is sufficient to use the load amplitude zero where favourable loads occur. However, the recommendation includes, that there might be cases, where the simplified rule is not sufficient, since the pressure may change the sign in the relevant areas.

Furthermore, it should be noted that the German DIN deviates from the recommended Eurocode-profiles. In DIN 1055, The gust velocity pressure for flat open country is obtained as:

$$q(z) = 2.1 \cdot q_{ref} \cdot \left(\frac{z}{10}\right)^{0.24} \tag{5}$$

q_{ref} - reference value of the mean velocity pressure = $\frac{1}{2} \cdot \rho \cdot v_{ref}^2$

This profile is also to occur in the German National Annex.

Australian/New Zealand Standard

Similar to the Eurocode, the new Australian/New Zealand Standard [1] specifies pressure coefficients for three regions: the upwind quarter, the centre half and the downwind quarter. It is important to note that for the upwind quarter two values have to be considered for the design. For the actual geometries, the recommended pressure coefficients are summarized in Table 3.

Table 3: Recommended pressure coefficients for the two arched roofs from AS/NZS 1170.2

	upwind quarter	centre half	downwind quarter
f/d = 0.1	-1.03 or 0	-1.05	-0.85
f/d = 0.2	-0.3 or 0	-0.85	-0.55

As reference pressure, the gust velocity pressure at the average height of the roof has to be used. The profile of the gust velocity pressure is given in terms of multipliers in tables. For flat open country, the respective factors are 0.933 for z = 6.25 m and 0.955 for z = 7.5 m. These factors apply to the design value of the gust velocity pressure at 10 m height.

The Designer's Guide to Wind Loading

A first consistent approach to the specification of the design wind loads has been developed by Cook [3] in the early 1980s. In part 2 of his Designer's Guide [4], pseudo-steady pressure coefficients are given

for many building shapes. Vaulted roofs are sub-divided in to six equal areas, labelled from a to f from the upwind to the downwind edge. The specified pressure coefficients are summarized in Table 4. The effects of favourable load contributions are not separately treated in the Designer's guide; however, it seems to be reasonable to adopt the Eurocode rule as well when applying the Cook-values. As reference pressure, the gust velocity pressure at the crest is used. The respective values are taken from the British Standard [2].

Table 4: Pressure coefficients as recommended by Cook

	a	b	c	d	e	f
f/d = 0.1	-0.58	-0.56	-0.64	-0.64	-0.48	-0.36
f/d = 0.2	±0.20	-0.58	-0.88	-0.72	-0.48	-0.48

Comparison of the gust velocity pressure profiles for flat, open country

In figure 4, the profiles of the gust velocity pressure of the Eurocode, the German DIN, the British Standard and the Australian/New Zealand Standard are compared to the expected range as given in ESDU. The differences at the respective reference heights are quite large. Only the specifications of the German DIN match with the specifications in ESDU. The other three codes specify larger values for the factor required to translate the mean velocity pressure to the gust velocity pressure. It is important to note that it is the product of the gust velocity pressure and the aerodynamic coefficient which finally specifies the design wind load. So it is still difficult to judge based only on the velocity pressure, which code represents the 'true' or best solution for the specification of the design wind load. However, it is clear that using one and the same set of aerodynamic coefficients with different gust velocity pressure profiles - as allowed in the Eurocode - will lead to different design wind loads, of which in the best case only one will be close to the 'true' solution.

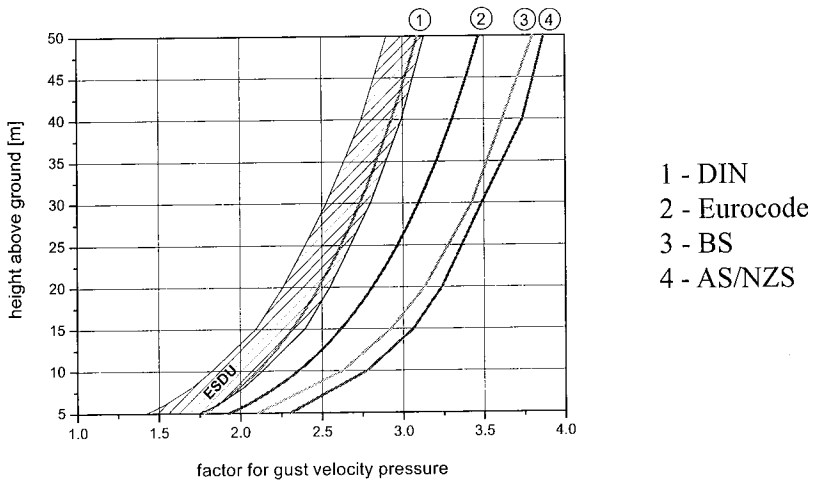

Figure 4: Comparison of the profile of the gust velocity pressures from some leading codes compared to the specification in ESDU

WIND TUNNEL RESULTS

Local pressures

In the following, the analysis is restricted to the local pressures along the centre arch of the building for a flow direction normal to the axis of the roof. It is important to note that the estimation of the statistical

parameters mean value and standard deviation based on a single run will contain some random scatter due to the confined ensemble. Therefore, in the following tables the statistical parameters are obtained from averaging over the complete set of 200 runs. The reference pressure is the 10-minute mean velocity pressure at eaves height.

Table 5 summarizes the results for the arch with f/d = 0.1, the results for the arch with f/d = 0.2 are shown in Table 6. For both arch geometries a change of sign is obtained for the pressures in the upwind quarter. This behaviour is only predicted by the Cook-values for the arch with f/d = 0.2. All other codes suggest that the pressures remain negative. In the wind tunnel experiments, a change of sign is also obtained for the downwind quarter of the roof. This behaviour is not predicted by any of the sources discussed above.

Table 5: Statistic parameters for the local pressures for the arch with f/d = 0.1

no.	$c_{p,mean}$	$c_{p,sdev}$	$\overline{c_{p,min}}$	$cov(c_{p,min})$	$\overline{c_{p,max}}$	$cov(c_{p,max})$
4	-0.64	0.223	-1.66	0.151	0.13	1.173
5	-0.48	0.165	-1.21	0.140	0.12	0.962
6	-0.49	0.149	-1.11	0.127	-0.01	6.715
7	-0.61	0.175	-1.31	0.126	-0.13	0.711
8	-0.66	0.190	-1.40	0.124	-0.18	0.557
9	-0.65	0.191	-1.39	0.122	-0.17	0.551
10	-0.61	0.184	-1.32	0.121	-0.15	0.573
11	-0.55	0.192	-1.32	0.108	0.01	8.606
12	-0.43	0.169	-1.11	0.107	0.09	0.714
13	-0.27	0.146	-0.87	0.109	0.23	0.256
14	-0.18	0.134	-0.73	0.119	0.30	0.216

Table 6: Statistic parameters for the local pressures for the arch with f/d = 0.2

no.	$c_{p,mean}$	$c_{p,sdev}$	$\overline{c_{p,min}}$	$cov(c_{p,min})$	$\overline{c_{p,max}}$	$cov(c_{p,max})$
4	-0.08	0.191	-0.68	0.156	0.87	0.189
5	-0.21	0.165	-0.78	0.138	0.61	0.261
6	-0.56	0.172	-1.25	0.099	0.08	1.661
7	-0.91	0.251	-1.89	0.098	-0.27	0.521
8	-1.05	0.298	-2.18	0.103	-0.37	0.463
9	-1.01	0.298	-2.12	0.105	-0.34	0.465
10	-0.93	0.287	-2.01	0.111	-0.29	0.481
11	-0.76	0.255	-1.78	0.107	-0.12	0.697
12	-0.51	0.223	-1.54	0.123	0.08	0.842
13	-0.29	0.164	-1.13	0.135	0.28	0.235
14	-0.22	0.147	-0.92	0.134	0.34	0.206

Global wind induced actions

The global wind induced actions drag and lift are normalized in the following with the span d. For both parameters, the reference pressure is the mean velocity pressure at eaves height. In Table 7, the results for the extreme global actions are summarized for the two arch geometries.

Table 7: Statistical parameters of extreme drag and extreme lift

	drag		lift	
	max_{mean}	cov (max)	min_{mean}	cov(min)
f/d = 0.1	0.08	0.146	-1.11	0.098
f/d = 0.2	0.11	0.185	-1.29	0.106

Support reactions

The statistical parameters of the support reactions are summarized in Table 8, presenting for the horizontal and vertical support the design-decisive values. For the arch with f/d = 0.1, the vertical support reaction (lift) at the upwind support becomes slightly larger than at the downwind position, while for the arch with f/d = 0.2 the downwind lift reaction is larger than the upwind lift reaction.

Table 8: Statistical parameters of the support reactions

f/d	position	horizontal		vertical	
		max_{mean}	cov (max)	min_{mean}	cov(min)
0.1	upwind	35.69	0.122	15.15	0.130
	downwind	36.43	0.123	13.10	0.117
0.2	upwind	24.72	0.113	15.88	0.098
	downwind	23.77	0.103	16.98	0.113

support reactions in [kN] per unit distance of the frames [m] per unit pressure [kN/m²]

Bending moments

The final evaluation of the quality of the load approach has to be based on the design-decisive structural response. Then, the wind induced actions effects have to be combined with the action effects induced by dead load and - depending on the climate at the actual site - eventually snow induced actions as well. As a simplification, in the following the largest positive and the largest negative bending moment are used. The respective statistical parameters are summarized in Table 9.

Table 9: Statistical parameters of the extreme bending moments along the arch

	positive bending moment		negative bending moment	
	max_{mean}	cov (max)	min_{mean}	cov(min)
f/d = 0.1	6.95	0.129	-5.67	0.155
f/d = 0.2	11.76	0.159	-6.90	0.171

bending moment in [kNm] per unit distance of the frames [m] per unit pressure [kN/m²]

DESIGN VALUES AND COMPARISON TO THE OTHER SOURCES

Local loads

The results for final design values of the local loads are summarized in Table 10 for the arch with f/d = 0.1 and in Table 11 for the arch with f/d = 0.2. Basically, the wind tunnel results show that at almost any position along the arch a change of sign may occur, i.e. along with considerable peak suction a positive pressure has to be considered. For the arch with f/d = 0.1, none of the other sources considers this wind induced action. For the arch with f/d = 0.2, the load proposal by Cook considers a positive pressure for the upwind region; however, the amplitude is too small by a factor of 2 and the affected region is too small.

The different codes specify clearly different large suctions at the leading edge. Only the Australian/New Zealand Standard predicts the peak suction on the safe side; the Eurocode underestimates the peak suction by almost 60%, Cook's proposal underestimates the peak suction by 33%. The peak suction near the crest is correctly predicted with the concept of the German DIN and with the Cook-proposal; the Eurocode overestimates the local loads by 10%, the Australian/New Zealand Standard by 44%. In the downwind

region of the roof, only the Australian/New Zealand Standard predicts too large peak suction loads, the other sources are more or less close to the wind tunnel results.

A different result is obtained for the arch with f/d = 0.2. The best agreement to the wind tunnel data is obtained for the Cook-proposal; however, the region of peak suction on the downwind part of the roof is underestimated. All sources underestimate the peak suction at the leading edge. The local pressures near the crest are underestimated by the Eurocode and the Australian/New Zealand Standard by about 20%; the German DIN underestimates these pressures by about 30%.

Table 10: Design values of the local pressures for the arch with f/d = 0.1

pos	wind tunnel		EC	DIN	AS/NZS	Cook
4	-2.18	0.45	-0.93	-0.84	-2.49 or 0	-1.47
5	-1.57	0.36				
6	-1.40	0.17				-1.42
7	-1.65	0.07	-1.96	-1.76	-2.54	
8	-1.77	0.03				-1.63
9	-1.75	0.03				
10	-1.66	0.03				
11	-1.62	0.14				-1.22
12	-1.36	0.22	-0.98	-0.88	-2.06	
13	-1.07	0.35				-0.91
14	-0.91	0.44				

Table 11: Design values of the local pressures for the arch with f/d = 0.2

pos	wind tunnel		EC	DIN	AS/NZS	Cook
4	-0.91	1.22	-0.75	-0.68	-0.76 or 0	±0.56
5	-1.01	0.94				
6	-1.51	0.34				-1.61
7	-2.28	0.03	-2.09	-1.88	-2.16	
8	-2.65	-0.01				-2.44
9	-2.59	-0.01				
10	-2.48	0				-2.00
11	-2.18	0.06				-1.33
12	-1.94	0.21	-1.04	-0.94	-1.40	
13	-1.45	0.42				
14	-1.18	0.49				

Global wind induced actions

The design values for the lift are simply obtained by obtaining the weighted sum of the specified pressures for each different source. The weighting coefficients are the relative tributary areas, using as reference the span d of the arch. For the estimation of the drag, as basic rule, all suction loads on the

upwind half of the roof are neglected. Hence, the estimated drag is the wind induced force in wind direction. In figure 5 and 6, the relative design values based on the different sources are summarized, normalizing the different design values by the wind tunnel results.

For the arch with f/d = 0.1, the predicted design values for drag and lift are quite close to the wind tunnel results with the exception of the Australian/New Zealand Standard, which leads to considerable overestimations. While for the arch with f/d = 0.2 all sources show a good agreement with the wind tunnel result for the lift, they are all overestimating the drag by 50% to 235%. The simple rule of neglecting favourable effects is obviously inappropriate to get a realistic design value of the drag.

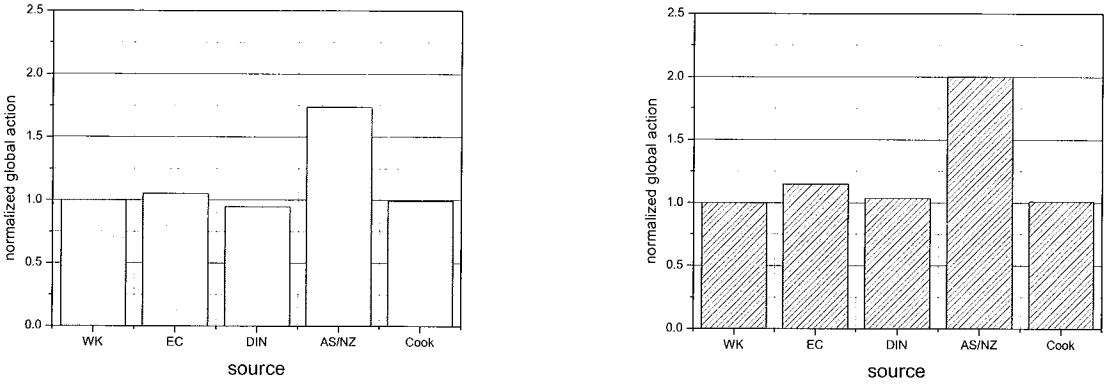

Figure 5: Relative design values of the global wind induced actions, f/d = 0.1 (WK-wind tunnel results, EC-Eurocode, AS/NZS-Australian/New Zealand Standard)

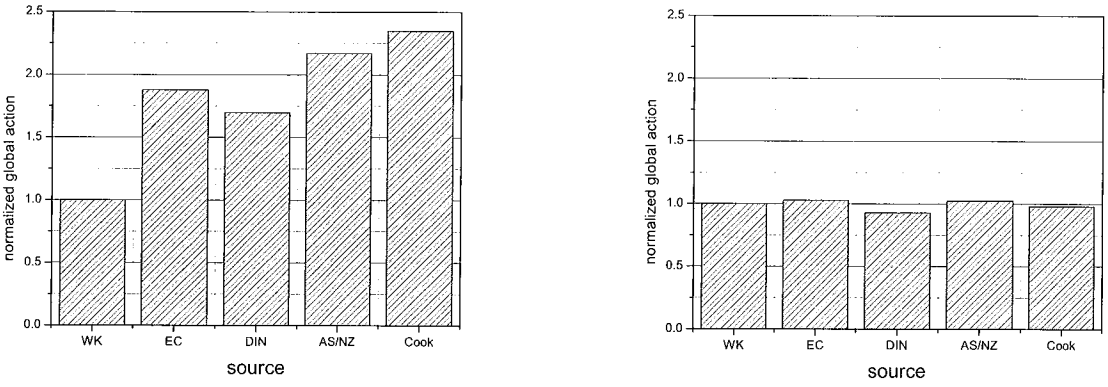

Figure 6: Relative design values of the global wind induced actions, f/d = 0.2 (WK-wind tunnel results, EC-Eurocode, AS/NZS-Australian/New Zealand Standard)

Support reactions

The design values of the support reactions are summarized in Table 12 for the vertical and horizontal direction, respectively. The observed shortcomings in the local pressures are averaged out; i.e. generally, there is a good agreement to the wind tunnel results. The only exception is the horizontal support reaction for the arch with f/d = 0.1, which is overestimated by the Australian/New Zealand Standard by about 60%. It is important to note, that for the analyzed arch structures it is not the wind induced drag which triggers the horizontal support reactions.

Table 12: Design values of the support reaction

		wind tunnel	EC	DIN	AS/NZS	Cook
f/d = 0.1	V	19.28	18.29	16.48	31.08	18.38
	H	45.87	50.53	45.52	74.67	44.36
f/d = 0.2	V	21.09	19.26	17.42	21.54	20.22
	H	28.90	25.86	23.39	26.90	26.36

Bending moments

For comparison, the bending moments obtained with the different sources are normalized with the respective value obtained based on the wind tunnel tests. In cases where a source specifies alternative load cases, the source occurs twice in the comparison. Additionally, for each source the influence of neglecting the favourable loads is analysed. In figure 7, the comparison for the largest negative bending and the largest positive bending moment is shown for the arch with f/d = 0.1. The original load distribution specified in the Eurocode leads to an underestimation of the largest negative bending moment by almost 50%. Neglecting the favourable load effects on the other hand leads to an overestimation by a factor of 2.2. A similar result is obtained when applying the reduced reference pressure as recommended in DIN. The DIN-results are smaller by about 10% than the EC-results. The new Australian/New Zealand Standard underestimates with one load distribution the negative bending moment by about 50%. The alternative load case overestimates the 'true' response by about 30%. Neglecting additionally all favourable loads, leads to an overestimation by a factor of 3.5. The load distribution by Cook is going to lead to the largest underestimation; the ratio to the 'true' load effect is only 0.36. If all favourable load contributions are neglected, again a considerable overestimation is obtained, in this case by a factor of 2.2.

The comparison leads to the same unsatisfactory result for the positive bending moment. The original Eurocode load underestimates the 'true' results by about 60%, applying the rule for favourable loads leads to an overestimation by a factor of 1.8. The two load distributions specified in the new Australian/New Zealand Standard produce either 20% or 200% of the 'true' load effect, neglecting additionally all favourable

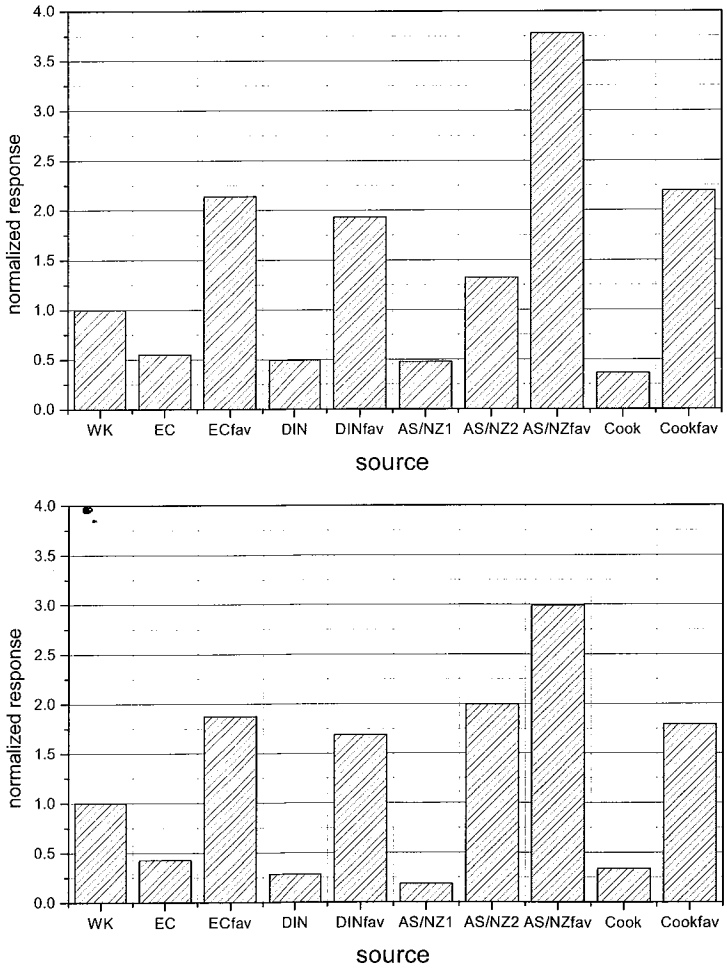

Figure 7: Comparison of the bending moments for the arch with f/d = 0.1 (all values with reference to the wind tunnel results)

loads increases the overestimation to a factor of 3.0. The load distribution proposed by Cook gives one third of the 'true' load effect, taking all favourable loads as zero overestimates the 'true' response by a factor of 1.8

The comparison for the arch with f/d = 0.2 (figure 8) leads to a slightly different result. Now, the alternative load case in the new Australian/New Zealand Standard also leads to an underestimation for the negative bending moment. The positive bending moment is almost correct with deviations of only 3%. If all favourable load effects are neglected, the obtained result with the Australian/New Zealand Standard will be conservative. However, the 'true' response is overestimated by a factor of 2.4 and 1.4 for the negative and positive bending moment, respectively. The Cook-proposal with two alternative load distributions does not perform any better. Severe underestimations are to be expected, unless all favourable loads are neglected. Then, however, the overestimations will be 2.2 and 1.4 for the negative and positive bending moment.

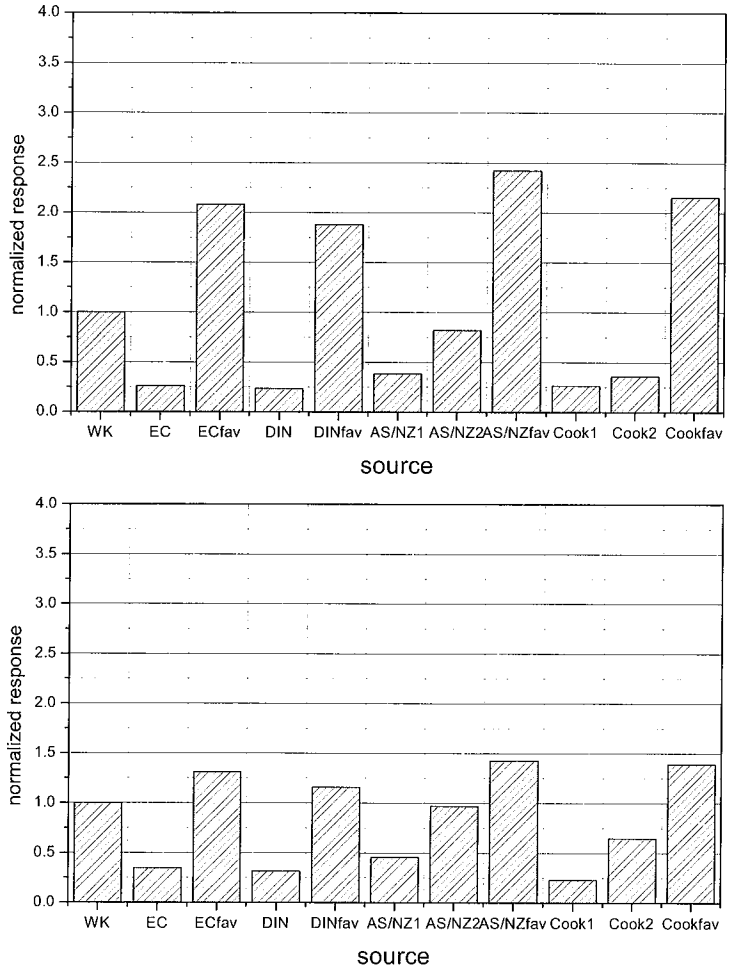

Figure 8: Comparison of the bending moments for the arch with f/d = 0.2 (all values with reference to the wind tunnel results)

EXAMPLES OF LRC-LOAD DISTRIBUTIONS

The recent version of ISO 4354 - wind actions on structures [8] recommends for the consistent codification of wind loads the following procedure:

- wind induced local actions are specified in tables, generally with two values covering both extremes
- additionally, figures with simultaneous pressure distributions are specified; the required number of figures depends on the different structural responses which have to be considered in the design; generally, at least two pressure distributions are required.

As one possible method for the identification of effective load distributions the ISO-Standard recommends the LRC-method [9], which obtains the simultaneous load distributions by the sum of the mean value of the pressures plus the weighted standard deviation of the pressures. Examples of two such pressure distributions are shown in figure 9, which lead to one of the required bending moments. It is worth mentioning that both distributions show a change of sign for the upwind part of the arched roofs.

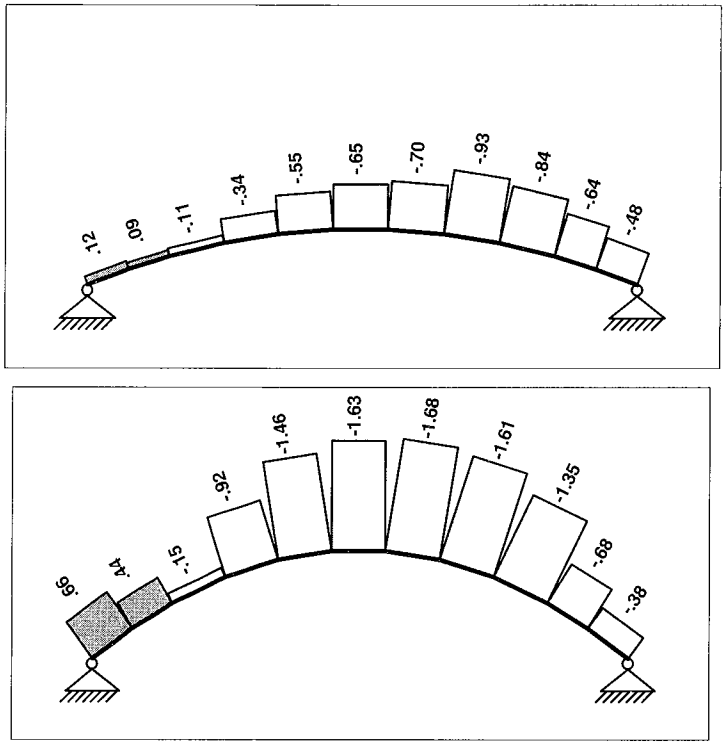

Figure 9: Examples of effective pressure distributions (all values with reference to the mean velocity pressure at eaves height)

CONCLUSIONS

Based on wind tunnel experiments, the paper studies the wind induced loads and the wind induced structural effects for two arched roofs. The wind tunnel results are compared to some leading codes and the recommendations of Cook's Designer's Guide. Since arched structures are sensitive to unbalanced load distributions, the specification of only the peak suction loads usually is not enough to enable a safe and economic design. A safe design is obtained applying the rule of neglecting all favourable load contributions. However it has to be stated

, that this rule may lead to considerable overestimations and therefore an uneconomic design. The LRC-method enables the wind engineers to specify effective load distributions which are able to fulfil both the demand for safety and the demand for economy. Therefore, the recent ISO-Standard "wind actions on structures" recommends this method as one possible tool to condense the amount of wind tunnel data to meaningful design wind loads for codification.

ACKNOWLEDGEMENT

The wind tunnel tests have been performed by Dipl.-Ing. Hassan Qrichate. This support is gratefully acknowledged.

REFERENCES

1. AS/NZS 1170.2 (2002), Australian/New Zealand Standard, Structural design actions, Part 2: wind actions, Standards Australia & Standards New Zealand
2. BS 6399-2:1997
   Loading for buildings. Code of practice for wind loads
   British Standards Institution / 15-Jul-1997 / 126 pages
   ISBN: 0580274470
3. Cook, N. J. and Mayne, J.R. (1980), A refined working approach to the assessment of wind loads for equivalent static design Journal of Wind Engineering and Industrial Aerodynamics 6, 125-137
4. Cook, N.J. (1990), The designer's guide to wind loading of building structures Part 2 Static structures, Butterworths, London 1990, ISBN: 0-408-00871-7
5. DIN 1055 Teil 4 - Windlasten März 2005
6. EN 1991-1-4 (2005), Eurocode 1: Actions on structures - Part 1-4: General actions - Wind actions
7. ESDU - Engineering Science Data Unit (1985, 1986), Characteristic of atmospheric turbulence near ground, Single point data for strong winds, ITEM 85020, Variations in space and time for strong winds, ITEM 86010
8. ISO 4354 Wind action on structures - DIS 05.2007
9. M. Kasperski, Extreme wind load distributions for linear and nonlinear design, Engineering Structures, Vol. 14, 1992, pp. 27-34.

Journal of Wind & Engineering, Vol. 5, No. 2, July 2008, pp. 31-39

THE EUROPEAN WIND LOADING STANDARD: PROVISIONS AND THEIR BACKGROUND

Hans-Juergen Niemann

Ruhr-Universitaet Bochum, Germany

THE FRAMEWORK

The Structural Eurocode programme comprises three topical types of codes which are briefly introduced to indicate the context of the wind loading code.

EN 1990: *Basis of Structural Design* deals with the fundamentals for the design of load carrying building components. A supplement has been added in 2005 containing the design values of actions on bridges and the load combinations, and includes rules for actions to be applied during erection.

EN 1991: *Actions on Structures* comprises 10 parts dealing with dead load, traffic loads, climatic loads, etc. Table 1 in Appendix-I summarizes the titles.

The codes EN 1992 – EN 1999 comprise detailed rules for the engineering design, structural analysis, and dimensioning of the load bearing structure. Table 2 in Appendix – I summarizes the topics of these codes. Generally, each code consists of several parts.

The design codes are in general rather detailed. As an example, table 3 in Appendix – I presents a list of the parts relating to the design of steel structures.

A structural design shall be performed in (i) the serviceability limit state, i.e. in view of comfort and appearance, and in (ii) the ultimate limit states, i.e. in view of collapse or other forms of structural failure such as fatigue. The partial factor method is applied, in which the structural load bearing capacity on one hand and the action effects on the other are represented by characteristic values weighted by individual partial safety factors. The characteristic values are defined in terms of appropriate quantiles of their probability distributions. The two parameters, the characteristic value and the partial factor are coupled to each other. They are set with the target that the operative failure rate amounts to 10^{-6} per year for collapse, and 10^{-3} per year for serviceability.

A typical load combination consists of permanent loads with characteristic values G_k, the dominant (or leading) non-permanent load Q_{k1}, and further non-permanent (or accompanying) loads Q_{kj} from n different origins:

$$\sum \gamma_{Gi} \cdot G_{ki} \oplus \gamma_{Q1} \cdot Q_{k1} \oplus \sum_{n} \gamma_{Qj} \psi_{0j} \cdot Q_{kj} \qquad (1)$$

In eq. 1, the partial load factors γ depend on the limit state under consideration: for wind loading, $\gamma_W = 1.5$ in the failure limit state. For serviceability and for fatigue, $\gamma_W = 1.0$. The combination factors ψ_0 are <1.0, accounting for the fact that the probability is very small that the characteristic extreme loads occur simultaneously. A value of $\psi_{0W} = 0.6$ is adopted for wind loading.

The corresponding characteristic value of a non-permanent load is the 2%-quantile of the yearly extremes. This is a rare event and describes an extreme storm intensity having an average return period of 50 yrs. The related mean wind speeds are depicted in wind maps. Observed wind data are available for 50 yrs or so. Since the return periods are in the order of the observation periods, the wind map data are rather realistic.

Alternatively, the design may be based on the so-called design values, i.e. the load values at the design point on the limit state function. The advantage would be that non-linear effects such as resonance are included in the procedure. However, the return period of the wind load is in this situation in the order of 2000 yrs. Extrapolation to such return periods is of course highly speculative. It is a rather fictitious event beyond our experience and does not seem very real. Moreover, the result depends very much on the probability function applied to the statistical data and on the parameter considered in it: whether it is the wind speed or its square representing the velocity pressure. It seems reasonable therefore to refer to wind data for which reliable prediction is feasible, and to include the uncertainties of the statistical model in the partial load factor.

THE WIND LOADING CODE

One of the major, if not the greatest, difficulty in developing a wind loading code is an adequate method of taking into account the load fluctuations, their non-simultaneous occurrence and their effect on the structural response. The most convenient way is to include these effects in an equivalent static load. The resonant gust response may be covered by a *dynamic factor*, the decay of correlation over the loaded area by a *size factor*.

In the Eurocode, a calculation procedure for the determination of wind actions is recommended along these lines. National annexes may choose to deviate from the given rules and parameters within certain limitations. The principal features are highlighted herein below:

The basic wind velocity v_b

The fundamental value, $v_{b,0}$ is "the characteristic 10 minutes mean wind velocity, irrespective of wind direction and time of year, at 10 m above ground level in open country terrain with low vegetation such as grass and isolated obstacles with separation of at least 20 obstacle heights." The *basic (mean) wind velocity* v_b is calculated from it:

$$v_b = c_{dir} c_{season} v_{b,0} \tag{2}$$

The *directional factor* allows for the effects of wind directionality. It is needed when the orientation of an individual building with regard to the wind speed rosette shall be considered. The *season factor* takes the seasonal variation of storm intensities over a year into account. It may be useful if temporary states of a structure are investigated. The recommended value for both factors is 1.

If the structure is designed for a longer or shorter lifetime than the usual value of say 50 yrs, a *probability factor* is given. It converts the annual exceedence rate of 0.02 of the characteristic wind speed into some required value p:

$$c_{prob} = \left(\frac{1 - K \cdot \ln(-\ln(1-p))}{1 - K \cdot \ln(-\ln(1-0.02))} \right)^n \tag{3}$$

The expression is derived from the Gumbel extreme value probability distribution. Values of the shape parameter K = 0.2 and the exponent n = 0.5 are recommended. Apparently it is assumed here that the observed frequencies of the squared velocity – not of the velocity itself – follow the Gumbel distribution.

The mean wind

The mean wind speed at a given location depends on height above ground, z, the terrain roughness, and the terrain orography. It is difficult to capture the latter effect in a realistic and sufficiently simple manner. Nevertheless, a procedure is given to calculate the *orography factor* c_O describing the wind speed-up over hills, cliffs, and escarpments.

The logarithmic wind profile is used to allow for the terrain roughness and the height above ground

$$v_m(z,z_0) = \frac{u_\tau(z_0)}{\kappa} \ln \frac{z}{z_0} \tag{4}$$

In equation (4), $\kappa = 0.4$ is the von-Kármán-constant. The roughness length, z_0, characterizes the terrain roughness. The so-called shear velocity u_τ depends on z_0. Five categories of terrain roughness are specified ranging from open sea with $z_0 = 0.003$ m, the reference terrain with $z_{0,ref} = 0.05$ m, and city centres with $z_0 = 1.0$ m. In order to deduce the mean wind speed in the actual terrain from the basic wind velocity in the reference terrain, a relation between the shear velocities in different terrain categories is needed. *Davenport's* approach is used with the standard plane and open terrain as a reference:

$$\frac{u_\tau(z_0)}{u_\tau(z_{0,ref})} = \left(\frac{z_0}{z_{0,ref}}\right)^{0,07} \tag{5}$$

Combining equations (4) and (5),

$$v_m(z,z_0) = k_r \cdot \ln\left(\frac{z}{z_0}\right) \cdot v_b \tag{6}$$

In equation (6), the terrain factor k_r has been introduced using $z_{0,ref} = 0.05$m.

$$k_r = \frac{1}{\ln(10/z_{0,ref})}\left(\frac{z_0}{z_{0,ref}}\right)^{0,07} = 0{,}1887 \cdot (z_0/0.05)^{0,07} \quad (z_0 \text{ in m}) \tag{7}$$

If the terrain varies with regard to the wind direction, the terrain factor should be calculated for each angular sector, within an angular width of 30°. The terrain roughness in a sector upwind of the site will in general vary between different terrain categories. The transition has to be considered eventually, and simplified procedures are recommended in Annex A.2.

Where cliffs, hills or escarpments increase the wind velocity at the building site by more than 5% the effects should be taken into account. The code applies an amplification factor c_O, the orography factor given in annex A.3.

The peak velocity pressure q_p

The peak velocity pressure q_p, is fundamental for the determination of all equivalent static wind loads specified in the code. Principally speaking, q_p comprises the mean value q_m and the rms-value σ_q of the turbulence induced velocity pressure fluctuations:

$$q_p = q_m + k_p \sigma_q = \left[1 + k_p I_q\right] \cdot q_m \tag{8}$$

in which k_p – peak factor; $I_q = \sigma_q / q_m$ – intensity of the pressure fluctuations.

The relation between intensity of the pressure fluctuations and the intensity of the velocity fluctuations can be derived from the time domain considering that the velocity pressure is linked to the square of the velocity. The result is:

$$q_m = \frac{1}{2}\rho \cdot v_m^2 (1 + I_v^2) \cong \frac{1}{2}\rho \cdot v_m^2 \tag{9}$$

$$I_q = 2I_v \frac{\sqrt{1 + \frac{1}{2}I_v^2}}{1 + I_v^2} \cong 2I_v \tag{10}$$

$$q_p \cong \frac{1}{2}\rho \cdot v_m^2 \left(1 + 2k_p I_v\right) \tag{11}$$

I_v denotes the intensity of turbulence, and equals σ_v / v_m with σ_v - rms-value of the wind speed fluctuations, v_m - mean wind speed; ρ is the mass density of air. The equations show also the customary linearization applied in the Eurocode. The simplified value of the mean velocity pressure is slightly too small, the intensity I_q is slightly overestimated. Considering two typical limits of turbulence intensity, it is seen that the peak pressure is 0.7% smaller where $I_v = 0.1$ and 4.2% smaller where $I_v = 0.3$. The deviations are small enough to justify the linearization.

The code adopts Prandtl's classical boundary layer theory for the intensity of turbulence. In it, the rms-value σ_v is constant throughout the height z. It depends on the roughness length z_0.

$$I_v = \frac{\sigma_v(z_0)}{v_m(z,z_0)} = \frac{1}{c_O \cdot \ln(z/z_0)} \tag{12}$$

The orography factor, $c_O \geq 1.0$, has been added to account for the speed-up of the mean wind speed over hills and escarpments. The speed-up of the mean wind diminishes at the same time the turbulence intensity. The peak velocity pressure is calculated from eq. 6

$$q_p(z,z_0) = [1 + 7I_v(z,z_0)] \cdot q_m(z,z_0) \tag{13}$$

In equation (13), q_m is the linearized mean velocity pressure

$$q_m = \frac{1}{2}\rho \cdot v_m^2 \tag{14}$$

The peak factor of $k_p = 3.5$ recommended in the code corresponds approximately to a 0.5 sec gust speed, meaning that a rather small loaded area of some m^2 is taken as a basis of the regulations. This implies loads which will be too high for larger areas. Therefore, national codes may provide different peak factors.

In order to simplify the application of the code, equation (13) is rewritten and referred to the velocity pressure of the basic wind speed according to equation (2):

$$q_p(z,z_0) = c_e(z,z_0) \cdot q_b \tag{15}$$

Herein, c_e is the so-called exposure factor, given in diagrams for the case of flat terrain, i.e. with a value of the orography factor of $c_O = 1.0$. The complete exposure factor is

$$c_e = \left(1 + \frac{7}{c_O \cdot \ln(z/z_0)}\right) \cdot (k_r c_O)^2 \cdot \ln^2(z/z_0) \tag{16}$$

The structural factor

The code introduces a so-called structural factor $c_s \cdot c_d$ to account for the effect of turbulence on the structural response. To exemplify the approach, consider the wind force F_w on a section of a stack:

$$F_w = c_s c_d \cdot c_f \cdot q_p(z_e) \cdot A_{ref}, \tag{17}$$

In equation 17 c_f – aerodynamic force coefficient; A_{ref} – reference area of the section considered; z_e – height above ground of the section considered. Fig 1 shows the factor for unlined steel stacks as an example. For a typical design, the structural factor is less than unity when the diameter is larger than 14% of the height. In these cases the design with the peak gust pressure is on the safe side. If the structural factor from fig. 1 is >1.0, a structure is considered as being vibrationally sensitive and the structural factor has to be calculated by the methods developed in the code (detailed procedure).

The calculation of the structural factor is based on *Davenport's* pioneering concept of the gust response factor G. The main difference is that Davenport referred G to the mean response (or the mean velocity pressure q_m) whereas the Eurocode chose the response to the gust wind load as the reference (peak velocity pressure q_p). Roughly speaking, the structural factor is typically of the order of 1, the gust response factor of the order of 2. Both approaches must of course lead to the same design load. Hence, the leading load effects E due to both equivalent wind loads should be the same:

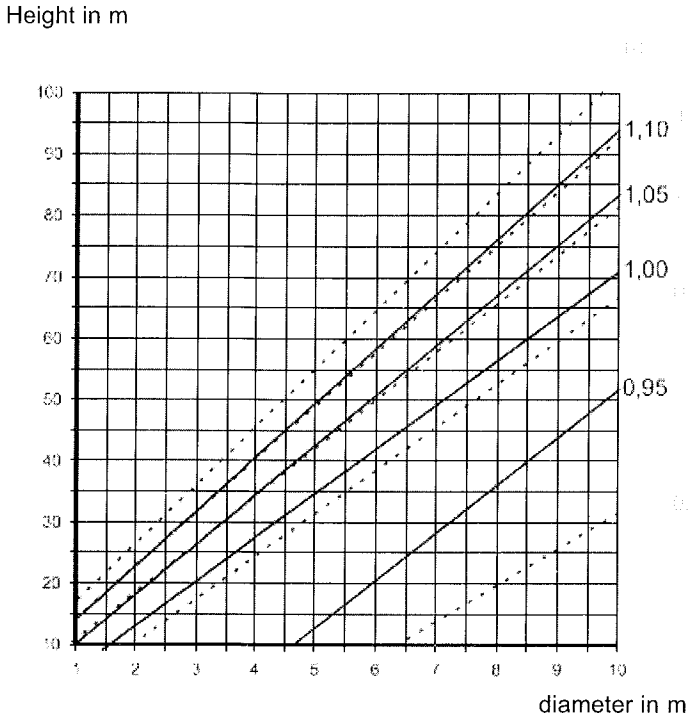

Figure 1: Structural factor for typical design of steel stacks without liners – full lines refer to terrain with roughness length z_0 = 0.05m, dotted lines to z_0 = 0.3m

$$E(c_s c_d \cdot q_p) = E(G \cdot q_m) \tag{18}$$

Consider structural response to the wind load, Y, to have, mean Y_m and standard deviation σ_Y. The response variance may be split into two contributions:

$$\sigma_Y^2 = \sigma_{YQ}^2 + \sigma_{YR}^2 \tag{19}$$

σ_{YQ} designates the standard deviation of the quasi-static response, σ_{YR} relates to the resonant response. The gust response factor G is defined as the ratio of the peak Y_p to the mean Y_m. It accounts for these contributions separately. It is written as:

$$G = 1 + k_p \frac{\sqrt{\sigma_{YQ}^2 + \sigma_{YR}^2}}{Y_m} = 1 + 2k_p I_v \sqrt{B^2 + R^2}\,, \tag{20}$$

in which:

$$B = \frac{\sigma_{YQ}}{Y_m}\frac{1}{2I_v}, \qquad \text{and} \quad R = \frac{\sigma_{YR}}{Y_m}\frac{1}{2I_v}.$$

B characterizes the contribution of background turbulence to the response; R stands for the resonant response to turbulence. Both contributions are normalized by the mean response and referred to twice the turbulence intensity. The factor 2 is due to the linearized approach mentioned earlier. Combining equations (18) and (20), and considering equation (11), the structural factor becomes:

$$c_s c_d = \frac{1 + 2k_p \cdot I_v(z_s) \cdot \sqrt{B^2 + R^2}}{1 + 7 \cdot I_v(z_s)} \tag{21}$$

Regarding a distinct structure, the structural factor has a fixed value. The turbulence parameters such as intensity, integral scale, spectral density etc refer to a reference height z_s which relates to the building height, see fig. 2.

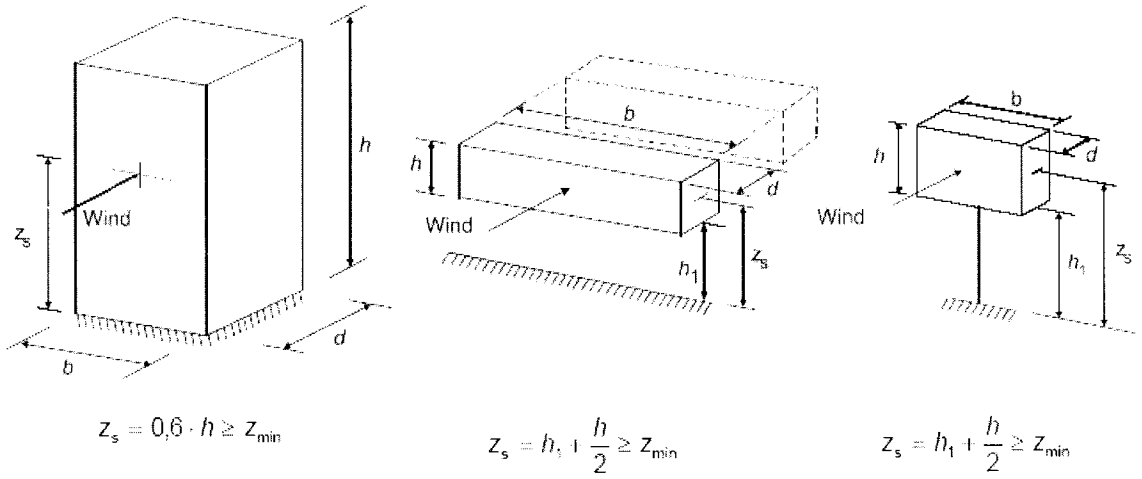

Figure 2: Reference height for calculating the structural factor

The background contribution B allows for the lack of full correlation of the wind pressure over the loaded area. The size factor, c_s is a reduction factor for the peak velocity pressure, accounting exactly for this effect. With a peak factor $k_p = 3.5$, c_s is given as:

$$c_s = \frac{1 + 7 \cdot I_v(z_s) \cdot \sqrt{B^2}}{1 + 7 \cdot I_v(z_s)} \tag{22}$$

Similarly, the resonant contribution R allows for the effect of resonance to turbulent excitation. The dynamic factor c_d is therefore an amplification factor, which in view of equations (19) and (20) becomes

$$c_d = \frac{1 + 2k_p \cdot I_v(z_s) \cdot \sqrt{B^2 + R^2}}{1 + 7 \cdot I_v(z_s) \cdot \sqrt{B^2}} \tag{23}$$

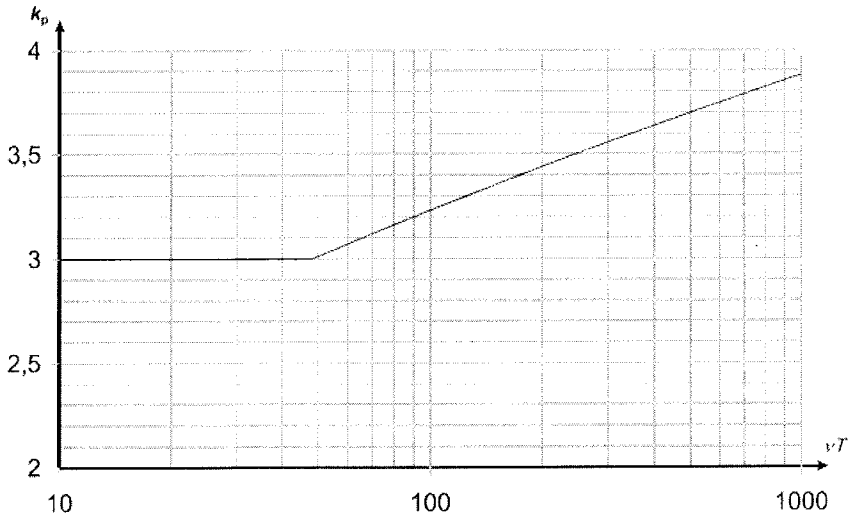

Figure 3: The peak factor

The peak factor k_p, is the ratio of the peak response to its standard deviation. It is related to the mean rate of up-crossings νT within the averaging time of the mean wind velocity, T = 600s. To calculate B and R, the Eurocode specifies two procedures, a recommended and an alternate procedure. Regarding the background factor, the principle is that it depends on the ratio of width b and height h of the structure or loaded area and

to the integral length scale of turbulence, L. This parameter depends on the height above ground level, z, and is given by

$$L = 300\left(\frac{z}{200}\right)^{0,67+0,05\cdot\ln z_0} \qquad \text{where z is in m} \tag{24}$$

The background factor in procedure 1 is

$$B^2 = \frac{1}{1+\left(\frac{b+h}{L(z_e)}\right)^{0,63}} \tag{25}$$

With procedure 2:

$$B^2 = \frac{1}{1+\frac{3}{2}\sqrt{\left(\frac{b}{L(z_e)}\right)^2+\left(\frac{h}{L(z_e)}\right)^2+\left(\frac{b}{L(z_e)}\frac{h}{L(z_e)}\right)^2}} \tag{26}$$

The difference of the result is small, generally less than 5%.

Regarding the resonance factor R^2, both procedures are similar in the principal approach:

$$R^2 = \frac{\pi^2}{2\cdot\delta} S(z_e, n_1)\cdot SR \tag{27}$$

where:

δ is the total logarithmic damping decrement including structural and aerodynamic damping;

S(n) is the spectral density of wind turbulence at the natural frequency of the mode considered;

SR is a size reduction function accounting for the correlation of load fluctuations at the natural frequency of the mode considered.

The difference of the two approaches concerns SR: procedure 2 offers the possibility to take the mode shape of the dominant mode in more detail into account. Again, for typical structures the choice is more a matter of convenience; the results do not deviate very much from each other. If torsion becomes important, the results of procedure 2 may be more realistic.

Wind pressures for cladding, fixings and structural parts

The wind pressures, w_e and w_i, acting on external and internal surfaces are given in the usual manner in terms of the peak velocity pressure multiplied by aerodynamic coefficients.

For cladding, fixings and structural parts no dynamic factor is specified; it is assumed that such elements are normally not prone to resonant vibrations due to wind turbulence. The size effect is taken into account to some extent in the external pressure coefficient: values are given for loaded areas of 1 m², the local coefficients $c_{pe,1}$, and for areas of 10 m², the overall coefficients $c_{pe,10}$. A typical region with a large difference between both coefficients is the corner of a flat roof with sharp eaves: here $c_{pe,1} = -2.5$ whereas $c_{pe,10} = -1.8$.

The internal wind pressure becomes important, when there are large spaces inside the building with no or just few partitions. The internal pressure is the result of the external pressures prevailing at the openings and at the background permeability of the building envelope. The contribution to the loading can be quite considerable. If there is a dominant opening at one of the building faces where an external pressure coefficient c_{pe} prevails, the Eurocode recommends for the internal pressure coefficient:

$$c_{pi} = 0.9\cdot c_{pe} \tag{28}$$

If doors and windows are normally closed in a storm, the condition of open doors and windows should be considered as an accidental design situation with a partial coefficient of $\gamma_w = 1.0$.

Wind forces

Wind forces acting on the whole structure, on sections of the structure or on structural components are calculated using aerodynamic force coefficients c_f. Alternatively, they may also be derived from pressures and friction forces by vectorial summation. The latter method becomes important for facade and roof elements, which are larger in area than 10 m² or vibrationally sensitive (natural frequency smaller than 5 Hz) because both, the size effect and the dynamic effect can then be allowed for.

The wind force is determined by the following expressions:

$$F_w = c_s c_d \cdot c_f \cdot q_p(z_e) \cdot A_{ref} \tag{29a}$$

$$F_w = c_s c_d \sum_{\text{surfaces}} w_e A_{ref} + \sum_{\text{surfaces}} w_i A_{ref} + c_{fr} \cdot A_{fr} \cdot q_p(z_e) \tag{29b}$$

where:

c_f is the aerodynamic force coefficient;

z_e is the reference height at which the peak velocity pressure has been taken as a reference for the aerodynamic force coefficient;

A_{ref} is the reference area for the aerodynamic force coefficient;

c_{fr} is the friction force coefficient;

A_{fr} is the external surface parallel to the wind.

The sum in equation (29b) indicates vectorial summation. It is interesting to note that in equation (29b), regarding the internal pressure no allowance is made for size and resonance effects. This corresponds to the fact that internal pressures are in general fully correlated and little energy is present at the high frequency end of their spectrum. The same behaviour is assumed also for the friction forces. This is conservative as far as the size effect is concerned.

The structural factor may be taken as unity in many cases, however if the structure is sensitive with regard to vibrations due to turbulence, the detailed procedure must be applied. It may be applied also for stiff structures to take advantage of the size effect reduction of the effective wind force. The structural factor may not be less than 0,85.

CONCLUSION

The new European wind loading code is an attempt to incorporate the present state of wind engineering into a tool for the daily work of practicing design engineers. A dilemma is due to the fact that the art of wind engineering has become a highly specialized field, and the practitioners right expect rules which are adequately simple *and* realistic at the same time. On the other hand, our buildings have changed in many ways to lighter designs, less material consumption, and they operate closer to the limit of their load bearing capacity. Therefore, methods which are more sophisticated compared to past codes had to be implemented.

REFERENCES

National versions of the Eurocodes are provided by the European Committee for Standardization in many languages. The German translations of the codes have been used in preparing the manuscript, and are therefore given as references, together with their English and French titles.

1. DIN EN 1991-1-4: Eurocode 1: Einwirkungen auf Tragwerke – Teil 1-4: Allgemeine Einwirkungen, Windlasten. Juli 2005
   Eurocode 1: Actions on structures – Part 1-4: General actions, Wind actions
   Eurocode 1: Actions sur les structures – Partie 1-4: Actions générales, Actions du vent
   CEN Brüssel
2. DIN EN 1990: Eurocode: Grundlagen der Tragwerksplanung. Oktober 2002
   Eurocode: Basis of structural design
   Eurocode: Bases de calcul des structures
   CEN Brüssel

Appendix – I

Table 1: The basic code EN 1990 and the action codes EN 1991

EN 1990:2002	Eurocode - Basis of structural design
EN 1990:2002/A1:2005	Eurocode - Basis of structural design(Amendment regarding bridge design)
EN 1991-1-1:2002	Eurocode 1: Actions on structures - Part 1-1: General actions - Densities, self-weight, imposed loads for buildings
EN 1991-1-2:2002	Eurocode 1: Actions on structures - Part 1-2: General actions - Actions on structures exposed to fire
EN 1991-1-3:2003	Eurocode 1 - Actions on structures - Part 1-3: General actions - Snow loads
EN 1991-1-4:2005	Eurocode 1: Actions on structures - Part 1-4: General actions - Wind actions
EN 1991-1-5:2003	Eurocode 1: Actions on structures - Part 1-5: General actions - Thermal actions
EN 1991-1-6:2005	Eurocode 1 - Actions on structures Part 1-6: General actions - Actions during execution
EN 1991-1-7:2006	Eurocode 1 - Actions on structures - Part 1-7: General actions - Accidental actions
EN 1991-2:2003	Eurocode 1: Actions on structures - Part 2: Traffic loads on bridges
EN 1991-3:2006	Eurocode 1 - Actions on structures - Part 3: Actions induced by cranes and machinery
EN 1991-4:2006	Eurocode 1 - Actions on structures - Part 4: Silos and tanks

Table 2: The design codes EN 1992 to EN 1999

EN 1992	Eurocode 2: Design of concrete structures
EN 1993	Eurocode 3: Design of steel structures
EN 1994	Eurocode 4: Design of composite steel and concrete structures
EN 1995	Eurocode 5: Design of timber structures
EN 1996	Eurocode 6: Design of masonry structures
EN 1997	Eurocode 7: Geotechnical Design
EN 1998	Eurocode 8: Design of structures for earthquake resistance
EN 1999	Eurocode 9: Design of aluminium structures

Table 3: Parts of Eurocode 3: Design of steel structures

EN 1993-1-1:2005	Eurocode 3: Design of steel structures - Part 1-1: General rules and rules for buildings
EN 1993-1-2:2005	Eurocode 3: Design of steel structures - Part 1-2: General rules - Structural fire design
EN 1993-1-3:2006	Eurocode 3 - Design of steel structures - Part 1-3: General rules - Supplementary rules for cold-formed members and sheeting
EN 1993-1-4:2006	Eurocode 3 - Design of steel structures - Part 1-4: General rules - Supplementary rules for stainless steels
EN 1993-1-5:2006	Eurocode 3 - Design of steel structures - Part 1-5: Plated structural elements
EN 1993-1-6:2007	Eurocode 3 - Design of steel structures - Part 1-6: Strength and Stability of Shell Structures
EN 1993-1-7:2007	Eurocode 3 - Design of steel structures - Part 1-7: Plated structures subject to out of plane loading
EN 1993-1-8:2005	Eurocode 3: Design of steel structures - Part 1-8: Design of joints
EN 1993-1-9:2005	Eurocode 3: Design of steel structures - Part 1-9: Fatigue
EN 1993-1-10:2005	Eurocode 3: Design of steel structures - Part 1-10: Material toughness and through-thickness properties
EN 1993-1-11:2006	Eurocode 3 - Design of steel structures - Part 1-11: Design of structures with tension components
EN 1993-1-12:2007	Eurocode 3 - Design of steel structures - Part 1-12: Additional rules for the extension of EN 1993 up to steel grades S 700
EN 1993-2:2006	Eurocode 3 - Design of steel structures - Part 2: Steel Bridges
EN 1993-3-1:2006	Eurocode 3 - Design of steel structures - Part 3-1: Towers, masts and chimneys - Towers and masts
EN 1993-3-2:2006	Eurocode 3 - Design of steel structures - Part 3-2: Towers, masts and chimneys - Chimneys
EN 1993-4-1:2007	Eurocode 3 - Design of steel structures - Part 4-1: Silos
EN 1993-4-2:2007	Eurocode 3 - Design of steel structures - Part 4-2: Tanks
EN 1993-4-3:2007	Eurocode 3 - Design of steel structures - Part 4-3: Pipelines
EN 1993-5:2007	Eurocode 3 - Design of steel structures - Part 5: Piling
EN 1993-6:2007	Eurocode 3 - Design of steel structures - Part 6: Crane supporting structures

Journal of Wind & Engineering, Vol. 5, No. 2, July 2008, pp. 40-49

EFFECT OF DESIGN WIND SPEEDS ON OPTIMUM DESIGN OF MICROWAVE TOWERS

Venkat Lute[1] and Akhil Upadhyay[2]

[1] Research Scholar; [2] Associate Professor
Department of Civil Engineering, Indian Institute of Technology Roorkee, India, 247667
vsraodce@iitr.ernet.in, akhilfce@iitr.ernet.in

ABSTRACT

In India a large number of microwave towers are under design or construction to meet the demands of its growing infrastructure. Wind loading is a prime design consideration for such towers. The present paper addresses the objective of finding the optimum design of such towers placed in different wind speed zones of the country. A genetic algorithm (GA) based optimum design tool is developed for the design of microwave towers. All the important design parameters related with size and configuration of the towers are taken as design variables to formulate a more general optimization problem. The design has to satisfy strength, stability and stiffness related constraints. The developed optimization tool is validated with a benchmark problem. Using the optimum design procedure, data base is prepared for the designers to find out the weight of a tower in a given wind speed zone as specified in the Indian Wind Loading Code- IS 875 (Part 3)-1987. A detailed study for 100m tower is carried out. Rigorous numerical experimentation is carried out by varying both the physical and genetic parameters so as to come up with an optimal set of parameters for this problem.

Key words: microwave towers, wind speed zones, genetic algorithms, optimization.

INTRODUCTION

With the rapid increase in the network of electronic communication systems, a large number of freestanding steel lattice towers have been constructed in India and other parts of the world. A great majority of these are microwave towers of heights ranging from 100m to 300m. In contrast to vertical load, lateral load effects on such structures are quite variable and increase rapidly with increase in height. Moreover, the velocity of wind increases with height and the wind pressures increase as the square of the velocity of wind. The continuing burgeoning of taller and more flexible structures has necessitated better understanding of wind effects on structures for improving the design and thus economize on the steel requirement. The microwave tower is a space frame and a higher order indeterminate structure. The overall optimization problem, which gives the least weight design for a given set of load combinations and functional requirements, is a very complex problem involving many design variables governing tower geometry and member size, as well as a number of behavioral and practical constraints related with strength, stability and stiffness. Wind loading is the main load on these towers and collapses of towers due to wind have been reported in India and abroad. Microwave lattice towers are used to support the antenna or relay equipments for transmission of TV and radio signals. In this regard the deflection / rotation control at the top becomes an important design criterion.

GA is a very robust tool for the optimum design of steel structures, particularly slender structures. Adeli and Cheng (1993) used GA for optimum design of space truss structures. Then in order to get solutions for constrained problems, Adeli and Cheng (1994a) presented a GA procedure for three dimensional truss structures using an augmented Lagrangian multiplier to transform the constrained problem to an unconstrained problem. Upadhyay and Kalyanaraman (2000) used the GA for the optimum design of fiber composite stiffened panels to study the robustness of GA in handling mixed type of variables as well as to prove the capability of GA to choose global minima in the presence of large number of local minima. Yoshida (2006) used the Genetic Algorithms for the optimum design of wind turbine towers considering the Aeroelastic characteristics of wind. Jasim and Galeb (2002) optimized free standing towers. They have used a traditional search technique for getting the optimum weight of tower. With traditional techniques there is a possibility to get stuck at local minima. Sivakumar et al. (2004) used genetic algorithms for optimizing lattice towers by object-oriented optimization approach and optimized the weight of a 26m tower considering each panel as an object. In discussing the efficiency and robustness of various optimization methods, (Rozvany, 1998) the optimality criteria methods are most efficient but least robust whereas the random search methods are least efficient but most robust. In this work Genetic Algorithm is chosen for the optimization since it is a directed random search approach and has the advantage of efficiency and robustness. The optimum design formulations available in the literature have limitations. While mostly size optimization is carried out there is a need to tackle all the levels of optimizations, i.e., sizing, configuration etc simultaneously. To fill this gap in the present work, sizing and configuration optimization of tower structure subjected to wind loads is attempted simultaneously using genetic algorithms.

Wind effects

Wind is a random three-dimensional force. However, for towers a two-dimensional wind analysis is generally sufficient. In the present work wind load is treated as being quasi-static. Also, natural frequencies for the tallest tower (100m) are calculated in this work and the lowest frequency is found to be 2.118Hz. As per codal provision of IS 875 (part 3)-1987 dynamic analysis is necessary when the lowest frequency lies below 1 Hz. Hence static analysis only is carried out.

LOAD CALCULATIONS

When a steady wind strikes a tall structure it induces pressure which is a constant at a particular section of the structure. The pressure is required for the calculation of wind force acting on a joint based on the panel area. Figure 1 shows the model of the tower studied, while, Fig. 2 shows the comparison of the main leg forces of the tower when the wind is (i) perpendicular to the face of tower, or (ii) diagonal. It indicates that diagonal wind exerts as much as 26% more force in the leg member compared to perpendicular wind.

The dead load of Antenna, ladder, cables and splices is applied to the tower. The static wind force is worked out as per uniform variation at particular level, and applied at the junction of two panels. For a given basic wind speed, the wind pressure (Fig. 3) on the tower is calculated panel-wise and the corresponding force coefficients (Fig. 4) are based on the solidity ratio (Eq.1) for each panel. Fig. 4 indicates that as the tower cross section remains unchanged the force coefficient remains unchanged. The force coefficient is more at the base of tower since the cross sectional area is more.

$$\text{Solidity ratio}(\phi) = \frac{obstruction \quad area \quad of \quad front \, face}{gross \quad area \quad of \quad the \, front \quad face} \tag{1}$$

Analysis and design aspects

Optimum design requires a number of analysis and reanalysis cycles to converge to the final solution and hence requires computationally efficient as well as reasonably accurate analysis approach. The tower can be analyzed as a spatial structure. However, it has been observed that such a three dimensional analysis

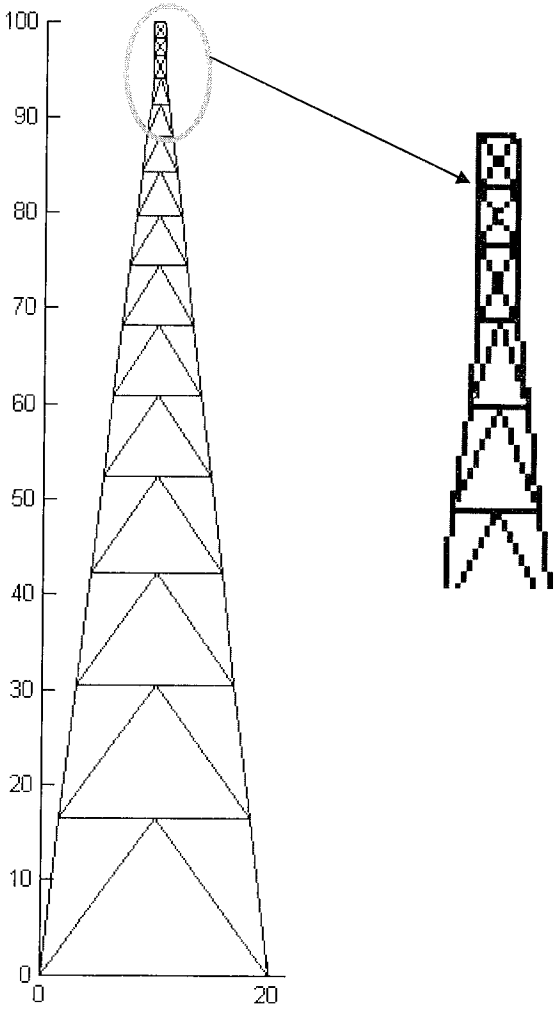

Figure 1. Tower plane frame details

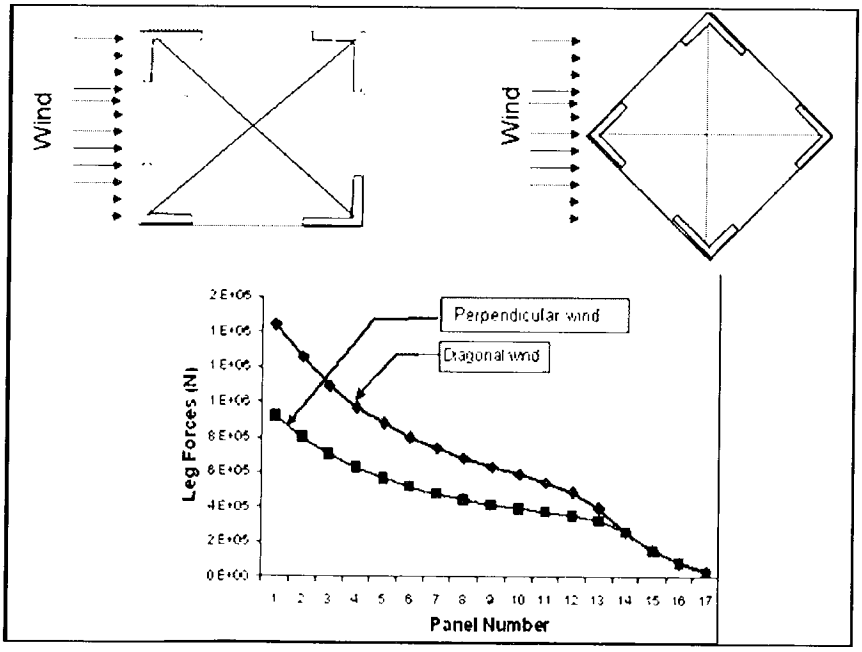

Figure 2. Member forces for perpendicular and diagonal wind

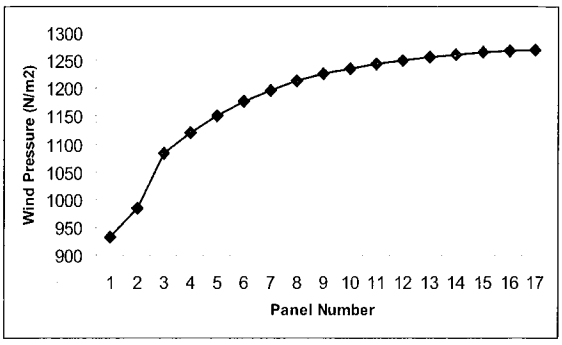

Figure 3. Wind pressure with tower height*

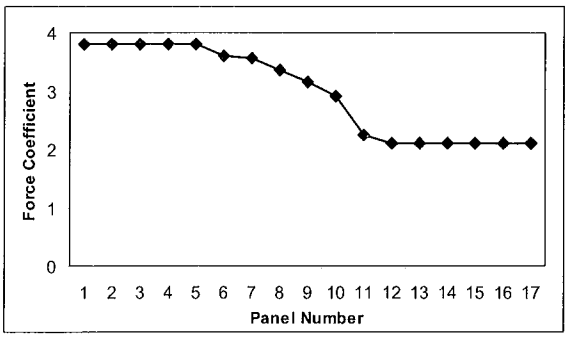

Figure 4. Force coefficient with tower height*

increases the computational work and memory requirement, by several times when compared to the plane truss analysis without appreciable variation in the results. While space truss analysis is ideal, the plane truss analysis of the free standing towers gives practically accurate results for the following reasons:

- The symmetry in the geometrical configuration of the tower
- The inclination of the legs with the horizontal plane is usually large, therefore the interaction between the two mutually perpendicular planes is very small
- The interconnection between the two planes is through horizontal members at panel points. No diagonal bracing between the diagonally opposite columns is usually provided
- The loads are simple and resolve themselves into two mutually perpendicular planes with comparatively small torque. The configuration of tower members is such that the torque is resisted by a pair of plane trusses.

Need and objective of optimization

Since a typical design of steel lattice towers can be used repeatedly for a large number of towers, it is worth optimizing these towers for configuration and member size. By optimizing these tower structures not only is there a saving in weight of steel but there is substantial amount of reduction in wind force on tower. So, rationalizing the tower design helps in saving the material and cost, including that of the foundation. The objective of this study is to see the effect of design wind speed on the design of microwave towers by developing a GA based optimum design procedure with the objective function being the minimum weight, as calculated in Eq (2).

PROBLEM FORMULATION

Objective function f(x): The minimum weight of tower,

$$Min(f(x)) = \sum_{j=1}^{nom} \rho A_j L_j \tag{2}$$

where ρ = density, A_j = member cross sectional area and L_j = member length

Design Variables: Important design parameters are considered as design variables in the present work. The variables are as follows:

- Number of panels in full height of tower (N_p),
- Cross sectional area of all the members of tower (A),
- Base width of tower (B),
- Height linking factor (ζ), in order to reduce the large number of design variables this factor is taken, which indicates the successive panel height in the tower, and
- Number of inclined panels in the tower (N_{Pl})

* Panel 1 is nearest to the base.

Constraints: Each member has to satisfy stress criteria according to design requirement with some factor of safety as recommended in IS specification. If the member is subjected to compressive stress it should be checked according to Eq. (3). The stability is determined in terms of slenderness ratio of member as given by Eq. (4) and the stiffness is checked using permissible deflection of the tower at the top.

Stress constraint is expressed as $$\sigma_{c,all} = \frac{f_y \times \sigma_E}{\left(f_y^{1.4} + \sigma_E^{1.4}\right)^{1/1.4}} \quad (3)$$

$$\lambda = l / r \quad (4)$$

where f_y is the yield stress, λ is the slenderness ratio, σ_E is elastic critical stress.

Methodology

In this work towers of all the usual heights are optimized ranging from 30m to 100m, each for three different design wind speeds. GA based optimization is implemented in MATLAB. The towers are analyzed for static wind loads. Dead load and wind load of tower members, four antennas, ladder, cable tray and other fixtures are included. Both perpendicular and diagonal wind cases are considered. Input data for the optimization program involves general specification of the tower, material specification, structural parameters, load conditions and combinations, variable upper and lower bounds, available sections and its properties, basic wind speed. The optimization program gives weight of each plane frame, separate weight of leg members and bracing members, chosen sections for the leg members and bracings along with the forces for each. The methodology is clearly explained with the help of flow diagram as given in Fig 5.

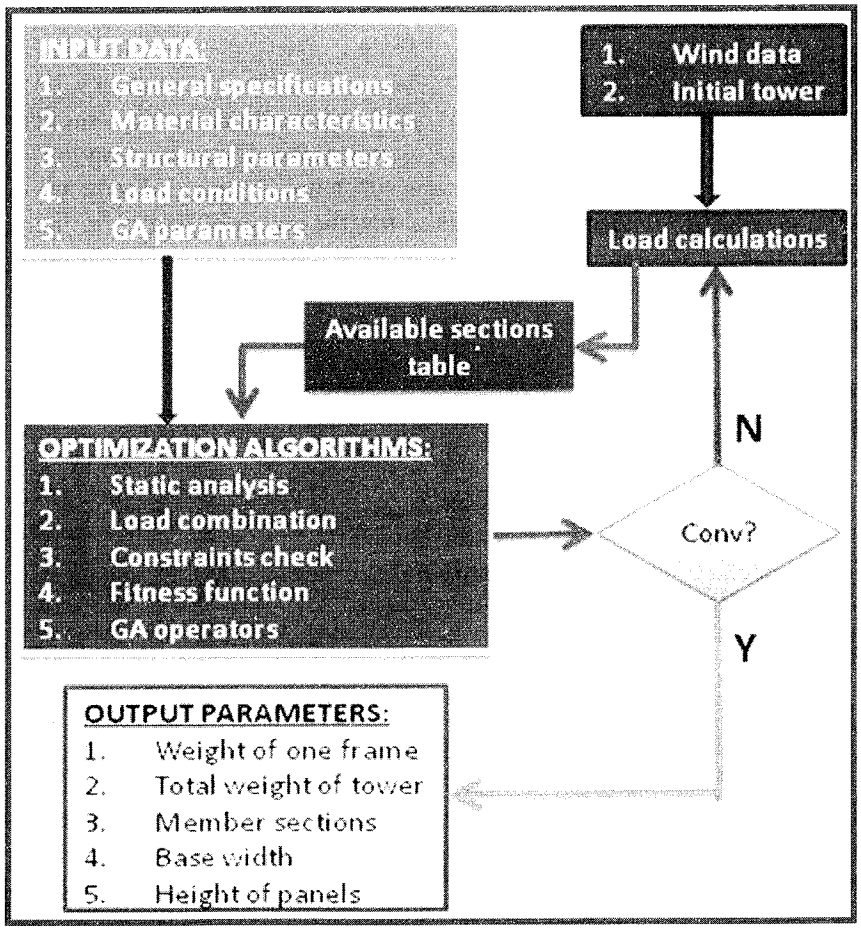

Figure 5. Design flow diagram

GENETIC ALGORITHMS

Genetic algorithms belong to the most popular optimization methods nowadays. These are based on biological principles of evolution and provide an interesting alternative to 'classic' gradient-based optimization methods, and are particularly useful for highly nonlinear problems, where computation time is not a primary concern. The variables in the design space are to be converted into genetic space by transforming the variables in binary form. As referred by Nabeel and Alaa (2002), in the case of discrete variables the set of values are distributed uniformly over a range whereas for continuous variables the selection is done by choosing nearest available discrete value. In this work binary encoding is implemented. The evaluation of GA from generation to generation is performed by three main GA operators: *selection*, *crossover*, and *mutation*. In this work, Roulette wheel selection and two- point crossover is used, wherein the binary strings between two randomly selected crossover sites in the chosen members of population are swapped. The Mutation operator involves switching (from 0 to 1 or 1 to 0) a randomly chosen binary character in the string and is used to improve the probability of finding the global optimum solution. After the genetic operations, the fitness of the solutions corresponding to the members of the new population is evaluated.

Validation of GA

The validation of GA is done taking one standard problem given by Rajeev and Krishnamoorthy (1992) as shown in Fig 6, 3- bar truss. For a given loading and geometry of the truss, design variables, and constraints, the analysis and design is carried out with the MATLAB program. The design variables are member areas and constraint is the limit of deflection. The outer members are assumed to be equal in cross section. The population size is taken eight in this problem and convergence is obtained after 20 generations. The details of 20th generation are shown in table 1. The optimum weight is reported as 146.67N.

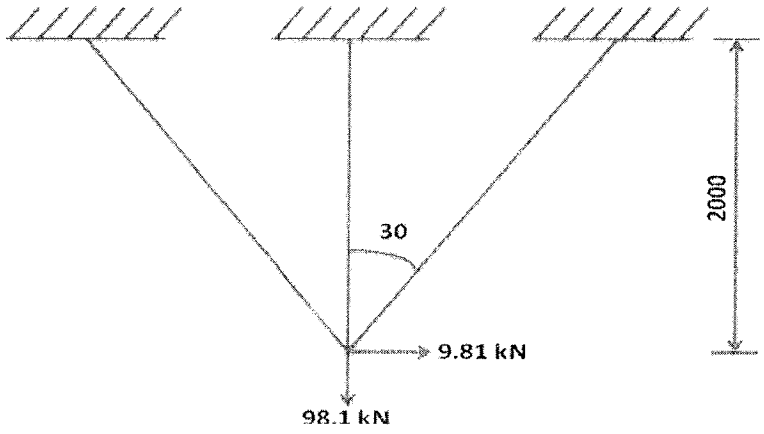

Figure 6. Three bar truss geometry

Table 1: Details of computations for 3-bar truss

Population	A_1 (mm^2)	A_2 (mm^2)	$f(x)$ (N)	σ_1 (MPa)	σ_2 (MPa)	σ_3 (MPa)	u_1 (mm)	u_2 (mm)	C	$\phi(x)$
1	220	440	148.84	145.99	56.77	135.14	1.03	-1.35	0.000	148.84
2	280	440	170.59	126.60	56.50	122.03	0.81	-1.22	0.000	170.59
3	300	340	162.14	133.55	68.12	134.47	0.75	-1.34	0.000	162.14
4	340	300	170.36	128.07	70.34	132.23	0.66	-1.32	0.000	170.36
5	400	260	185.83	118.91	69.84	125.79	0.56	-1.25	0.000	185.83
6	300	300	155.86	139.40	73.96	142.20	0.75	-1.42	0.000	155.86
7	340	180	151.52	147.21	89.48	157.75	0.66	-1.57	0.072	261.37
8	240	380	146.67	147.26	65.47	141.78	0.94	-1.41	0.000	146.67

PARAMETRIC STUDIES

To study the effect of change in various genetic algorithm parameters, parametric study is carried out. The parameters include the number of panels, heights of panels, and size of population. The effect of variation in the above parameters on the optimum tower weight is illustrated with Figures.

1. Population size: Appropriate population size in GA is needed to avoid trapping in local minima. For 100m tower optimization four different population sizes are tried. The convergence study (Fig.7) indicates that when the population size is approximately equal to the design variables, i.e. 60 the optimum weight is obtained. With this population size, one tower design problem is solved at five different times and maximum deviation from the mean optimum weight is found to be 2.4%. This indicates that the selected size of population is appropriate for the current problem.

2. Number of panels: In a given tower the optimum number of panels is a very important parameter to decide. For three different wind speeds, keeping all other parameters constant, and tower height of 100m, the optimum number of panels are given in Fig.8. For wind speeds of 44 m/s and 50m/s, the optimum number of panels is 14 where as for 39m/s basic wind speed the optimum number of panel is 15. This indicates that optimum number of panel reduces with increase in wind speed.

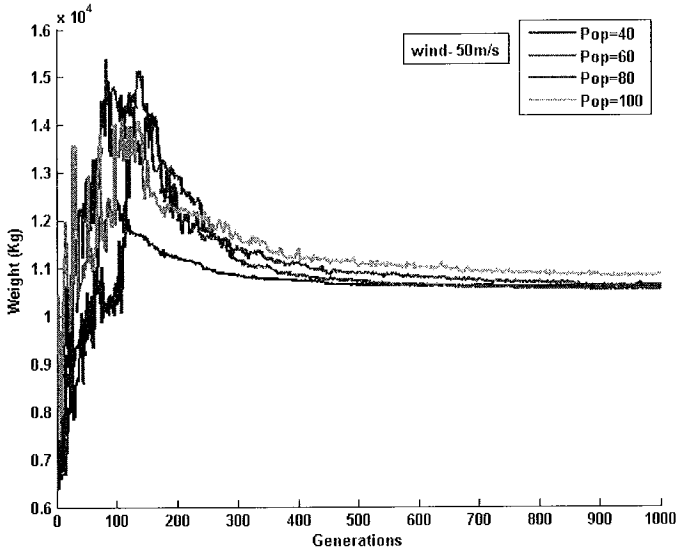

Figure 7. Effect of variation in population size

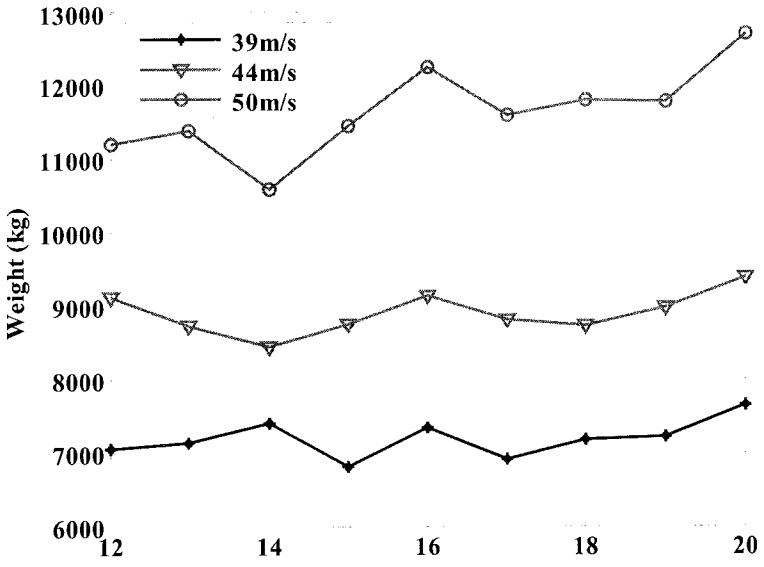

Figure 8. Variation of panels with weight

3. Tower weights v/s wind speeds: The study is conducted for six different towers with practical tower range from 30m to 100m. Figure 9 shows that at lower height the variation in wind speed does not have any significant variation in design. However for larger heights the design gets affected by the wind speeds. For 30m tower, difference in weight for wind speeds 39m/s and 50m/s is 20%, while for 100m tower it increases to 55%.

4. Optimum design Results: The generation history for 100m tower for 500 generations for all the parameters as indicated in Fig.10 shows that the optimization algorithm will converge for 350 generations. The initial high fluctuation is because of violation in the design constraints.

Optimum design studies are carried out for 100 m tower for three different wind zones keeping all other parameters constant and the optimum weight and details of optimization output is given in Fig.11. This study gives the data base for the designers for preliminary estimation of the cost of tower for different wind speeds.

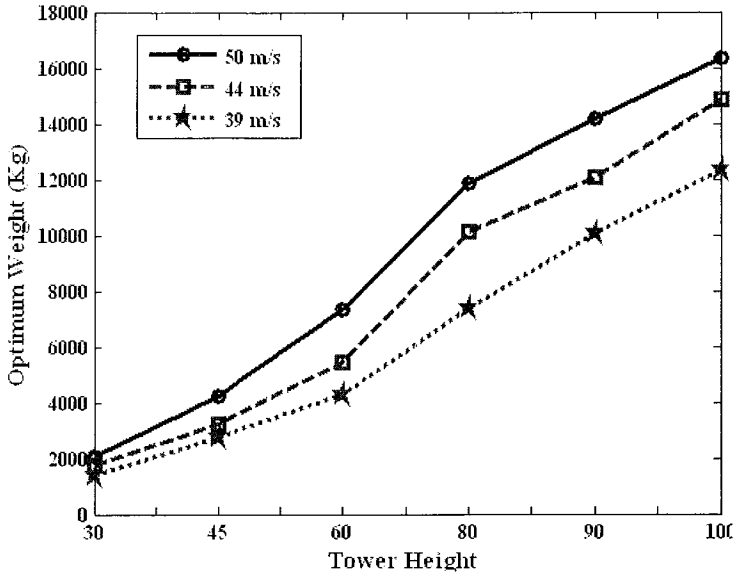

Figure 9. Optimum weights for different design wind speeds

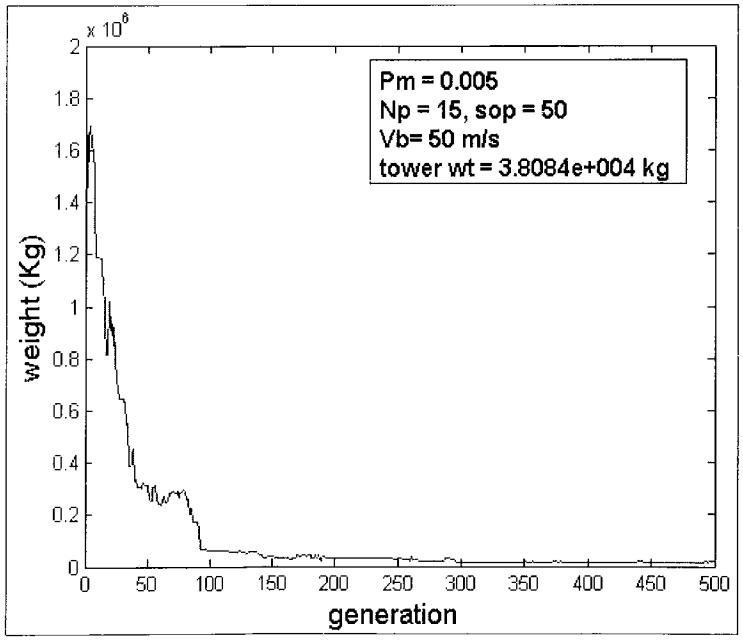

Figure 10. Generation history for 100m tower

Panel Number	Wind Zone (Vb = 39m/s)					Wind Zone (Vb = 44m/s)					Wind Zone (Vb = 50m/s)				
	section			Panel Height (m)	Leg forces (Kgf)	section			Panel Height (m)	Leg forces (Kgf)	section			Panel Height (m)	Leg forces (Kgf)
	Leg Member	Diagonal Bracing	Horizontal Bracing			Leg Member	Diagonal Bracing	Horizontal Bracing			Leg Member	Diagonal Bracing	Horizontal Bracing		
1	200x25	65x8D	70x8	17.26	133630	200x25	65x10D	60x6D	20.73	167170	200x25	65x10D	60x10D	19.55	217750
2	200x25	65x5D	60x5D	14.50	112720	200x25	60x8D	60x5D	16.58	136430	200x25	60x10D	60x6D	15.90	180660
3	200x18	50x5D	55x8	12.18	97221	200x25	55x10D	70x8	13.27	114300	200x25	60x8D	60x8D	12.93	152630
4	200x15	55x8	55x10	10.23	84995	200x18	55x5D	60x5D	10.61	97770	200x25	60x6D	55x8	10.52	131450
5	150x18	55x8	60x5	8.59	75596	200x15	50x5D	50x5	8.49	85450	200x25	60x5D	65x5	8.55	114990
6	150x18	60x8	70x6	7.22	67961	150x18	50x6	55x5D	6.79	76088	200x18	55x10	60x5	6.96	102310
7	150x15	50x6	50x5	6.06	61849	200x15	50x5D	50x5D	5.43	68547	200x18	50x5D	60x5	5.66	92351
8	150x15	65x6	65x8	5.09	57221	150x15	55x6	50x5	4.35	62424	200x18	55x5D	50x6	4.60	84327
9	150x15	50x5	60x5	4.28	53587	150x18	50x6	60x8	3.48	56997	150x18	65x5D	55x6	3.74	77663
10	130x15	50x5D	50x5	3.59	50673	150x12	50x6	55x5	2.78	51717	150x18	50x5	60x10	3.04	71564
11	150x12	50x6D	60x6D	3.02	48180	110x15	50x5D	55x6	2.23	45908	150x15	60x5D	55x5D	2.48	65092
12	110x15	55x6	65x5	2.54	45753	110x15	50x5	50x5D	1.78	38696	150x15	60x8	60x5D	2.01	57100
13	130x10	55x10	-	2.13	34791	110x12	50x5D	-	1.42	29017	110x15	55x10D	-	1.64	42733
14	100x10	60x5	-	1.79	17963	75x8	55x8	-	1.14	14500	90x12	55x10	-	1.33	21484
15	90x6	65x8	65x6	1.50	5800.6	75x5	55x6	50x5D	0.91	4839.3	75x6	55x8D	55x8D	1.08	6727.5
	Tower height (m) =				**100**	**Tower height (m) =**				**100**	**Tower height (m) =**				**100**
	Base width (m) =				**19.03**	**Base width (m) =**				**20**	**Base width (m) =**				**20**
	No. of inclined panels =				**12**	**No. of inclined panels =**				**12**	**No. of inclined panels =**				**12**
	Number of panels =				**15**	**Number of panels =**				**15**	**Number of panels =**				**15**
	Total weigth (Kg) =				33389	**Total weigth (Kg) =**				39742	**Total weigth (Kg) =**				**44959**

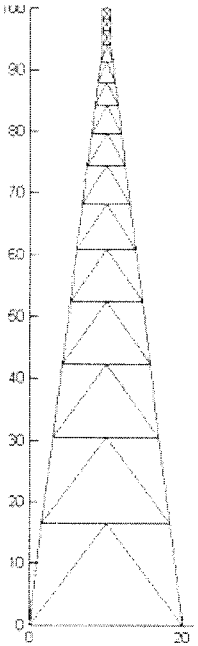

Note: 1.Panel numbering is from bottom to top
2. All the sections are equal angles

Figure 11. 100m Optimum tower design detail

SUMMARY AND CONCLUSION

Wind sensitive structures are a potential area where the designer may gain savings. However as indicated by this study these savings become significant for taller structures. In order to evaluate the efficiency of the optimum design procedure, several design studies were carried out and the observations are as follows:

- The present procedure is efficient in handling large and mixed type of design variables and capable of giving practical feasible optimum designs.
- The effect of wind speed on towers of lower height is less than on higher towers. For 30m tower, the increase in the weight of tower for a wind speed increase from 39m/s to 50m/s is 20%, whereas for 100m tower it is 55%.
- The optimum number of panels for a 100m tower is obtained as 15. It is observed with respect to the optimum number of panels that towards the lower side (13 panels) the weight is 24% more, and towards the higher side (17 panels) the weight is 15% more.
- For a given height of tower, as wind speed increases, the number of panels in optimum design reduces

REFERENCES

1. IS 875(part 3)-1987 (Nov.1998) "Indian Standard Code of Practice For design loads (other than Earthquake) for buildings and Structures", *Bureau of Indian standards, New Delhi.*
2. MATLAB version 7.1
3. Nabeel, A.J. and Alaa,C.G, "optimum design of square free-standing communication towers" *J. of Constructional Steel Research*, 2002, Vol. 58, pp 413-425.
4. Jasim, N.A. and Galeb, A.C., "Optimum design of square free-standing communication towers" *J. of Constructional Steel Research 58*, 2002, pp413–425
5. Rajeev, S. and Krishnamoorthy, C.S., "Discrete optimization of structures using genetic algorithms", *ASCE J. Of Str. Engg.*, 1992, Vol.118 (5).
6. Rozvany, G.I.N., "Topology optimization of multipurpose structures" in: Steven G.P, Querin, O.M, Guan,H., Xie,YM., editors. *Proceedings of the Australasian conference on structural optimization.* Australia: Oxbridge Press (1998).
7. Sivakumar, P., Rajaraman, A.,and Knight, G. M. S., Ramachandra murthy, D.S. "Object-Oriented Optimization Approach Using Genetic Algorithms for Lattice Towers", *J. of Computing in Civil Engg.*, 2004, Vol. 18(2), pp 162-171.
8. Upadhyay, A and Kalyanaraman, V., "Optimum design of fibre composite stiffened panels using Genetic Algorithms" *Engineering optimization,* Vol. 33, 2000, pp. 201-220
9. Yoshida, S. "Wind Turbine Tower Optimization Method Using Genetic lgorithm" *Wind Engineering Volume 30,* No. 6, 2006, pp 453-470.

Journal of Wind & Engineering, Vol. 5, No. 2, July 2008, pp. 50-59

e-wind: AN INTEGRATED ENGINEERING SOLUTION PACKAGE FOR WIND SENSITIVE BUILDINGS AND STRUCTURES

Chii-Ming Cheng, Jenmu Wang, Cheng-Hsin Chang

Wind Engineering Research Center, Tamkang University, Taipei, Taiwan

ABSTRACT

This article introduces "*e-wind*" program that is currently under development at Wind Engineering Research Center at Tamkang University. *e-wind* is an effort to integrate the available wind engineering tools, such as wind code, aerodynamic database and analytical procedure, towards an efficient wind resistant design process for building designers. Special IT tools, such as Artificial Neural Network and Expert System are used to integrate all the components together forming a solution package that can be used by an average structural engineer. The latest information and web technologies were adopted to construct a user friendly interface so that the system would be easily accessible and constantly updated. The current status of the wind engineering components and the IT keys for *e-wind* are briefly discussed.

Keywords: Wind Code, Wind Load, Interference, Aerodynamic Database, Expert System, Buildings, Wind tunnel, CFD, Neural Network.

INTRODUCTION

The Wind Engineering Research Center at Tamkang University (WERC-TKU) has set its long term goal to be a pioneer to explore the new frontiers of wind engineering. At the time WERC-TKU has also set a pragmatic self-positioning for the next 5~10 years as a regional research institute aiming to promote wind engineering education, collaborative research activities and acting as a wind engineering solution provider of that region. Under such guideline, research resources have been allocated to programs related to these ends. Currently, two long term wind engineering research programs are in progress at WERC-TKU, and these are: field monitoring and *e-wind*. The field monitoring program covers three areas, viz. wind field characteristics, tall buildings and cable stayed bridge responses. The objectives of the monitoring program are to generate data for future building wind code revisions and also to provide lead to directions of future research. The objective of *e-wind*, is to apply the latest information and web technologies to integrate several key components of wind engineering and develop an engineering solution package for wind sensitive buildings and structures. This article will be focused on the *e-wind* program.

There are two different types of wind engineering issues for buildings and structures: appropriate structural design for the global and local wind pressures, and suitable environment for building inhabitants and pedestrians nearby. In the case of structural wind resistant design of buildings and structures, there exist two common practices: wind codes are used to provide design wind loads for the majority of buildings and structures, and wind tunnel tests for some high-rise and large span structures. In most wind codes, the aerodynamic assumptions of isolated and regular shaped (rectangular) building coupled with the simplified structural models were adopted to evaluate buildings design wind loads. Nevertheless, for many structural

engineers, the wind resistant design posts a much more difficult challenge than earthquake design due to lack of basic training in wind engineering. It is not unusual to find errors in wind resistant design practice. For buildings and structures with irregular shape and/or structural properties, wind tunnel tests are used. However, in many cases, building geometry and structural system are decided based on the wind code prior to the wind tunnel test. Since wind codes may not be appropriate for these special buildings and structures, it will be time consuming and costly to make major design changes. Therefore, an alternative approach is needed to provide an economic yet reasonably accurate solution for the design of wind sensitive buildings and structures; at least at the stage of preliminary design. The idea of *e-wind* has originated from these needs of engineering practice.

Incorporating the information and web technologies with aerodynamic database to assist wind resistant design is by no means a new idea. Kareem (1990) constructed an aerodynamic database based on the HFFB measurements of building models with several cross-sectional shapes and various aspect ratios, in two different turbulent boundary layer flows; and later on integrated those data into the first interactive wind load database (Zhou *et al*, 2003). At Wind Engineering Research Center of Tamkang University (WERC-TKU), an aerodynamic database for high-rise buildings (Cheng *et al*, 2003) based on wind tunnel experimental data was established and a wind load expert system for tall buildings utilizing the database was developed shortly after (Wang and Cheng, 2005). Several databases, including wind pressure, cross ventilation and air pollution, are under continuous development as part of the COE program of Tokyo Polytechnic University (Quan *et al*, 2007). NIST's aerodynamic database of low-rise buildings and database-assisted design approach (Kopp and Chen, 2006) are alternative design methods and their development is in progress.

The aforementioned are only a few examples among numerous efforts being made at various wind tunnel labs across the world that develop database and software technology to adapt wind engineering to the computer era. However, it is the authors' observation that almost all existing aerodynamic databases are limited in industrial applicability and often require certain degree of wind engineering expertise to be able to use them properly. There is not yet any aerodynamic database that is sufficient in both wind engineering contents and accessibility to provide wind resistant design solutions to the general structural design community. During the course of developing the expert system for Taiwan building wind code and the prototype expert system for tall building resistant design, the authors felt that most building designers feel themselves to be aliens to the modern building wind codes and the increasingly sophisticated analytical wind load estimation procedures. To benefit the building design community, the aerodynamic database needs to have not only the relevant wind engineering contents but also user friendly interface and good accessibility. These thoughts shape the program of *e-wind*.

THE FRAMEWORK OF *e-wind*

The success of *e-wind* is built on three pillars; they are: abundant wind engineering elements, appropriate IT keys to integrate the wind engineering components, and the latest information and web technologies to facilitate the user friendliness and easy accessibility. The common wind engineering issues are: design wind loads for structural system, design wind pressures for cladding, motion uneasiness of building inhabitants, pedestrian comfort near buildings, air quality and energy conservation through ventilation. Generally, codes, regulations and criteria are the basis of engineering design to meet these needs. For special buildings and structures, advanced analytical models, wind tunnel simulations or CFD are used to solve these problems. Excluding the

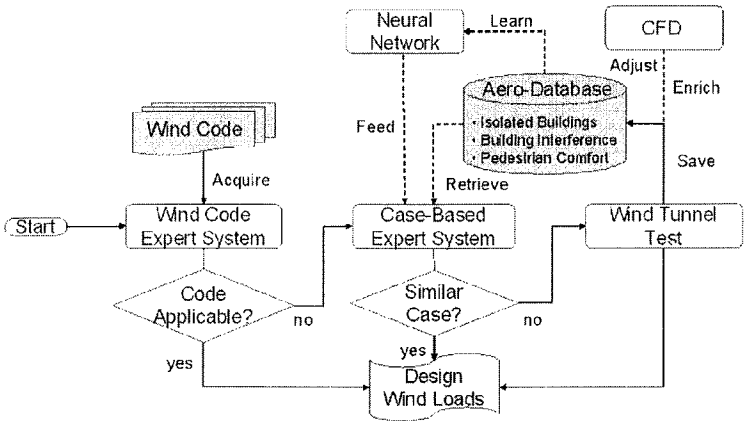

Figure 1: The framework of *e-wind*

time consuming and costly full-blown wind tunnel or CFD simulation, the wind engineering elements of *e-wind* should include the necessary codes and criteria, wind tunnel aerodynamic databases, and databases consisting of case studies by either analytical model or CFD simulations. Finding a solution of a multi-parametric problem from several databases is a challenging task even for a well trained wind engineer. Integration of all the components in developing a solution package that can be used by an average structural engineer requires special IT tools. Based on the reports in the literature and some experience, Artificial Neural Network (ANN) and Expert System (ES) are chosen for this purpose. The next important feature of *e-wind* is applying the latest information and web technologies to construct a user friendly interface and to make the system easily accessible and constantly updated. Figure 1 shows the framework of *e-wind*. Solid lines are the working links between components, and dashed lines represent the links which are not yet fully developed. The essential components of *e-wind* will be discussed in detail in the following sections.

WIND ENGINEERING ELEMENTS

An on-line program for education and applications of building wind code

The *Specifications for Building Wind Resistant Design* (ABRI, 2006) became the official wind load provisions of Taiwan building code in 2007. Since it was a major overhaul from an obsolete building wind code, WERC-TKU is developing an on-line education and application program to assist the building designers to have better comprehension of the new wind code.

A web-based building wind code expert system

The design codes and standards for wind resistant design are often complex and prone to misinterpretations. The comprehension of wind code and calculation of design wind loads are difficult and time-consuming for designers who have insufficient wind engineering training. Therefore, a web-based building wind code expert system was developed by WERC-TKU and put to on-line service in 2007, in which, Taiwan's new wind code and the logical flow of calculations were coded in rules, and a rule-based online expert system was developed for generating design wind loads according to the design standards. The user interface is built on Internet browsers using mostly Java Server Page (JSP), and the knowledge base and inference engine are on a MS IIS server. Engineers can go through a guided process to input building geometry, surroundings and structural properties in a step by step manner. The expert system finds the appropriate section of the code and calculates the necessary coefficients and parameters. Finally, it works out the wind load distributions for structural designs. The application areas of the system cover the evaluation of design wind loads for structural systems and design wind pressures for claddings. The generated wind loads and pressures can be listed in tables, and downloaded in both text and Excel formats. Various loading curves can be plotted using web-charting software. For documentation and explanation purposes, calculation procedures, including the equations and coefficients used, can be generated at the end of each session for viewing and printing. Screen shots of the system are shown in Figure 2.

The latest version of the wind code expert system has the ability to import data from and export data to a popular structural analysis package. Building geometry and structural properties can be imported from the input files of the package to avoid repeated data inputs. The final wind load analysis results can be inserted into the input file for structural analysis.

Wind code e-learning program

Even though Taiwan is located in a region with frequent occurrence of strong typhoons, there are only limited number of colleges and universities that offer any form of wind engineering courses. As a result, most of the practicing structural engineers and many design offices do not have sufficient expertise to perform appropriate wind resistant designs. Misinterpretation of the building wind code is not a rare event. In order to provide wind engineering education to the practicing structural engineers in Taiwan, an *e-*

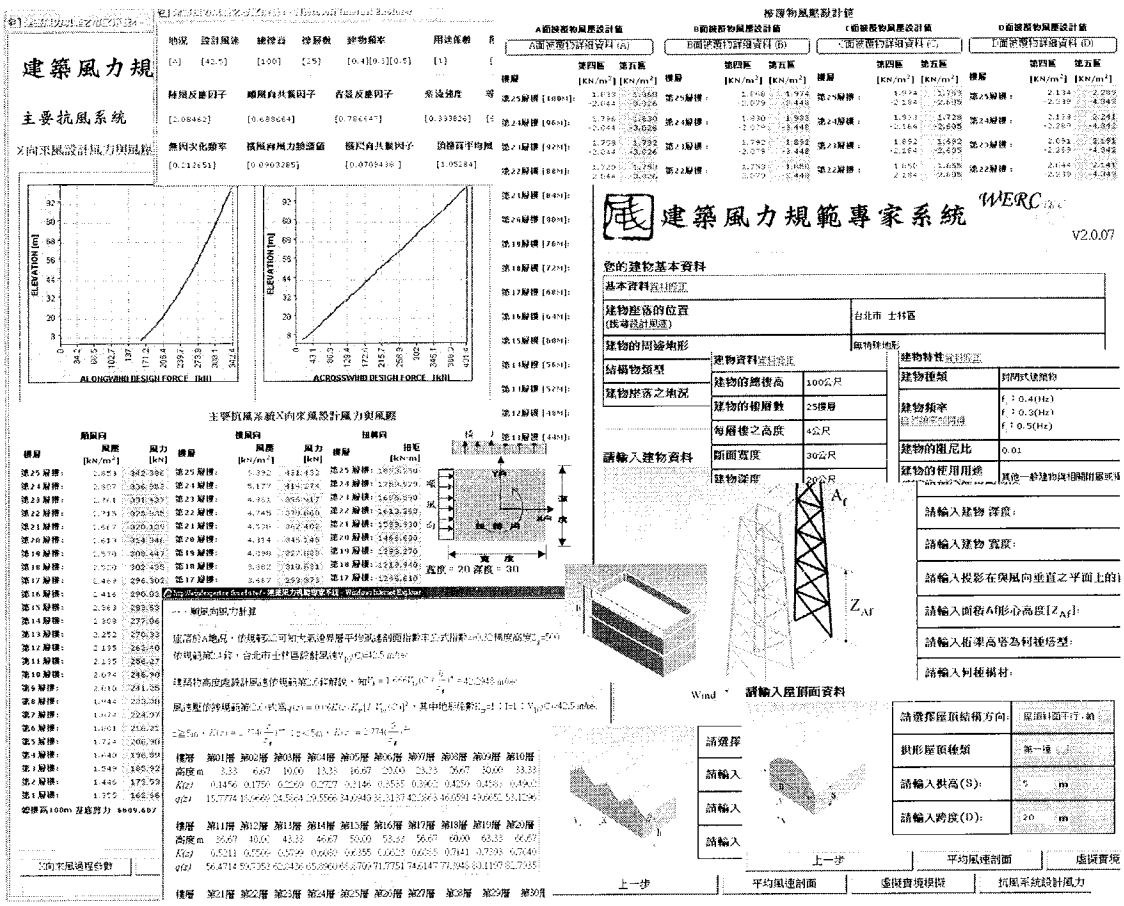

Figure 2: The user interfaces of the building wind code expert system

learning program dealing with the building wind code is under preparation and will be put on-line in the first half of 2008. The so called *e*-learning contains lectures on: atmospheric boundary layer, building aerodynamics, building wind code and examples on design wind load calculations. Utilizing the latest video compression and streaming techniques, the lectures of the above subjects, being composed of presentation slides and instructor's voice elucidations, can be viewed directly on the web.

Design wind loads aerodynamic database

Aerodynamic database for isolated tall buildings

Wind tunnel measurements and their analysis of various generic building shapes have been performed to establish the base of the expert system. A total number of 70-plus building shapes have been studied so far. Most of the building models were tested in both open terrain and city environment flow fields (α=0.15, 0.32). Some models were tested in suburban and coastal environments (α=0.25, 0.10). The wind force coefficients and reduced force spectra in the alongwind, acrosswind and torsional directions of most models were measured through HFFB, whereas some were measured through multi-channel electronic pressure scanning system. The database can be categorized into five sets of models. The first set consists of various generic building shapes functioning as the core of the database; it includes: (i) rectangular with different cross sectional side ratio, (ii) polygons (circular, triangular and rectangular), (iii) L shaped cross-sections and (iv) a few irregular shapes. The second set of building models have square cross-section with a secondary cross sectional modifications, including different aspect ratios, corner chamfering, and two types of recess sections. The third set consists of models with multiple of cross-sectional parameter variations, which will also be used as the validation of the model selection procedure. The fourth set consists of the rectangular

shaped pressure models with different side ratios and aspect ratios. The fifth set consists of the pressure models of the "real life" buildings. For the fourth and fifth sets, besides the global wind loads, the characteristics of local wind loads are also available through the simultaneous pressure measurements.

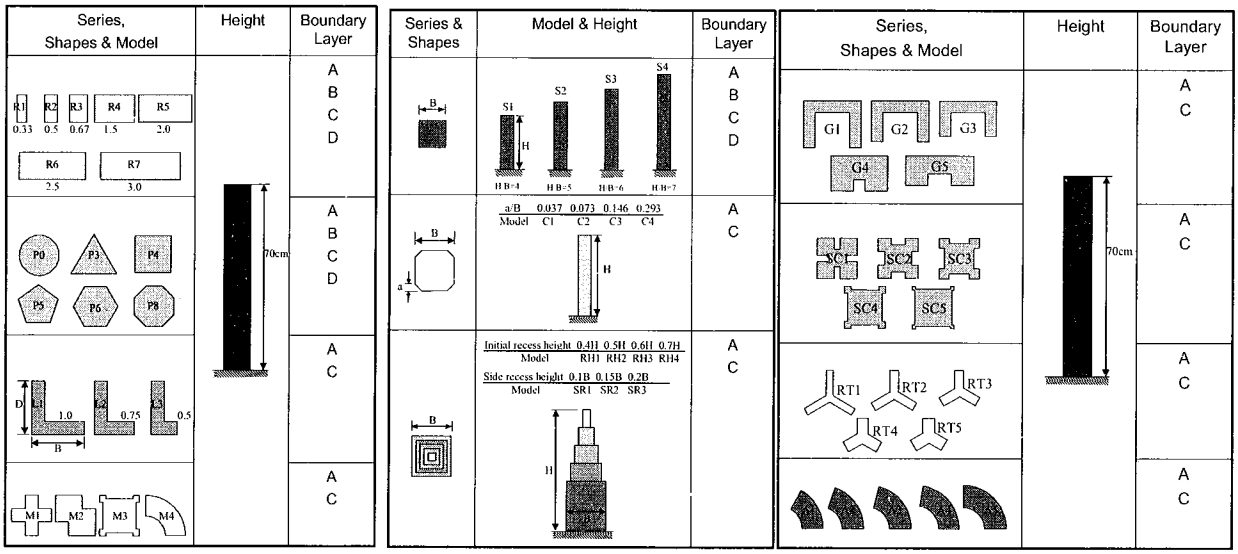

Figure 3: Geometric shapes of the isolated tall building aerodynamic database

Aerodynamic database for the interference effects of two adjacent tall buildings

The current aerodynamic database for building interference can be divided into three parts. The first part focuses on the interference of a pair of identical square shaped prisms. The second part of the database consists of the geometric effects of the principal building while the interfering building remains to be the square shaped prism. In the present database, rectangular prisms of aspect ratio H/"A=6, and side ratio, B/D=0.5 & 2.0 and circular cylindrical models were used as the principle building. The geometric variations will be extended to other cross-sectional shapes and aspect ratios in future. The third part consists of the interference effect of a square shaped principal building under the influence of another rectangular shaped building with width ratio R_B= 0.75, 1.0, 1.5, and height ratio R_H= 0.75, 1.0, 1.25. All the three parts of wind tunnel tests were repeated for the three turbulent boundary layers, BLA ($\alpha = 0.32$), BLB ($\alpha = 0.25$) and BLC ($\alpha = 0.15$). Using HFFB technique, the alongwind, acrosswind and torsional wind loads of the principal building were measured when the interfering building was placed at different locations over an area of x:(-3B, 13B) × y:(-6B, 6B), in which x is the alongwind axis and y is the acrosswind axis. In order to obtain sufficient information when the two buildings are standing closeby, extra measuring points were considered for the spacings less than 1.0 B. Due to the geometrical symmetry, actual wind tunnel measurement covered only half of the area of interest as shown in Figure 4. Total of 131 measurements were taken for the case of

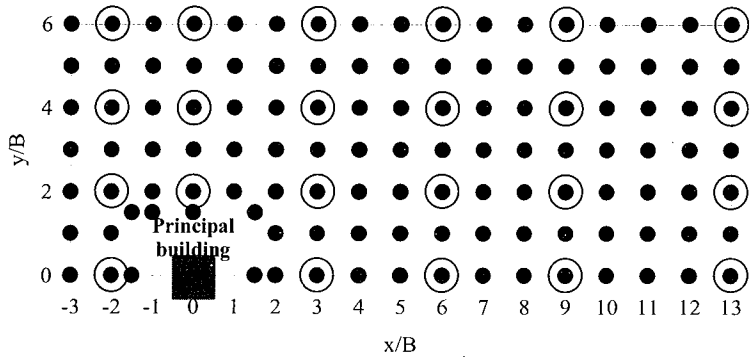

Figure 4. Grid system for the wind tunnel experiment • measurement points for two identical square shaped buildings ⊙measurement points for building with geometry variations

two identical square shaped buildings, and 23 measurement points for the rest of the wind tunnel test cases.

A fourth set of interference studies considering the cases of closely placed group of buildings in the same development site, will be added to the database. Tentatively, pressure model will be used for this set of data to evaluate interference of both global wind loads and local cladding pressures.

Aerodynamic database for other buildings and structures

Besides tall buildings, the aerodynamic databases for the other two building types are under preparation. They include low-rise buildings and spherical roof domes. Systematic wind tunnel pressure model measurements were conducted to build an aerodynamic database for low-rise buildings (Ho and Chen, 2007). Regarding wind loads on low-rise buildings, the significance of the geometry was the most important factor. The basic shapes of the testing models include gable buildings, cylindrical structures and domes. The variation of depth-to-height ratio, slope of roof and angle of attack of approaching flow were also considered. A simulated turbulent boundary layer with open terrain characteristics was used as the approaching flow. Prior to including the data into database, a 1/50 scale model of the Texas Tech Building was tested and the results were compared with the field measurements for validation. The mean, fluctuating and peak pressure coefficients of all the models were calculated and the contour maps were accordingly drawn. Furthermore, for the investigation of suitable design wind loads on low-rise buildings, a simply supported frame was set as the analysis target. The structural responses of the structure were estimated by the covariance integration method, and the results taken as the design limits. Based on this principle, a more systematic procedure for evaluating the design wind load for low-rise buildings will be developed to put the aforementioned aerodynamic database into full usage.

Similarly, wind tunnel testing on a typical spherical roof dome, representing a large span stadium, is underway. This work is currently at the initial stage of determining the proper wind tunnel testing condition to eliminate the possible Reynolds number effects. Tentatively, this database which is under development will exhibit mean, RMS and peak pressure distributions on spherical dome models with various roof-rise/span ratio and wall-height/span ratio. Analytical procedures for equivalent static design wind loads and the time domain analysis for large span dome structures are currently under study.

CFD on aerodynamic database

HFFB and electronic pressure scanning system have simplified the work load of wind tunnel tests significantly, and make the aerodynamic database a valid wind resistant design tool. Still, wind tunnel experiments have their inherent shortcomings. One of the most severe limitations is the Reynolds number discrepancy of the scaled model, especially for curve shaped buildings and some of the cross-sections with obtuse angle such as octagons. Reynolds number effect on curve shape bluff bodies is a generally understood problem, yet extremely difficult to resolve by physical modeling procedures. Rapid developments in both computer hardware and software have created a possible environment for the practical applications of CFD to simulate flows within and around buildings and other structures in recent years. CFD can play two important roles in *e-wind*, these are: (i) adjustment for Reynolds number effects; (ii) alternatives to enrich the aerodynamic database, especially for secondary parameter variations. Currently, WERC-TKU is developing an efficient scheme of digital turbulent boundary layer flow field for CFD simulation on building models.

An on-line real time scheme for pedestrian comfort assessment

Wind induced pedestrian comfort is an important issue of the environmental impact assessment of a sizeable urban development project. Since there are too many factors which influence the pedestrian level wind characteristics, it is extremely difficult to quantify the effects of the geometric shape of the building and orientation on the pedestrian wind level at planning stage. The basic concept of this project is to perform a preliminary on-line analysis that could produce sufficient data to form a design guide on pedestrian comfort

assessment at planning stage. To achieve this goal, the solution package requires two ingredients: a time efficient CFD simulation scheme for pedestrian wind assessment and an aerodynamic database for sheltering effect by different windbreak facilities.

CFD simulation for pedestrian wind assessment

The basic scheme of the CFD simulation on the pedestrian level wind characteristics is as follows:

i Building designer provides the size and basic geometric shape of the main building, and basic geometric shape and the relative location of the surrounding buildings within the CFD computational domain. All the buildings are modeled with basic 3D elements such as rectangular prisms. The designer also has to provide the information of terrain category for choosing the power law index α and the gradient height δ of approaching wind velocity profile.

ii After all the data as described above are provided to the system, it automatically produces CFD executable files. Under the high-speed computation core, the executable files can automatically generate computational domain and meshes, inflow velocity profile and other boundary conditions. The wind speed contours at pedestrian level can then be calculated.

iii From the CFD simulation results, the significant wind speed acceleration regions around the main building can be identified.

Currently, several CFD codes that have potential to meet these requirements are under evaluation.

Aerodynamic database for sheltering effect by different windbreak facilities

When the orientation and geometric shape of the main building have been determined, the influence of wind speed on pedestrians can be improved by constructing landscapes and wind sheltering facilities. The affiliated constructions that can be chosen to lower the wind speed at pedestrian level are provided below:

i Trees: Tree planting can reduce airflow to lower the wind speed influence on pedestrians.

ii Canopies: Strong wind always happens at the bottom of tall buildings. It can be improved by constructing canopies or rainproof structures to reduce the direct effects of the downwash flow on pedestrians.

iii Fences: Windbreak fences or wind-break nets can act as sheltering and filtering devices to the surface wind field.

An aerodynamic database focusing on the sheltering effects of trees, canopies and fences, with parameters such as sizes, geometric shapes and relative distances to the high wind-speed spots, will be developed to provide a solution package on pedestrian comfort.

IT KEYS FOR *e-wind*

Artificial Neural Network scheme for the integration of aerodynamic databases

Building aerodynamic database with sufficient contents for practical purpose is a tedious and time consuming task. To integrate the components of the aerodynamic database and make it functional is a much more difficult challenge. Since the design wind loads on buildings with different geometrical shapes and under the influence of adjacent buildings are functions of multi-variables in non-linear form, it is almost an intractable task to derive a set of general purpose empirical formulae for this complicated phenomenon. In order to merge all the databases into one package that yield on-line solutions, an alternative approach is to apply proper IT techniques that are suitable for this kind of task. Currently, the Artificial Neural Network (ANN) technique is adopted to integrate the information in different compartments of the aerodynamic database. ANN has been used by several researches for the problem of building interference (Khanduri et al, 1997, English and Fricke, 1999, Zhang and Zhang, 2004). The basic theory and the rules of application

of neural networks on building interference phenomenon were well explained by Khanduri *et al.* (1997). However, past works on the ANN application were all on rather confined domains, such as a specific interference effects on wind loads on a specific shape of principal building. The aim of *e-wind* is not only to estimate the effect of building interference, but also for the complete building wind resistant design when it is used together with the wind code or/and single building database. ANN may not be able to carry the designated task by itself; nevertheless, it could be one of the key IT tools to integrate various wind engineering components. Figure 5 shows the prediction of the Interference Factors by RBF Neural Network. The two data points that strayed away from the exact line are predictions outside the range of experimental parameters, i.e., extrapolation of database. In other words, the initial work suggests that neural network prediction should be limited to interpolation of aerodynamic database.

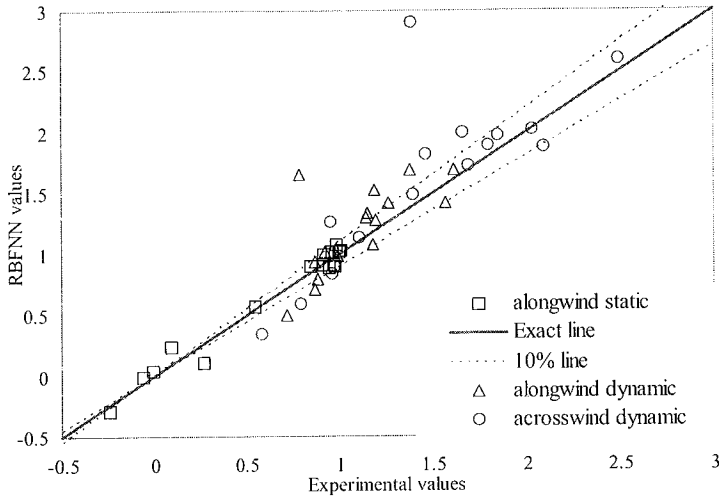

Figure 5: Predictions of Interference Factors by RBF neural network

A web-based expert system for easy access and application of aerodynamic database for tall building wind resistant design

A case-based expert system based on the aforementioned aerodynamic database for isolated tall buildings was developed. The expert system incorporates not only the aerodynamic database but also analysis procedures of structural dynamics, wind load modification methods and heuristic knowledge of wind engineering. Case-based reasoning and web programming techniques were used to implement the system. Based on the client-server architecture, the user interface was built on Internet browsers mostly using Java Server Page (JSP). Similar cases can be selected, and design wind load modifications can be performed using correction factors calculated by numerical programs written in Fortran and MATLAB. In addition, web-charting software is used to produce figures of wind spectra and loading distributions. Typical screen shots of the system are shown in Figure 6. The system can be used at the preliminary design stage to get reasonably accurate design wind loads without performing costly and time-consuming wind tunnel tests.

INFORMATION AND WEB TECHNOLOGIES FOR *e-wind*

A powerful cyber infrastructure is essential to support the operation of *e-wind*. Because of the wide range of tools and software being involved, the operation of *e-wind* can be complicated. Hiding away the computational details and providing a user-friendly interface of the *e-wind* environment are very important. A simple off-the-shelf software solution is not possible. The system has to be built using the appropriate IT and web technologies.

The implementation of the *e-wind* environment is based on a three-tier client-server architecture. The first tier is the presentation tier, which is usually called the client or front-end. Clients process user inputs,

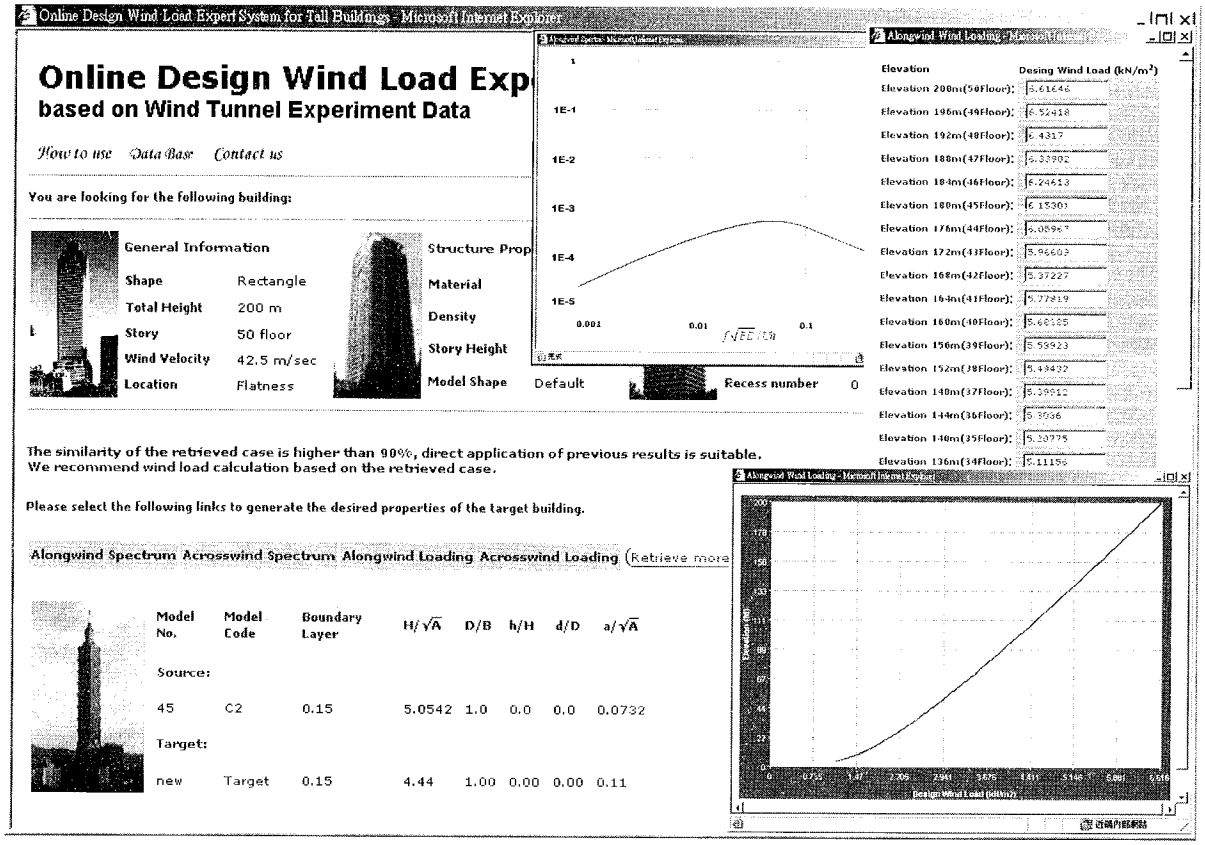

Figure 6: The user interfaces of the case-based design wind load expert system.

send requests to the server, and show the results of these requests to the user. In the *e-wind* environment, client is made up of a number of dynamic HTML pages that one can access with a web browser. The second tier is the application tier, which consists of several servers that process the requests of all clients and perform all the specified functions. The *e-wind* environment currently has three components in this tier: reasoning, calculation and charting engine. The reasoning engine is powered by two expert system shells, CBR-Works (2008) and KnowledgeWright (2008). The calculation engine contains Fortran, MATLAB and CFD software. The charting engine uses WebCharts3D and MATLAB to perform graphic functions. The third tier is the database tier, which contains the database management system that manages all the wind tunnel experimental data and aerodynamic databases. The interfaces between the tiers use CGI and SOAP web service techniques. Information can then be exchanged between the presentation, application and database tiers.

CONCLUDING REMARKS

A wind engineering program with an integrated engineering solution package for wind resistant design of buildings and structures called *e-wind* is under development at Wind Engineering Research Center at Tamkang University. Among the many branches of this program, various aerodynamic databases are the core of *e-wind*; therefore, more efforts will be spend to expand and enrich their contents. A web-based building wind code expert system has been completed and put to on-line service to local building designers since 2007. A prototype of aerodynamic data based expert system for tall building wind resistant design was also built and put to trial; further improvement of this system is needed and is being pursued.

REFERENCES

1. Kareem, A. 1990. Measurements of pressure and force fields on building models in simulated atmospheric flows. Journal of Wind Engineering and Industrial Aerodynamics, 36, 589–599.
2. Zhou, Y., Kijewski, T., Kareem, A. 2003. Aerodynamic load on tall buildings: an interactive database. Journal of Structural Engineering, ASCE, 120, 394-404.
3. Cheng, C.M., Liu, C.T., Lu, P.C. 2003. A wind tunnel database for wind resistant design of tall buildings. Proc. of Second International Structural Engineering and Construction Conference, Rome, Italy, Vol. 3, 2383-2389.
4. Wang, J., Cheng, C.M. 2005. Web-enabled design wind load expert system for tall buildings. Proc. of The 6th Asia-Pacific Conference on Wind Engineering, Seoul, Korea, 329-339.
5. Quan, Y., Tamura, Y., Matsui, M., Cao S.Y., and Yoshida, A. 2007. TPU aerodynamic database of low-rise buildings, Conference Preprints. Proc. of 12th International Conference on Wind Engineering, Cairns, Australia, Vol. 2, 1615-1622.
6. Kopp G.A., Chen, Y. 2006. Database-Assisted Design of Low-Rise Buildings: Aerodynamic Considerations for a Practical Interpolation Scheme, Journal of Structural Engineering, 132, 909-917.
7. Taiwan Architecture and Building Research Institute (ABRI), 2006. Specifications for Building Wind Resistant Design. (in Chinese)
8. Ho M.G., Chen, J.H. 2007. A study on the wind effects on the low-rise industrial buildings with gable roofs. Journal of Architecture, Special Issue on Technology, No.1, 99~116. (in Chinese)
9. Khanduri, A.C., Bedard, C., and Stathopoulos, T. 1997. Modeling wind induced interference effects using back-propagation neural networks. Journal of Wind Engineering and Industrial Aerodynamics, 72, 71-79.
10. English, E.C., Fricke, F.R. 1999. The interference index and its prediction using a neural network analysis of wind-tunnel data. Journal of Wind Engineering and Industrial Aerodynamics, 83, 567-575.
11. Zhang, A., Zhang, L. 2004. RBF neural networks for the prediction of building interference effects. Computers & Structures, 82, 2333-2339.
12. CBR-Works 4, accessed 2008. http://www.ai-cbr.org/tools/tecinno.html.
13. KnowledgeWright 4.2, accessed 2008. http://www.amzi.com/products/knowledgewright.html.

Journal of Wind & Engineering, Vol. 5, No. 2, July 2008, pp. 60-73

QUALITY ASSURANCE OF URBAN FLOW AND DISPERSION MODELS – NEW CHALLENGES AND DATA REQUIREMENTS

Bernd Leitl

University of Hamburg, Center for Marine and Atmospheric Research
Environmental Wind Tunnel Laboratory, Hamburg, Germany

ABSTRACT

Numerical modeling is a commonly accepted tool for predicting wind flow and pollutant dispersion in urban areas. In order to assure the quality of micro-scale meteorological models predicting flow and dispersion modeling in urban and industrial areas, a COST action has been launched. The main objective of the action is to develop and establish a commonly accepted model evaluation procedure and to provide data qualified for model validation purposes. A brief introduction into the methodology developed by the COST action is given and future challenges in the provision of qualified validation data sets are outlined. The role of physical modeling as a via-media between field data and the results from numerical modeling is highlighted.

Keywords: micro-scale meteorological modeling, wind tunnel modeling, model validation.

INTRODUCTION

Numerical modeling is a commonly accepted tool for predicting wind flow and pollutant dispersion in urban areas. An immense amount of new models of prognostic or diagnostic type have been developed recently and they are applied on a more or less routine basis, for example for modeling pedestrian wind comfort or pollutant transport in complex urban areas. The emergence of increasingly powerful computers enables the development and use of CFD even for complex urban type applications, whereas the focus of flow and dispersion modeling is shifting from predicting (annual) mean flow and dispersion patterns to the prediction of transient flow and dispersion phenomena such as peak wind loads or maximum hourly pollutant concentration. Numerical models also play a more and more important role in environmental assessment and urban climate studies which are expected to quantify the effects of human activities on air quality and the local climate as well as their feedback to climate change at larger scales. The increasing use of such models on one hand and the possible differences of model results for one and the same problem on the other hand lead to an increasing awareness that most of the models have never been evaluated rigorously. Moreover, the diverging model results obtained in different competitive model evaluation exercises have been triggering doubts on model quality, and they often cause a lack of confidence in the modeled results although most of the models were validated before.

Analyzing the reasons why even 'validated' numerical codes can lead to a variety of model results reveals a number of different sources for diverging model predictions. Since there is – not yet – a commonly accepted standard on how a certain type of micro-scale flow and dispersion model should be evaluated, it is more or less up to the model developer or user, when the model can be referred to as being validated. In this regard, a crucial question is how model- and application-specific the evaluation process must be. If, for example, a time-dependent model code (URANS- or LES-based) is predicting mean flow and dispersion in a reasonable manner, the question remains whether the code is validated for predicting transient flow and dispersion phenomena as well. From a physical point of view, one would need to stretch this subject even

further. The question then would be, for example, whether a code validated successfully for simulating time dependent dispersion phenomena for a continuously emitting source can be assumed to be validated for modeling puff releases as well. Depending on how the driving physical phenomena such as turbulence modeling or even chemistry processes are implemented in the code, the answer would be certainly very different from case to case. As stated by Hanna et al. (1982), most of the practical micro-scale problems to be modeled are, unfortunately, of an intermediate type between puff dispersion and continuous dispersion either because of intermediate release duration or because of a relatively short evaluation/sampling period. Consequently, most of the standard micro-scale model applications would call for a model 'validated' for both continuous and instantaneous release conditions.

A second problem related to model evaluation is a general lack of reference data qualified for model validation. Thus, model- and application-specific evaluation strategies require model- and application-specific reference data as well. In order to illustrate the problem we just consider the numerous field trials in order to measure mean concentration data for dispersion over flat uniform roughness (e.g. Barad (1958) or Haugen (1959)). The data is certainly qualified to be used for validating Gaussian-type dispersion models, and it is of value, though limited. In fact, when a more complex CFD code is tested and provides - in a physical sense - nearly no valuable information at all for validating LES-based models. Strictly speaking, validation of a CFD code based on data from the prairie grass experiments is merely amounts to documenting the ability of the code to simulate (mean) Gaussian type dispersion problems, and, forcing a LES-code developer or user to reproduce statistically representative mean flow and concentration fields is perhaps far too laborious. To complicate matters further, far less data is available for different types of complex urban structures, so that there is actually not much data available to choose from.

Further, model validation is also largely relying on the measures used for quantifying the fitness for purpose of a particular code. A wide range of (so-called) quality measures have been defined in the past, but not all of them can or should be used for all existing types of models and model applications and the results ('quality scores') obtained are still subject of a rather flexible interpretation. The problem is illustrated, for example, by considering an agreement of model prediction and reference values within a factor of two to be suitable, if the long-term development of mean concentrations of traffic induced pollutants within an urban area is to be predicted for a local climate assessment. The same 'model quality' will be referred to being unacceptable if the results are expected to be used for air quality control and monitoring or the assessment of health hazards. Usually, the threshold score used to separate acceptable model results from those unacceptable is defined not even based on physical or model application requirements but based on what 'most models can match'. A typical example for this approach of defining desired scores is a model evaluation guideline for validating urban-type micro-scale flow and dispersion models to be used for predicting car-induced air pollution in urban areas (VDI 3783/9).

Summarizing the above, model validation and model evaluation can be understood as a problem in a three-dimensional space spanned by model application specificity, the requirement of suitable data and the formulation of suitable quality measures. Each of the basic types of commonly used models (Gaussian, RANS, LES) can be assigned a very different 'operating point' in model validation space and the transitions are smooth.

Defining a reliable standard for quality assurance of urban-type flow and dispersion models and improving the quality of numerical modeling - also at the applied/application level - is certainly one of the new frontiers in the fields of Wind Engineering and Technical Meteorology. Driven by the very need for physically sound model validation strategies, the COST Action 732 'Quality Assurance and Improvement of Micro-Scale Meteorological Models' was initiated in March 2005. This European-wide activity is intended to define commonly accepted quality standards for modeling/predicting flow and dispersion phenomena in urban or industrial environments.

COST 732 - OBJECTIVES AND METHODOLOGY

The main objective of action COST 732 is to improve and maintain the quality of micro-scale meteorological models applied for predicting flow and transport processes in urban or industrial environments. In particular, the action intends

- to develop a coherent and structured quality assurance procedure for the given type of models, including guidance on how to properly verify model quality and how to apply models properly.
- to provide a systematically compiled set of data qualified for model validation.
- inviting developers and users from participating countries to apply the procedure and prove its applicability.
- to build a consensus within the community of developers and users regarding the usefulness of the procedure.
- stimulating a widespread application of the process based on standardized quality assurance protocols and proving the 'fitness for purpose' of micro-scale meteorological models.
- to contribute to a proper use of this type of models by disseminating information on the range of applicability, potential and also on the limitations of such models.
- to establish a consensus on best practices in current model use and
- to give recommendations for focused experimental programs in order to improve the extent and quality of data available for model validation.

The action is expected to have a fundamental impact on the community by improving the 'culture of modeling'. The very existence of an accepted European standard for quality assurance for provision of test data qualified for model validation will support the improvement and reliable application of micro-scale meteorological models. It will also reveal the need for further model- and application specific research activities regarding model development and the supply of reference data sets. In this context, the COST action is not only affecting numerical modeling but also the community of experimentalists who is expected to provide the data required for model testing.

COST 732 – PRESENT STATUS

The action COST 732 was started with a joint ESF/COST exploratory workshop on 'Quality Assurance of Micro-Scale Meteorological Models'. In the workshop proceedings (Schatzmann and Britter, 2005) a state-of-the-art report on former quality assurance initiatives in the field of micro-scale meteorological models is given, referring for example to the 'General Requirements for a Quality Assurance Project Plan' by Borrego and Tchepel (1999), the 'Guidelines for Model Developers' and the 'Model Evaluation Protocol' prepared by the Model Evaluation Group (MEG, 1994) under the CEC's Major Industrial Hazards Programme or the US Environmental Protection Agency's requirements for quality assurance of atmospheric dispersion models (Irwin, 1998 and 1999). The review also takes into account similar activities in related fields of applied numerical modeling, such as the EMU project (Hall, 1997), the thematic network QNET-CFD or COST action C 14, focusing on industrial and engineering applications of CFD codes. Finally, several recommendations as well as national standards such as the Quality Assurance Guidelines released by a task force of UK's Royal Meteorological Society (1995) and the German 'VDI Commission on Clean Air' (2002) were carefully considered. Regarding the need for data qualified for validation purposes, considerations outlined in Schatzmann et al. (2002, 2003) were taken into account, resulting in standards for validation of data which can be met only by data sets based on a combination of field and wind tunnel experiments.

As stated by Popper (1959), strategies for assuring the quality of a numerical model can only be based on very generic scientific principles such as the principle of falsification. Building a consensus within the scientific community, about which tests should be applied for model validation and which data sets should be used for comparison, is essential. Hence, a first version of the evaluation procedure and the underlying motivation was drafted at an early stage of COST 732. A background and justification document (Britter and Schatzmann 2007a) and a more practical model evaluation guidance and protocol document (Britter and Schatzmann 2007b) were released, whereas the first document provides detailed explanations concerning the general model evaluation philosophy and the methodology to be applied. A list of six tasks to be processed in the course of a model evaluation is defined as follows:

1. Model Description – a brief description of the characteristics of the model, the intended range of application of the model as well as the theoretical background of the model
2. Database description – description of the database which is employed for the evaluation procedure, including the reasons as to why a specific set of data was chosen and what variability or scatter is expected in the reference database
3. Scientific Evaluation – description of the equations employed, the physical and chemical processes the model has been designed to include and the choice of the numerical modeling procedures as well as the resulting limits in the intended application of the model
4. Code Verification – documentation of the capability of the model to produce results in accordance with the actual physics and mathematics that have been employed in order to identify and reduce errors in the transcription of the mathematical model into a computational code and the (analytical or numerical) solution
5. Model Validation – structured comparison of model predictions with experimental data based on statistical analyses of selected variables in order to identify and quantify the difference between model predictions and the evaluation datasets and to provide quantitative evidence as to how well the model approximates reality, as much as possible.
6. User-oriented Assessment – a more general evaluation of the model from a pure users point of view, regarding the availability of a comprehensive documentation of the model, sufficient technical description of the code or a user manual and an evaluation documentation, covering the issues like the range of applicability of the model, computing requirements, installation procedures and troubleshooting advice

It is obvious; that the most crucial and complex step of the entire evaluation procedure is the model validation step, and quite often, model evaluation studies consist of a model validation only. Because of the stochastic nature of atmospheric flow and dispersion problems, no matter whether measured in the real atmosphere or physically modeled, a number of questions need to be addressed properly. With the type of model and the intended range of model applications in mind, the evaluator must specify which quantities should be compared, at what point(s)/area(s) a comparison should take place or at which level of detail the comparison should take place (point by point or area-averaged). Only if the purpose of the model is stated precisely, the concerning questions can be answered properly. The various matrices possible to be used for quantifying the model performance can give a wide range of evaluation results even for one and the same model and the same test case. Consequently, the validation matrices must be selected carefully and – even more important – agreed upon amongst the model developer and user community.

Because the quality of the reference database is directly controlling the quality and outcome of model validation, substantial efforts within COST 732 were dedicated to define model- and application-specific validation data requirements. As stated by Yoshie et al. (2007), the COST 732 is claiming for a suite of data sets with increasing geometrical complexity to be used for systematic testing of micro-scale meteorological models. The data sets must be 'complete', in the context of providing sufficient information to set up a model run without further assumptions concerning the model input parameters and the uncertainty of the reference data must be documented. The latter is of substantial importance for any kind of reference data but very difficult to obtain particularly from field measurement programs. If uncertainty is understood as the possible difference between an individually measured value and a statistically representative result ideally to be used for validation purposes, it becomes clear that data uncertainty cannot only be defined based on the accuracy of the measurement instrumentation used. What is required is a quantification of the repeatability of experimental results for similar experimental boundary conditions as well as an evaluation of the spatial and temporal representativeness of the experimental results with respect to the specific flow and dispersion problem. Since this information cannot be gathered from field measurements only, COST 732 suggests validation data sets that comprise combinations of field and laboratory experiments.

The 'Model Evaluation Guidance and Protocol Document' is summarizing the model evaluation strategy developed by COST 732. It gives a step-by-step guidance on how to assure the quality of a micro-scale meteorological model. This document will be updated continuously as the evaluation procedure is tested by

the COST 732 members. The final guidance and protocol document will come along with recommendations for data sets that should be used during the validation work. Recommended data sets will be made available in a unified data format via a www data base.

Another factor identified as being of major concern is the qualification of the user running a model. Generally speaking, numerical simulation is a knowledge based activity. Appropriate knowledge can be transferred to users by recommendations concerning the proper use of models. For obstacle resolving CFD codes this information is not straight forward and so one of the activities within COST 732 is to draft, as a third document, a 'Best Practice Guideline for the CFD Simulation of Flows in the Urban Environment' (Franke et al. 2007a).

The entire evaluation procedure is tested presently by the action itself. As a first combined data set, results from the Mock-Up Urban Setting (MUST) field experiment have been prepared together with corresponding wind tunnel tests. Although the test geometry is still a rather simple one (idealized building array formed by 256 standard size shipping containers), it reveals the complexity of a model evaluation. Within COST 732 a total of 11 groups of numerical modelers (9 CFD / 2 non-CFD) started a model evaluation based on the MUST case, strictly following the evaluation guideline. Besides a comparison of the model results, a major focus of the ongoing work is to identify the strengths and weaknesses if the different evaluation metrics are applied and to give clear recommendations for a fair model comparison.

A general conclusion drawn from the COST 732 activities so far is that the type and quality of reference data used for model validation is very crucial. As the complexity of models is increasing and the evaluation time frame gets shorter, the provision of qualified reference data is getting more and more difficult.

DATA REQUIREMENTS AND NEW CHALLENGES

The data requirements specified in the COST 732 documents clearly state, that validation data must qualify for model validation not only in terms of the quality or accuracy of the data but also in terms of the type of data needed for validating a specific type of model for a particular type of application. Depending on the type of model, for example, the required input data will differ significantly. So far, most of the test data available for complex urban model applications is providing mean flow and dispersion measurements for mean boundary conditions assumed to be representative for a given dispersion situation. However, from a statistical point of view it remains an open question if the results from field tests allow for a statistical averaging in general. Measurements taken at full scale are characterized by a permanent change of the physical boundary conditions and averaging normally does not account for the different spatial and temporal representativeness of the data collected for different boundary conditions or at different measurement locations. Let us consider an experimental setup where wind speeds are measured within a street canyon and above roof level simultaneously. A typical averaging period for field data would be for example 30 minutes and a wind profile plot would be presented showing mean data points at different elevations. Strictly speaking, the data points must not be compared directly because each of the points is representing a different spatial and temporal representativeness and most likely none of them will be giving a true mean value. Since the time scales of turbulent wind fluctuations and gusts are in a range of seconds up to tens of minutes, the measurements taken at the lower mean wind speeds present at street level are less representative than the half hourly mean measured at higher wind speeds above roof level. The higher mean wind speed present above roof level enables a larger ensemble of turbulent motions to be considered in the process of averaging over a fixed period of time, approaching a representative mean value more closely than at the lower mean wind speeds within a street canyon. In order to quantify this substantial uncertainty and the required confidence interval of any kind of measured data, repetitive measurements under more or less identical boundary conditions are required. Unfortunately, for field measurements it is nearly impossible to repeat individual measurements under identical boundary conditions and, thus, the physical uncertainty of field data can hardly be quantified relying on the field data only. On the other hand, if the uncertainty and confidence interval of a measured mean is not known, it might not be wise to use the data for the purpose of validation. In plain words it means, if the reference data is of unknown uncertainty and representativeness the entire validation will be of lower value as well.

In order to add vital information on uncertainty and representativeness to field data, physical modeling in boundary layer wind tunnels can act as a via-media between field data and numerical modeling. Although, a wind tunnel model of an urban area is a model itself, it provides substantial and reliable information on processes hard to be captured and measured by field measurements but necessary for model validation. As an example, a RANS-based CFD code requires the boundary conditions at least at the inflow plane of the computational domain to be specified in a RANS-compatible format as statistically representative mean flow plus information on the turbulent fluctuations. Whereas the required inflow conditions cannot be measured directly and completely at full scale, a physical model in a boundary layer wind tunnel can deliver the information necessary because the mean flow conditions can be carefully controlled and kept constant until all required inflow information is measured with sufficient accuracy and statistical representativeness for quasi-stationary boundary conditions. What delivers a substantial increase in information at the inflow boundary of a computational domain, of course works also for measurements taken within complex urban geometries. Based on a very careful physical modeling and using instrumentation suitable for measuring three-dimensional turbulent flows, sufficiently long statistically representative time traces of wind measurements and concentration fluctuations can be captured under quasi-stationary conditions. A subsequent analysis of the long time series for evaluation periods equivalent to the averaging period at full scale enables quantification of the minimum uncertainty or scatter to be expected in the corresponding averaged field data. It is obvious, that with this information added to the field data, a model validation in many cases will deliver a different outcome than for a situation where field data with low confidence level are used.

Access to qualified reference data is even more difficult, if newer Large-Eddy-Simulation type flow and dispersion models are supposed to be validated for predicting transient flow and dispersion processes. LES based models provide a far better physical potential for example for predicting dispersion from accidental releases in urban areas (puff dispersion) or simulating the gustiness of winds in complex urban geometries but also these models need to be validated considering their intended use. For characterizing the corresponding inflow conditions of a model domain and to provide the required reference data for model validation, representative mean values are no longer sufficient. In this case, the temporal and spatial distribution of flow and dispersion patterns needs to be characterized and provided for validation. The need for a statistically representative set of mean flow and dispersion data is replaced by the need for a statistically representative probability distribution of reference quantities/variables. In this situation the limiting factor of field experiments and the corresponding data is, among other things, that individual experiments cannot be repeated sufficiently often in order to derive the required distribution functions safely. For example, providing validation data for the dispersion of clouds of pollutants resulting from accidental releases would require simulating several hundred releases at full scale for fixed boundary conditions in order to increase the probabilistic representativeness of the ensemble of results to a level acceptable for model validation purposes. At this point again, the combination of field and laboratory data and complementary experimental work can increase the quality of reference data substantially. Using state-of-the-art instrumentation and a contemporary approach for modeling atmospheric boundary layer flows in a boundary layer wind tunnel, laboratory data can at least partially bridge the existing gap between numerical model results and full scale measurements.

It must be emphasized clearly, that compiling validation data in a boundary layer wind tunnel requires substantially higher experimental standards than regular wind tunnel modeling and testing. In particular when it comes to modeling atmospheric boundary layer flows at large model scales and if transient flow and dispersion phenomena are supposed to be modeled and measured, the improved meteorological knowledge currently available must be incorporated appropricately. Most of the existing physical modeling guidelines do not adequately consider the specific needs of the upcoming modeling requirements since they are still based on the standards defined in the seventies and early eighties. For wind tunnel modeling continuing to be a part of the prospective research on urban flow and dispersion processes it is essential or even critical that the standards of physical modeling are raised to a contemporary and application-driven level, taking into account the needs of modern wind tunnel applications and considering the new potential resulting from significantly improved measurement techniques as well.

VALIDATION DATA FOR URBAN DISPERSION MODELING – AN EXAMPLE

In order to illustrate what type, extent and quality of validation data can be achieved, some recent research efforts of the Environmental Wind Tunnel Laboratory at Hamburg University are outlined. In summer 2003, one of the biggest urban type dispersion studies, the JOINT URBAN 2003 (JU2003) field experiment took place in Oklahoma City (USA). The main purpose of this large experimental field campaign was to simulate and study pollutant dispersion from accidental releases in complex urban terrain at full scale. The data collected is intended to be used for the purpose of model validation, particularly in the context of validating emergency response tools and models predicting puff dispersion in urban areas. An immense experimental effort was spent to realize several intense operation periods, for which data from several consecutive pollutant releases were collected. An overview of the JU2003 experiment can be found in Allwine et. al (2003). The JU2003 data are one of the few experimental test cases for which extensive combined wind tunnel and field data are currently available. At an early stage of JU2003, the Environmental Wind Tunnel Laboratory at Hamburg University was given the task to support the field campaign by corresponding wind tunnel tests. The wind tunnel tests were intended to support efficient and proper instrumentation citing and data interpretation and the wind tunnel was asked to extent the field data set by systematic measurements in order to provide the type of systematic data needed for a more safe validation of numerical models.

In a first step, the atmospheric boundary layer flow across Oklahoma City was replicated at a scale of 1:300 in the test section of the large boundary layer wind tunnel facility at EWTL. The large cross section of the tunnel allows a large city area to be modeled at a sufficiently large model scale. Using a sufficiently large model scale is important particularly for marinating a high spatial and temporal resolution of the laboratory data. The area covered by the model is covering about 2 km by 2 km. Figure 1 shows the model mounted in the test section of the large wind tunnel facility WOTAN. Following the boundary layer documentation standards established at the EWTL, the approach flow evaluation and documentation consisted of:

- documentation of spatial and temporal homogeneity and stability of the modeled boundary layer flow
- representative mean flow profiles for all three components of the wind vector
- representative profiles of turbulence intensities
- representative profiles of vertical and lateral turbulent fluxes
- integral length scales derived from component-resolving high resolution flow measurements
- power spectral density distributions for several heights above ground
- temporal and angular analysis of turbulent wind direction fluctuations in order to estimate temporal representativeness of the wind tunnel experiment.

In order to achieve a constant shear layer in the lower fraction of the model boundary layer flow, the longitudinal pressure gradient was minimized along the test section using the adaptable ceiling of the tunnel. As Figure 2 shows, the non-dimensional pressure gradient stays below the threshold value defined in VDI 3783/12 (2000) even with the model blockage present in the wind tunnel. As illustrated in Figure 3, the mean wind profile of the modeled boundary layer flow agrees well with the wind conditions expected at full scale in Oklahoma City. Both, the power law exponent of the wind profile and the corresponding roughness length derived from the logarithmic wind profile are consistent and in agreement with the standard assumptions for a boundary layer flow over moderately rough terrain. In Figure 4, the corresponding turbulence intensity profiles are plotted. The data is in good agreement with the profiles documented in ESDU (1985). Later on, a comparison with field data from JU2003 revealed a good agreement with the wind conditions present during a large fraction of the field tests as well. The vertical shear stress profile measured upstream of the city model is plotted in Figure 5. A proper modeling of the vertical turbulent fluxes is essential especially for a reliable dispersion modeling and the sufficient and physically correct representation of turbulent flow and transport phenomena in the model. The measured profile shows a nearly constant shear stress as it is expected for the entire so-called Prandtl-layer. As in full scale, for elevations above the Prandtl-layer the vertical fluxes are gradually decreasing. The physically consistent modeling of turbulent structures is also documented by the good agreement of turbulence length scales

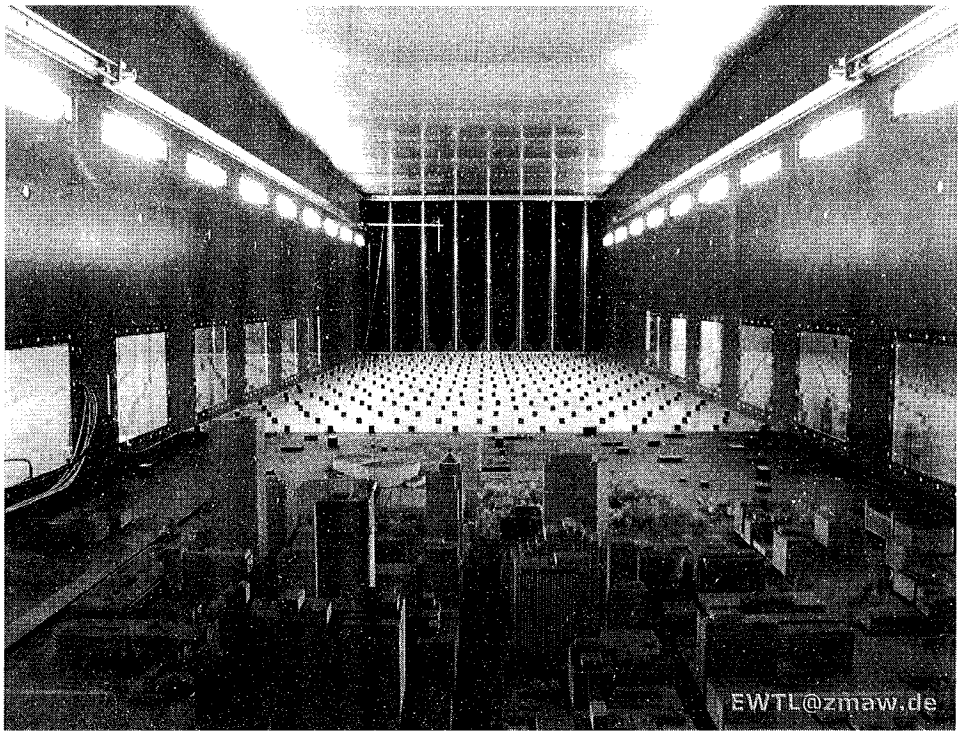

Figure 1: The 1:300 scale model of the Central Business District of Oklahoma City, mounted in the test section of the large boundary layer wind tunnel at EWTL.

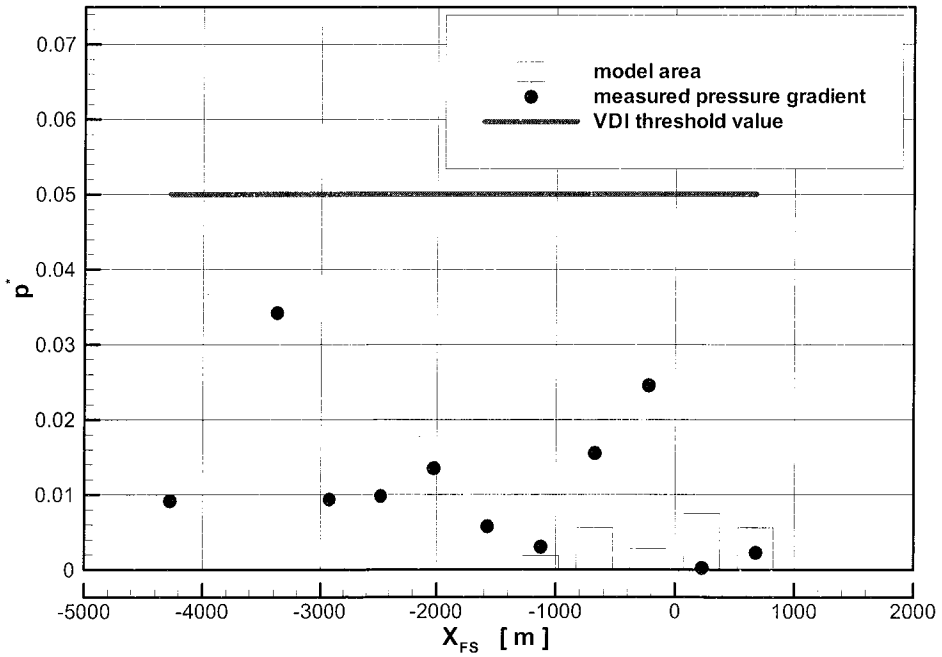

Figure 2: Non-dimensional longitudinal pressure gradient measured along the test section of the wind tunnel. The red line indicates the allowable limit value defined in VDI 3783/12.

derived from wind velocity measurements at different heights above ground. Figure 6 shows the modeled length scales in comparison with field data from Counihan (1975). As documented in Figure 7, the spectral distribution of turbulent kinetic energy is matching well with reference spectra as well. The final step of boundary layer documentation delivers essential information on the lateral and vertical wind direction fluctuations modeled in the wind tunnel. Often wind tunnels are said not to be capable of replicating large

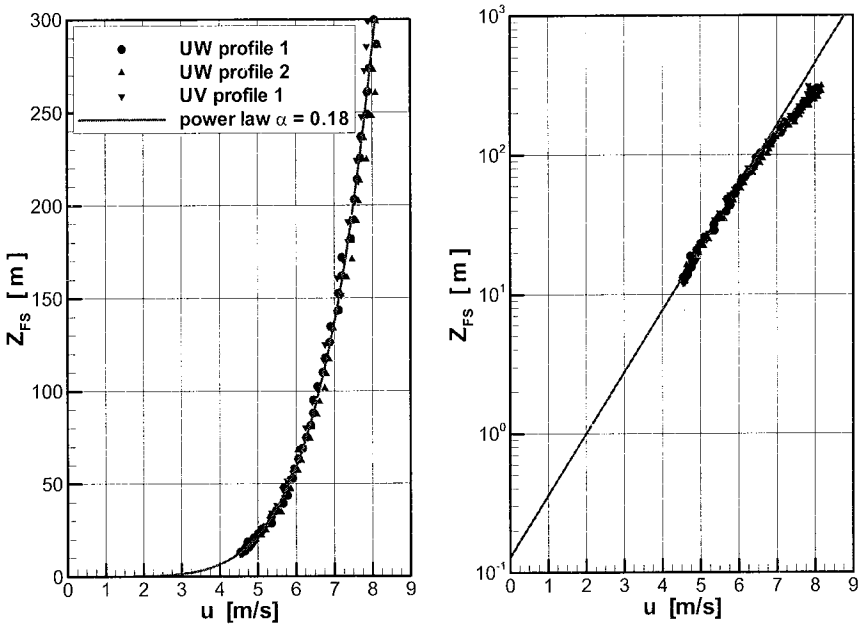

Figure 3: Mean wind profile of the modeled atmospheric boundary layer flow.

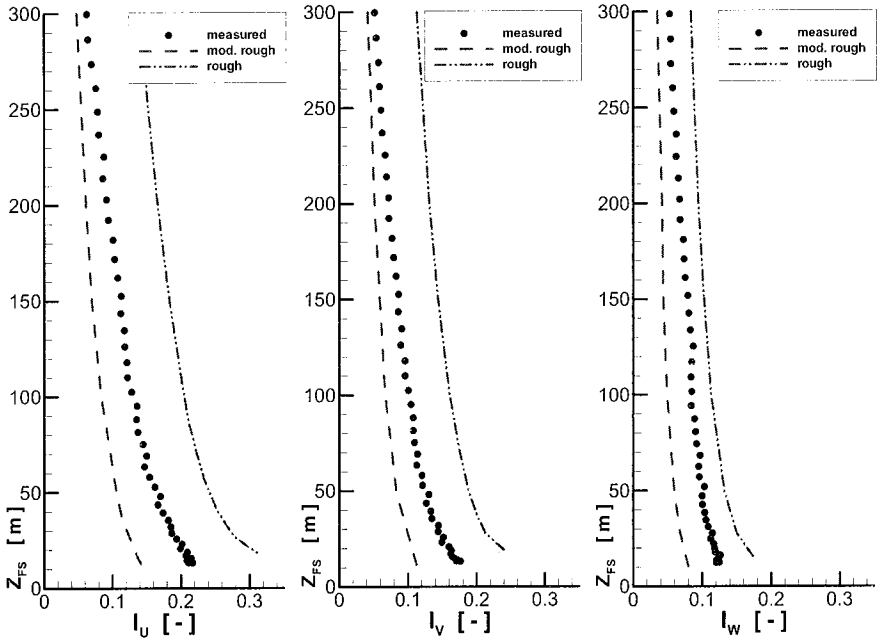

Figure 4: Mean vertical turbulence intensity profiles measured in the modeled approach flow.

scale turbulence fluctuations of the wind directions properly because of the duct-like flow. However, if sufficient care is taken in boundary layer modeling and in the choice of a proper model scale, almost the entire low frequency range of the micro-scale turbulence spectrum can be modeled properly. Figure 8 shows the frequency of occurrence of measured lateral wind direction deviations from the mean wind direction, measured in the wind tunnel. Measurements at different heights above ground are plotted, covering almost the entire model boundary layer. From a comparison with field data it can be concluded, that the model boundary layer sufficiently covers all turbulent fluctuations present up to about 45 to 60 minutes at full scale, even with respect to the temporal behavior of the wind direction fluctuations. All data essential for documenting the modeled boundary flow are found to be essential for specifying the inflow boundary conditions for a RANS-based CFD simulation as well. Even more experimental effort is necessary for

documenting the approach flow conditions necessary when an LES-model has to be validated. For characterizing the dominating turbulent structures (~ large eddies), correlated flow measurements can be carried out in cross-flow planes upwind of the model. In order to reconstruct turbulent structures locally it is essential that not only statistically averaged results are stored/provided, it is necessary that also the underlying time series of all measurements are kept for further analysis. Figure 9 gives an example for correlation patterns derived from correlated flow measurements taken upwind of the OKC model.

The second part of a reference data set is of course the data from within the model area itself which is to be used in the context of applying different validation metrics. The data requirements again depend on the type of model to be validated and its intended application. For atmospheric flow and dispersion modeling, it is mandatory to provide the driving flow fields. If the type of model to be validated is RANS based, representative mean flow fields with sufficient spatial resolution need to be measured and stored. The area density of measurement points should be chosen high enough to continuously resolve all essential flow

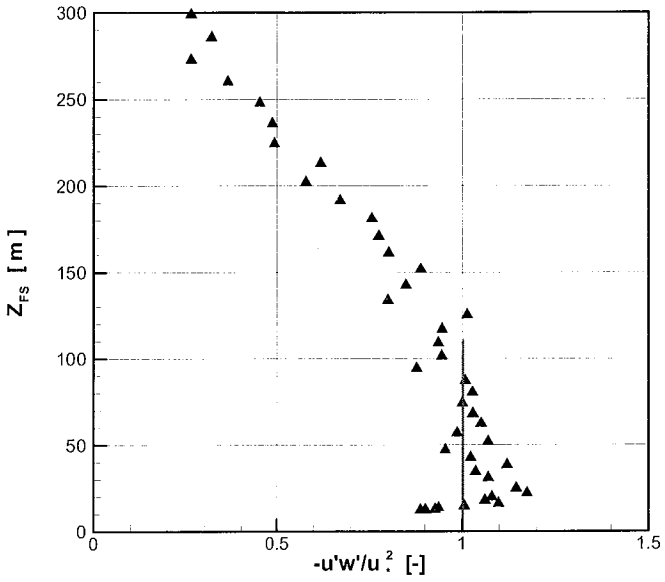

Figure 5: Vertical shear stress distribution measured upwind of the model. The red line indicates the approximate thickness of the modeled constant shear layer.

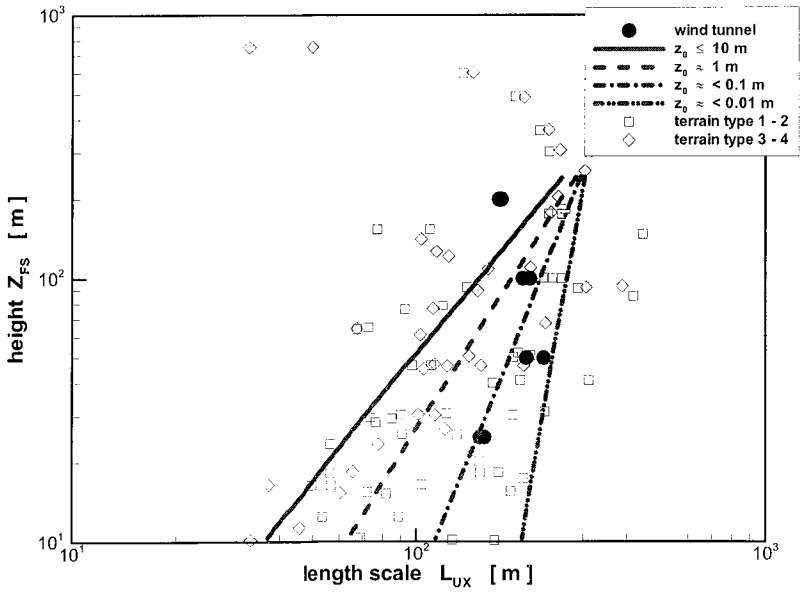

Figure 6: Vertical distribution of integral length scales derived from wind speed measurements in the modeled boundary layer flow (reference values adopted from Counihan 1975).

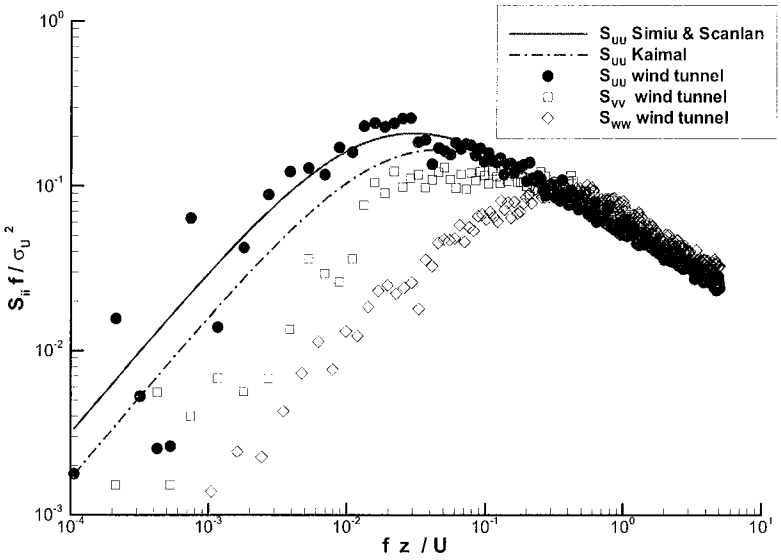

Figure 7: Turbulent spectra measured in the wind tunnel at a height of 25.9 m above ground (full scale). The empirical curves were derived for neutral or near-neutral atmospheric conditions.

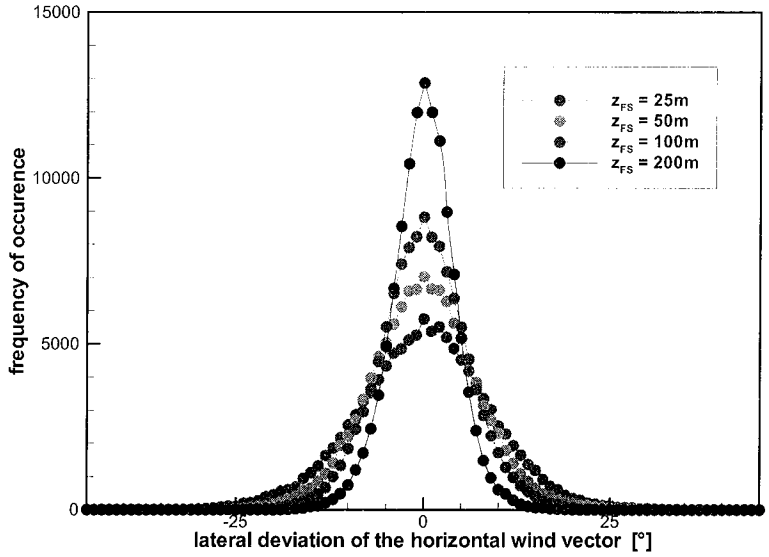

Figure 8: Histogram of lateral wind direction fluctuations measured at different heights above ground.

structures reasonably. Figure 10 shows component resolved mean flow fields measured in a dense grid of measurement points for the core area of interest. For a substantial number of measurement locations, non-consecutive repetitive measurements were carried out in order to quantify the overall reliability, the uncertainty and the confidence interval of the measured values. Provision of data consisting of a sufficient number of reference points, the more or less automated use of validation metrics, like the ones suggested by COST 732, is required to provide reliable results. A similar amount of data is required also for validating dispersion modeling based on a RANS approach.

Assuming that an LES-based model might be validated for quasi-stationary flow and dispersion situations at first, the type and quality of validation data illustrated so far is useful for LES code validation as well. However, the particular strength of a model resolving essential scale features of turbulence is to model transient, non-stationary flow and dispersion phenomena explicitly. Consequently, LES codes require validation procedures and validation data for basically instantaneous processes such as puff dispersion, instantaneous wind loads or wind gusts. This essentially means that adequately long and sufficiently resolved time traces of flow and dispersion measurements must be recorded, archived and analyzed off-line. Since

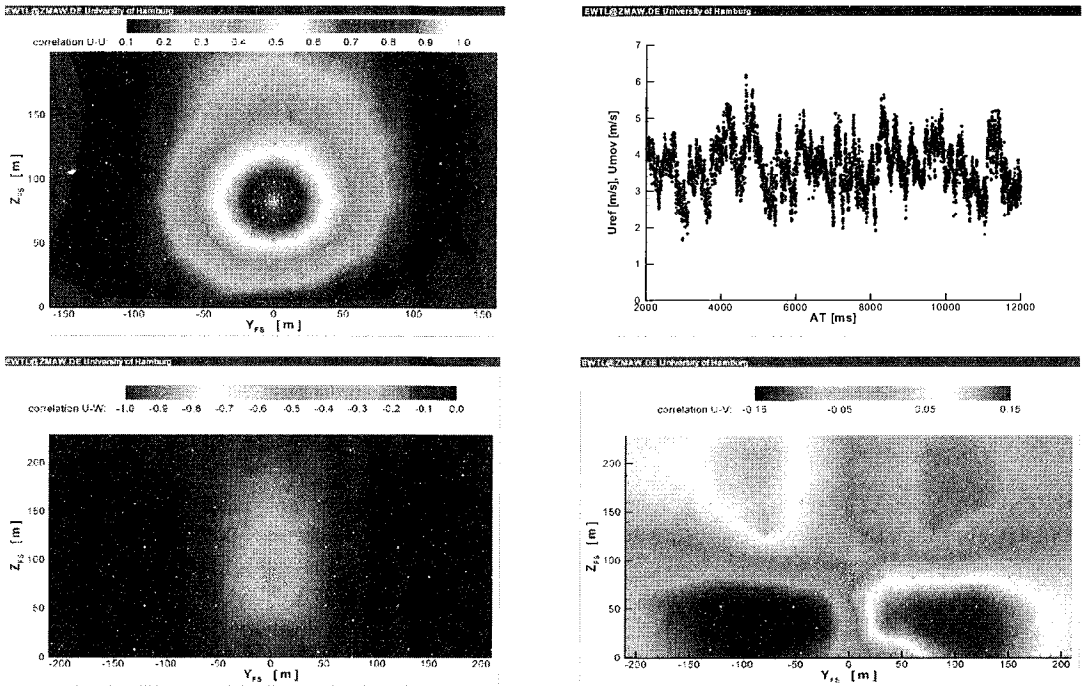

Figure 9: Correlation patterns derived from correlated, component resolving wind speed measurements in the modeled boundary layer flow.

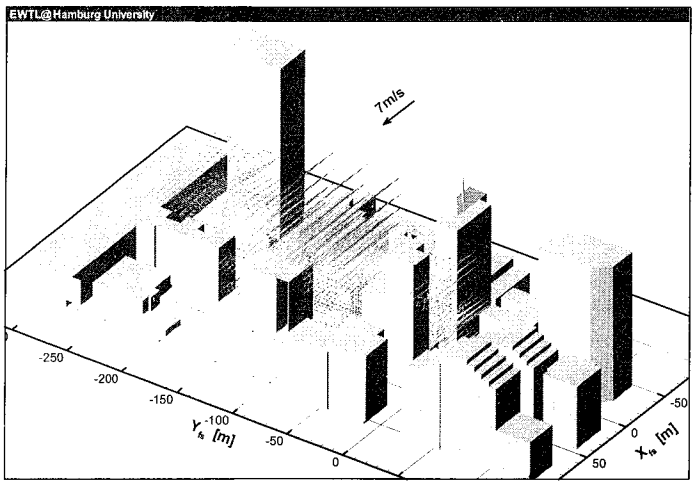

Figure 10: Selected results of representative mean flow measurements in a dense grid within a part of the model area.

model evaluation based on singular events is not sufficient, LES model validation will require a systematic analysis of the statistics and probability of measured/modeled quantities and their comparison based on a probabilistic approach. In order to illustrate the problem, Figure 11 shows a typical result from puff dispersion modeling and measurements carried out in the wind tunnel. Scaled clouds of tracer were released in the OKC wind tunnel model and the resulting puff dispersion signal was recorded at numerous locations within the model area. As expected, the time traces recorded at one location vary significantly from release to release. In order to achieve sufficiently large ensembles of individual releases the experiment was repeated several hundred times for quasi-stationary mean flow conditions. Subsequently, the entire set of data for a particular release configuration was analyzed regarding the frequency distributions of relevant dispersion parameters such as puff arrival time, peak concentration, dosage and decay time. Furthermore, a systematic ensemble analysis of the wind tunnel data revealed that typically the data from more than 150 individual releases is required to define frequency distributions within a range of confidence acceptable for model validation purposes. Based on a comparison with field data available from the JU2003 field trials it could be documented that the ensemble of possible dispersion signals captured in the wind tunnel is embedding

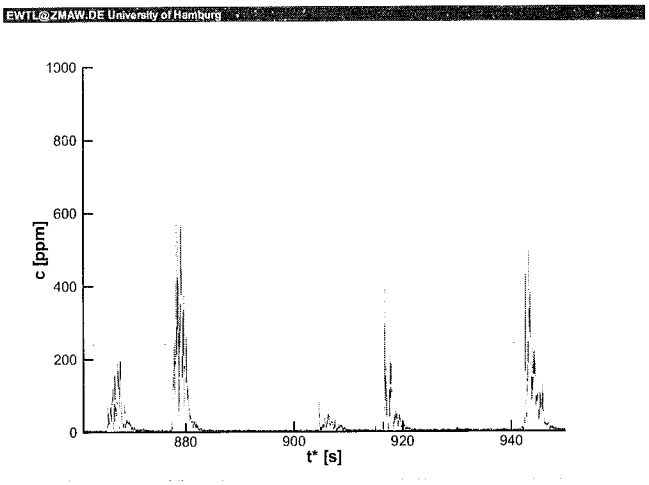

Figure 11: Typical section of a high frequency concentration time series measured for multiple puff releases under quasi-stationary approach flow conditions. Please note the high variability in the shape of the individual puff signals.

the field results as well. However, the uncertainty range or confidence interval which must be assigned to the results from a very limited number of field releases is certainly questioning the use of field data for 'validating' complex LES codes.

As stated in the very beginning, the example documents the clear change in the data requirements for the validation of numerical flow and dispersion models with their increase in complexity. Not necessarily the quantities measured but certainly the quality and the type of the data required is being shifted significantly. It will be one of the future challenges in wind engineering to improve the quality standards for physical modeling of atmospheric flow and dispersion phenomena in order to provide the type and extend of data vital for validating more and more complex numerical models.

CONCLUSIONS

As one of the first cross-national activities, COST 732 is stimulating a Europe-wide discussion on model quality assurance, on the use of suitable reference data as well as on a best practice in applied urban-type transport and dispersion simulations. The action will harmonize modeling approaches in order to form an accepted standard for numerical transport and diffusion modeling in urban areas. In addition, the strengths and weaknesses of particular types of models, parameterizations or closure schemes are determined. COST 732 is also understood as an opportunity to develop common views about the most appropriate way of applying different types of models to urban type flow and dispersion problems. The general goal is to improve the culture of numerical modeling more than to rank different types of models with respect to their performance.

COST 732 reveals clearly, that a true validation of numerical models requires more than just the replication of a finite number of individual test cases. In order to validate state-of-the-art RANS- or LES-based transport and diffusion models, it requires a sufficient amount of systematic data of sufficient quality and quantity which are currently not yet available. It will be one of the future challenges in wind engineering to support the further development and improvement of numerical modeling with suitable experimental data from field and laboratory experiments.

ACKNOWLEDGEMENTS

The support by the members of COST action 732 is gratefully acknowledged. The experimental data outlined was partly gathered within the scope of a scientific cooperation between the School of Meteorology at the University of Oklahoma and the Meteorological Institute at Hamburg University and a joint research project between the Naval Research Laboratory in Washington and the Environmental Wind Tunnel Laboratory in

Hamburg, funded by DTRA. In particular, the author wants to thank Mr. Rick Fry, Dr. Petra Klein and Dr. Gopal Patnaik for their cooperation.

REFERENCES

1. Allwine, K.J.; Leach, M.J.; Stockham, L.W.; Shinn, J.S.; Hosker, R.P.; Bowers, J.F.; Pace J.C. (2004): Overview of Joint Urban 2003 – and atmospheric dispersion study in Oklahoma City. Symp. on Planning, Nowcasting and Forecasting in the Urban Zone, January 11-15, Seattle, WA, AMS J7.1
2. Barad, M.L. (Ed.) (1958): Project Prairie Grass, A Field Program in Diffusion. Geophysical Research Paper, No. 59, Vols. I and II, Report AFCRC-TR-58-235, Air Force Cambridge Research Center.
3. Borrego, C.; Tchepel, O. (1999): General requirements for a Quality Assurance Project Plan. Proc., 3rd SATURN Workshop, Aveiro, Protugal.
4. Britter, R.; Schatzmann, M. (Eds.) (2007a): Background and justification document to support the model evaluation guidance and protocol document. COST Office Brussels, ISBN 3-00-018312-4.
5. Britter, R.; Schatzmann, M. (Eds.) (2007b): Model evaluation guidance and protocol document. COST Office Brussels, ISBN 3-00-018312-4.
6. Counihan, J. (1975): Adiabatic Atmospheric Boundary Layer: A Review and Analysis of Data from the Period 1880-1972, Atmospheric Environment, vol. 9, no. 10, pp 871-905
7. ESDU (1985): Characteristics of atmospheric turbulence near the ground. Part II: Single point data for strong winds (neutral atmosphere). published in: ESDU International 85020, 1985
8. Franke, J.; Hellsten, A.; Schlünzen, H.; Carissimo, B. (Eds.) (2007): Best Practice Guideline fort he CFD simulation of flows in the urban environment. COST Office Brussels, ISBN 3-00-018312-4.
9. Hall, R.C. (1997): Evaluation of modeling uncertainty – CFD modeling of nearfield atmospheric dispersion. EU Project EV5V-CT94-0531, Final Report. WS Atkins Consultants Ltd., Woodcote Grove, Ashley Road, Epsom, Surrey KT18 5BW, UK
10. Hanna, S.R.; Briggs, G.A; Hosker, R.P. (1982): Handbook on Atmospheric Diffusion. Technical Information Center, U.S. Department of Energy, DOE/TIC-11223, ISBN 0-87079-127-3
11. Haugen, D.A. (1959): Project Prairie Grass, A Field Program in Diffusion. Geophysical Research Paper, No. 59, Vol. III, Report AFCRC-TR-58-235, Air Force Cambridge Research Center.
12. Irwin, J.S. (1998): Statistical Evaluation of Atmopsheric Dispersion Models. Proc. 5th Int. Conf. on Harmonization within Atmospherics Dispersion Modelling for Regulatory Purposes, Rhodes, Greece
13. Irwin, J.S. (1999): Effects of Concentration Fluctuations on Statistical Evaluations of Centerline Concentration Estimates by Atmospheric Dispersion Models. Proc. 6th Int. Conf. on Harmonization within Atmospheric Dispersion Modelling for Regulatory Purposes, Rouen, France.
14. Model Evaluation Group (1994): Guideline for model developers and Model Evaluation Protocol. European Community, DG XII, Major Technological Hazards Programme, Brussels, Belgium
15. Popper, K.R. (1959): The Logic of Scientific Discovery. Basic Books, New York.
16. Royal meteorological Society (1995): Atmospheric Dispersion Modeling. Guidelines on the Justification of Choice and Use of Models, and the Communication and Reporting of Results. RMS, 104 Oxford Road, Reading, RG1 7LJ, UK
17. Schatzmann, M.; Britter, R. (Ed., 2005): Quality Assurance of Microscale Meteorological Models, COST732/ ESF Workshop Proc., ISBN 3-00-018312-4
18. Schatzmann, M.; Leitl, B. (2002): Validation and application of obstacle resolving urban dispersion models. Atmospheric Environment, 36, pp 4811-4821
19. Schatzmann, M.; Grawe, D.; Leitl, B.; Müller, W.J. (2003): Data from an urban street monitoring station and its application in model validation. Proc. 26th Int. Tech. Meetingon Air Pollution Modelling and its Application. Istanbul, Turkey, May 26-30.
20. Yoshie, R.; Mochida, A.; Tominaga, Y.; Kataoka, H.; Harimoto, K.; Nozu, T.; Shirasawa, T. (2007) Journal of Wind Engineering and Industrial Aerodynamics 95 (2007), pp. 1551-1578
21. VDI Guideline 3783/9 (2002): Environmental meteorology – Prognostic Microscale Windfield Models – Evaluation for flow around buildings and obstacles. Kommission Reinhaltung der Luft, Beuth Verlag GmbH, 10772 Berlin, Germany
22. VDI Guideline 3783/12 (2000): Environmental meteorology – Physical Modeling of Flow and Dispersion Processes in the Atmospheric Boundary Layer, Application of Wind Tunnels. Kommission Reinhaltung der Luft, Beuth Verlag GmbH, 10772 Berlin, Germany

ERRATUM

In the paper entitled "Recent Developments in the Specification of Wind Loads on Transmission Lines" By J.D. Holmes, published in Vol. 5, No.1, January 2008 of the Journal, on page 14, the equation (9) given below was inadvertently missed in typesetting the paper –

$$SRF = \frac{1 + 2gI_u\sqrt{B}}{1 + 2gI_u} \qquad (9)$$

ABOUT THE JOURNAL

Aims

The aim of the Journal is a continuous and timely dissemination of research developments and applications. The Journal is an inter disciplinary forum for Wind and Engineering and publishes referred papers on the latest advances on the subject and their application to industrial wind engineering, wind induced disasters, environmental issues and wind energy. Papers on relevant and innovative practice and engineering application as well as those of an interdisciplinary nature are strongly encouraged. Discussions on any paper previously published in the Journal are also considered for publication. Articles submitted to the Journal should be original and should not be under consideration for publication elsewhere at the same time.
Besides regular issues containing contributed research papers, it will be the endeavour of the editors to bring out specialty issues covering a specific area of interest to include invited state-of-the-art papers.

On the other hand two-page notes describing preliminary ideas on a proposed area of future research will also be considered for publication.

Members may also send news items, memoirs, book reviews for publication.

The Society is not responsible for statements and opinions expressed by the authors in the Journal.

Subscription

The journal will be brought out biannually. For ISWE members, subscription to ISWE Journal is included in the membership fee. The rates per issue for non-members are given below:

Regular Issue	: Rs. 150.00 (US$ 25.00, by air mail)
Special Issue	: Rs. 500.00 (US$ 50.00, by air mail)
Library Membership (Annual)	: Rs. 1000.00 (US $ 100.00 by air mail)

There are no page charges for the Journal of Wind and Engineering.
A copy of the journal will be sent by post to all corresponding authors after publication. Additional copies of the journal can be purchased at the author's preferential rate of Rs. 150.00 per Volume.

Preparation of the Manuscript

a. **Paper Length** : The length of paper should normally be restricted to 10 pages maximum.

b. **Headings and subheadings** : Headings should be in bold uppercase and not numbered. Sub- headings should be in bold lower case and may be numbered.

c. **Figures and Tables:** These should be numbered consecutively in Arabic numerals and should be titled. Figure captions should be given on a separate sheet. Figures should be very sharp.

d. **Photographs, Illustrations:** Good glossy bromide prints of these must accompany the manuscript and not be attached to the manuscript pages.

e. **References:** These should be listed alphabetically at the end of the text and numbered serially, cited in the text by the last name(s) of authors followed by the year of publication in parenthesis. In case of more than two authors, the last name of the first author followed by et al. and the year of publication is to be cited in the text. References are to be listed in he following format only:

1. Walker, G.R., Roy, R.J. 1985. Wind loads on houses in urban environment. Proc. of Asia Pacific Sym. on Wind Engg., University of Roorkee, Roorkee, India, Dec. 5-7.
2. Holmes, J.D., Melbourne, W.H. and Walker, G.R. A commentary on the Australian Standard for wind loads. Australian Wind Engineering Society, 1990.
3. Krishna, P., Kumar, K., Bhandari, N.M., (2005), "Review of Wind Loading Codes", A study sponsored by Gujarat State Disaster Management Authority, India.

f. **Abstract**: This should not exceed 150 words and be an abbreviated, accurate representation of the contents of the article. It should be followed by a list of 3 to 5 key words of these contents.

g. **Units:** All quantities should be in SI units. Other units may be enclosed in parenthesis after the SI units, if necessary.

Submission

Manuscript of the paper should be transmitted by e-mail, or, alternatively, the original manuscript together with a soft copy on CD should be submitted to the Editor-in-Chief / Editors for possible publication in the Journal.

Please make sure your contact address is clearly visible on the outside of all packages you are sending to the Editors.

Editorial Office: Located at Boundary Layer Wind Tunnel,
Indian Institute of Technology Roorkee Campus,
ROORKEE -247667, India.
E-mail: iswe@iitr.ernet.in; iswe1993@gmail.com;
http://www.iswe.co.in

All enquiries may be addressed to the Editor-in-Chief / Editors, at this address.

Submitting a Paper to Journal

1. In order to maintain annonymity during any referring process, authors are requested to refrain from, or keep to a minimum, self-referencing.
2. In consideration of the publication of your Article, you assign us with full title guarantee, all rights of copyright and related rights in your Article. So that there is no doubt. This assignment includes the right to publish the Article in all forms, including electronic and digital forms, for the full legal term of the copyright and any extension or renewals. You shall retain the right to use the substances of the above work in future works, including lectures, press releases and reviews, provided that you acknowledge its prior publication in the Journal.
3. We shall prepare and publish your Article in the journal. We reserve the right to make such editorial changes as may be necessary to make the article suitable for publication; and we reserve the right not to proceed with publication for whatever reason. In such an instance, copyright in the Article will revert to you.
4. You hereby assert your moral rights to be identified as the author of the Article according to the Indian Copyright Designs & Patents Act.
5. You warrant that you have secured the necessary written permission from the appropriate copyright owner or authorities for the reproduction in the Article and the Journal of any text, illustration, or other material. You warrant that, apart from any such third party copyright material included in the Article, the Article is you original work, and cannot be construed as plagiarizing any other published work, and has not been and will not be published elsewhere.
6. In addition, you warrant that the Article contains no statement that is abusive, defamatory, libelous, obscene, fraudulent, nor in any way infringes the rights of others, nor is in any way unlawful or in violation of applicable laws.
7. You warrant that, wherever possible and appropriate, client or participant mentioned in the text has given informed consent to the inclusion of material pertaining to themselves, and that they acknowledge that they cannot be identified via the text.
8. If the Article was prepared jointly with other authors, you warrant that you have been authorized by all co-authors to sign this Agreement on their behalf, and to agree on their behalf the order of names in the publication of the Article.

THE INDIAN SOCIETY FOR WIND ENGINEERING

MEMBERSHIP FORM

Name : ..... Father's Name .....

Position : .....

Organisation : .....

Address : .....

.....

Res. Address : .....

.....

Tel : ..... Fax : .....

E-mail: .....

Nature of work and period of active involvement:

1. I/We wish to become the Individual/ Institutional member of the Indian Society for Wind Engineering (ISWE).
2. A Demand Draft for Rs. ..... payable to Indian Society for Wind Engineering at Roorkee as Membership fee is enclosed.

Date: Signature

Supported by :

Name	**Membership No.**	**Signature**
1.		
2.		

Please send this completed form to :
Secretary, Indian Society for Wind Engineering, Located at Boundary Layer Wind Tunnel,
Indian Institute of Technology Roorkee Campus, Roorkee - 247667, India,
Website- http://www.iswe.co.in

OBJECTIVES OF THE INDIAN SOCIETY FOR WIND ENGINEERING

(a) The Society shall provide a necessary forum to the individuals and institutions connected with, or, interested in industrial aerodynamics, which includes wind effects on structures and buildings, land and sea transportation vehicles; mitigation of disasters due to cyclones, tornadoes, blizzards, sand storms, etc.; wind energy generation; study of atmospheric pollution and dispersion; and, related matters to come together and exchange ideas for the advancement and dissemination of knowledge in the field of Wind Engineering
(b) The Society shall promote research and development work in the field of Wind Engineering and shall maintain close liaison with the International Organisations working with allied objectives.
(c) The Society shall promote research results in professional practice.
(d) The Society shall make efforts to involve field engineers and professional organisations in its activities by arranging seminars, symposia, etc.
(e) The Society shall bring out a periodical publication.
(f) The Society shall institute awards and prizes to recognize excellence of research and application in Wind Engineering.

MEMBERSHIP OF THE SOCIETY

The Society shall have the following categories of membership:

(a) Individual (b) Institutional
(c) Honorary

Subscription: The life membership rates for different categories shall be as follows:

Individual Membership			
Indians and SAARC Nationals	Life	Rs.	1500.00
Other Foreign Nationals	Life	US$	100.00
Institutional Membership	Annual	Rs.	3,000.00
	Regular	Rs.	30,000.00

ISWE EXECUTIVE COMMITTEE

President	Dr. N. Lakshmanan	SERC, Chennai
Vice-President	Dr. P.D. Porey	SVNIT, Surat
Hon. Secretary	Dr. Achal K. Mittal	CBRI, Roorkee
Jt. Secretary	Dr. Naveen Kwatra	Thapar University Patiala
Treasurer	Dr. Akhil Upadhyay	IIT, Roorkee
Members	Dr. Abhay Gupta	ERA Building Systems Ltd., Noida
	Dr. Ajay Gairola	IIT, Roorkee
	Dr. L.M. Gupta	VNIT, Nagpur
	Dr. M.M. Pandey	MITS, Gwalior
	Sri R.K. Mittal	MANIT, Bhopal
	Dr. Santosh K. Rai	Delhi
	Dr. Siraj Ahmad	MANIT, Bhopal
	Sri Sujit Kumar Dalui	Research Scholar, IIT Roorkee

COMMUNICATION

Communication regarding change of address, subscription renewals, missed numbers, membership and Society publications should be addressed to —

HON. SECRETARY
Indian Society for Wind Engineering,
Located at the Boundary Layer Wind Tunnel,
Indian Institute of Technology Roorkee Campus,
Roorkee - 247667, India.
Telefax: + 91 1332 284549
E-mail: iswe@iitr.ernet.in, iswe1993@gmail.com
http://www.iswe.co.in

ISSN : 0973 – 0613

JOURNAL OF WIND & ENGINEERING

Vol. 5 No. 2 July 2008

CONTENTS

Published by : Indian Society for Wind Engineering, Located at Boundary Layer Wind Tunnel, Indian Institute of Technology Roorkee Campus, Roorkee – 247667, India

***Printed and Produced by**: Elite Publishing House Pvt. Ltd. 302 JMD House, 4B Ansari Road, Daryaganj, New Delhi – 110 002, Tel: 011-41004299:*